NASA CR-152391

NASA-CR-152391-VOL-1

19810014497

ANALYSIS OF WIND TUNNEL TEST RESULTS FOR A 9.39-PER CENT SCALE MODEL OF A VSTOL FIGHTER/ATTACK AIRCRAFT

VOLUME I - STUDY OVERVIEW

DR. J. R. LUMMUS
G. T. JOYCE
C. D. O'MALLEY

NATIONAL AERONAUTICS AND SPACE ADMINISTRATION

1. Report No. NASA CR-152391	2. Government Accession No.	3. Recipient's Catalog No.
4. Title and Subtitle Analysis of Wind Tunnel Test Results for a 9.39-percent Scale Model of a VSTOL Fighter/Attack Aircraft		5. Report Date October, 1980
		6. Performing Organization Code
7. Author(s) Dr. J. R. Lummus, G. T. Joyce, C. D. O'Malley		8. Performing Organization Report No.
		10. Work Unit No.
9. Performing Organization Name and Address General Dynamics/Fort Worth Division P. O. Box 748 Fort Worth, Texas 76101		11. Contract or Grant No. NAS2-10344
		13. Type of Report and Period Covered Contractor Final Report Sept. 10, 1979–Feb. 10, 1981
12. Sponsoring Agency Name and Address NASA, AMES Research Center, Moffett Field, Ca 94035		14. Sponsoring Agency Code

15. Supplementary Notes

AMES Research Center Technical Monitor W. P. Nelms
(415) 965-5880

16. Abstract

    The results of a series of NASA AMES wind tunnel tests of a General Dynamics vectored-engine-over wing, Navy VSTOL fighter/attack configuration have been analyzed to (1) assess prediction method capabilities, (2) evaluate geometry variations such as multiple canard longitudinal locations and strake shapes, and (3) evaluate the effects of configuration changes associated with varying the propulsive lift system from a jet-diffuser ejector to a Remote Augmentation Lift System (RALS). Configuration modification and additional testing and analysis are recommended to adequately evaluate the configuration potential.

    This document is presented in four volumes – Volume I – Study Overview, Volume II – Evaluation of Prediction Methodologies, Volume III – Effects of Configuration Variations from Baseline E205 Configuration on Aerodynamic Characteristics, and Volume IV – RALS R104 Aerodynamic Characteristics and Comparisons with E205 Configuration Aerodynamic Characteristics.

17. Key Words (Suggested by Author(s)) CANARD, STRAKE, AERODYNAMIC PREDICTION METHODS	18. Distribution Statement

19. Security Classif. (of this report) UNCLASSIFIED	20. Security Classif. (of this page) UNCLASSIFIED	21. No. of Pages	22. Price

N81-23030 #

VOLUME I - STUDY OVERVIEW

TABLE OF CONTENTS

LIST OF FIGURES

LIST OF TABLES

LIST OF SYMBOLS

a. English Symbols

A	axial force, lb (N)
a.c.	aerodynamic center, $\%\bar{c}$
AR	aspect ratio
b	span, in. (m)
$\bar{c}$, MAC	mean aerodynamic chord, in. (m)
C_A	axial force coefficient
$C_{A_{ejector}}$	axial force coefficient due to ejector
C_D	drag coefficient
$C_{D_{AERO}}$	aero-only drag coefficient (no thrust increments included)
$C_{D_{min}}$	minimum drag coefficient
C_{D_E}	equivalent drag coefficient
$C_{D_{RAM}}$	ram-drag coefficient (engine inlet)
C_{D_t}	total drag coefficient
C_L	lift coefficient
$C_{L_{buffet}}$	buffet-onset lift coefficient
C_{L_E}	equivalent lift coefficient
$C_{L_{max}}$	maximum lift coefficient
$C_{L_{aero}}$	aero-only lift coefficient (no thrust increments included)
C_{L_t}	total lift coefficient
C_l	rolling moment coefficient

C_{l_β} — rolling moment derivative due to sideslip, 1/deg

C_{m_E} — equivalent pitching moment coefficient

$C_{m_{X_{\overline{c}}}}$ — pitching moment coefficient about x percent $\overline{c}$

C_{m_o} — zero lift pitching moment coefficient

C_{m_t} — total pitching moment coefficient

C_N — normal force coefficient

C_n — yawing moment coefficient

C_{n_β} — yawing moment derivative due to sideslip, 1/deg

C_T — thrust coefficient, $\dfrac{T}{qS_{REF}}$

C_Y — side force coefficient

C_{Y_β} — side force derivative due to sideslip, 1/deg

CMU, C — ideal thrust coefficient, $\dot{w}\, Vj/gqS_{REF}$

D — drag, lb(N)

e — span efficiency factor

ESF — engine scale factor, $\dfrac{T}{T_{ESF = 1.0}}$

IGE — in ground effect

L — lift, lb(N)

L_Γ — lift due to supercirculation, lb(N)

l — rolling moment, ft lb (Nm)

M — Mach number

m — pitching moment, ft lb(Nm)

NPR — nozzle pressure ratio, $\dfrac{\text{Total Pressure}}{P}$

N   normal force, lb(kg)

n   yawing moment, ft lb   (N_m)

OGE   out of ground effect

$\cdot P$ freestream static pressure, lb/ft^2 $(\frac{N}{m^2})$

P_o freestream total pressure, lb/ft^2, $(\frac{N}{m^2})$

q   freestream dynamic pressure, lb/ft^2 $(\frac{N}{m^2})$

S_C canard exposed area, ft^2 (m^2)

S_{ref} reference area, ft^2(m^2) (usually equal to S_W)

STOL   short takeoff or landing

S_W area of trapezoidal wing extended to centerline, ft^2(m^2)

Sv_T exposed area of vertical tail, ft^2(m^2)

T   thrust, lb(N)

V_∞ freestream velocity, ft/sec, knots (m/sec)

V_j jet velocity based on isentropic expansion from nozzle camber total pressure to freestream static pressure, ft/sec (m/sec)

VSTOL   vertical or short takeoff or landing

VTOL   vertical takeoff or landing

VEO-Wing   vectored engine over wing

$\dot{w}$ weight flow, lb/sec (kg/sec)

X_{cp} action point of circulation lift relative to leading edge of MAC

LG:mb/10344-FW#060-15
3 February 1981

Subject: Contract NAS2-10344
            Contract Compliance Submittal
            Final Report - NASA CR-152391

To: National Aeronautics and Space Administration
            Ames Research Center
            Moffett Field, California 94035

Attention: W. P. Nelms
            N-227-2

Enclosure: (A)   One (1) reproducible and twenty-five (25)
                  copies of NASA CR-152391 "Analysis of Wind
                  Tunnel Test Results For A 9.39-Per Cent
                  Scale Model of a VSTOL Fighter/Attack Air-
                  craft" Final Report September 10, 1979 -
                  February 10, 1981, dated October 1980

                  Volume I   - Study Overview
                  Volume I   - Evaluation of Prediction
                                Methodologies
                  Volume III - Effects of Configuration
                                Variations From Baseline
                                E205 Configuration on
                                Aerodynamic Characteristics
                  Volume IV   - RALS R104 Aerodynamic
                                Characteristics and Compari-
                                sons with E205 Configuration
                                Aerodynamic Characteristics

            (B)   Distribution List for NASA CR-152391

1. The Report, submitted as Enclosure (A), covers work conducted
by General Dynamics under NASA Contract NAS2-10334 for the joint
AMES/NSRDC VSTOL Aerodynamic Technology Program.

2. Enclosure (A) is submitted in compliance with Article II.C.1.c
and Article V.B.3 of Contract NAS2-10344.

3. Distribution is being made in accordance with Enclosure (B)
list supplied by Mr. W. P. Nelms, Contract Technical Monitor,
NASA-Ames Research Center.

                              GENERAL Dynamics
                              Fort Worth Division

                              H. J. Kauffman
                              Director of Engineering
                              Administration

To: NASA/W. P. Nelms

cc: w/Encl. (A)
Ames Research Center
Patent Counsel
N200-11A

Ames Research Center
Technology Utilization Office
N240-2

cc:

Ames Research Center Technical Information Division
N241-12

Ames Research Center
Contracting Office, Carolyn S. LaFollette
N241-1

Direct transmittal is approved by the
Air Force. Your answer, if any, will
be forwarded through regular Air Force
channels to General Dynamics,
Fort Worth Division, Fort Worth, Texas.

Page 3
10344-FW#060-15

To: NASA/W. P. Nelms

cc:

J. R. Lummus, 2882
W. R. Kayl, 2870
T. M. Pettigrew, 1649
L. G. Graham, 2236 (2)
Engr. Files, 2228
Corres. Control, 1137
Contract Records, 6699

DISTRIBUTION LIST FOR NASA CR-152391

Mr. W. S. Aiken, RJ-2
National Aeronautics &
  Space Administration
Washington, D.C.   20546

Mr. John Ward, RJL-2
National Aeronautics &
  Space Administration
Washington, D.C.   20546

Mr. Jack Levine, RJH-2
National Aeronautics &
  Space Administration
Washington, D.C.   20546

Mr. P. J. Bobbitt
M.S. 285
NASA Langley Research Center
Langley Station
Hampton, VA   23665

Mr. R. V. Harris
M.S. 407
NASA Langley Research Center
Langley Station
Hampton, VA   23665

Mr. L. W. Gertsma
M.S. 500-208
Lewis Research Center
NASA
21000 Brookpark Road
Cleveland, Ohio   44135

Mr. H. R. Chaplin
NRDC, Room 219, Bldg. 7
Corderock, Maryland   20034

Mr. James H. Nichols, Jr. 3 Cys.
NSRDC, 208A, Bldg. 13
Corderock, Maryland   20034

Mr. Hal Andrews
Room 412
Jefferson Plaza #1
1411 Jefferson-Davis Highway
Arlington, VA   20306

Mr. M. W. Brown
Room 904
Jefferson Plaza #2
1421 Jefferson-Davis Highway
Arlington, VA   20360

Capt. D. C. Troutman
Project Manager, V/STOL
Room 674
Jefferson Plaza #1
1411 Jefferson-Davis Highway
Arlington, VA   20360

Mr. R. F. Siewert
OUSDR&D
Room 3D1089
Pentagon
Washington, D.C.   20301

Mr. T. J. Brennan
Naval Air Development Center
Code IVA
Warminster, PA   18974

Co. Peter J. Butkewicz
Chief, Aeromechanics Div.
AFWAL/FIM
Flight Dynamics Laboratory
Wright-Patterson AFB, Ohio
45433

Mr. John Chuprun, Jr.
ASD/XRHD
Wright-Patterson AFB, Ohio
45433

b. Greek Symbols

α	alpha	angle of attack, deg
β,	beta	angle of sideslip, deg
Γ		supercirculation
γ		flight path angle, deg
δ_C, δ_i		canard deflection (positive, leading-edge up), deg
δ_{TE}, δ_F		VEO-Wing nozzle and outboard flaperon deflection, deg; except for aileron action the flaperons and VEO-Wing nozzle flaps always deflect together.
θ		pitch attitude angle, deg
θ_J		jet thrust deflection out of VEO-Wing nozzles when deflected, $_{TE}$, deg
Λ_{LE}		leading-edge sweep angle, deg
λ		taper ratio, $\dfrac{\text{tip chord}}{\text{root chord}}$
ϕ		ejector measured thrust/isentropic supply thrust (where isentropic supply thrust is the thrust which would be obtained from supplied air at the nozzle exit of pressures and flow rates expanded at isentropically to ambient pressure)

c. Model Symbols

B_1 VSTOL ejector configuration E-205 basic fuselage with fuselage strake that blends the fuselage to the inboard section to the wing.

B_2 VSTOL RALS configuration R-104 basic fuselage

C_1 All moveable nacelle-mounted horizontal canard of VSTOL ejector configuration E-205 in the mid-location

C_2 Horizontal canard in VSTOL E-205 or RALS R104 fwd-location

C_3 Horizontal canard in VSTOL E-205 or RALS R104 aft-location

N VSTOL ejector configuration E-205 or RALS R104 VEO-wing nacelle

S_1 Baseline strake on E205 configuration

S_2 High sweep strake on E205 configuration

S_3 Low sweep strake on E205 configuration

V All moveable vertical tail of VSTOL ejector configuration E-205 or RALS R104

W_1 VSTOL ejector configuration E-205 wing with linear elements between SS 96.496 and SS 223.695

W_2 VSTOL RALS configuration R-104 wing with linear elements between SS 87.231 and SS 214.430

1.0 SUMMARY

This document presents the analysis of a series of NASA AMES wind tunnel tests of two General Dynamics Vectored-Engine-Over (VEO-) Wing, Navy VSTOL fighter/attack configurations; the airplane configurations and wind tunnel models were developed during a previous NASA AMES contracted effort described in Reference 1. The two configurations differ primarily in the propulsive lift systems employed for VTOL operations, the jet-diffuser ejector (E205 configuration) and the Remote-Augmentation-Life System (RALS R104 configuration); both configurations employ the VEO-wing concept for improved maneuver and STOL performance.

The wind tunnel data has been analyzed to (1) assess the prediction method capabilities, (2) evaluate geometry variations such as multiple canard longitudinal locations and strake shapes and (3) evaluate the differences in the aerodynamic characteristics of the two configurations, i.e., the effect of the propulsive lift system on the airplane arrangement and subsequent performance.

The existing prediction methods were found to be surprisingly effective for such unusual configurations but areas of concern were uncovered where improvements in prediction capabilities are certainly worthwhile. The experimental data base gathered in this series of tests forms one of the most complete, systematic parametric variations of configuration variables existing in the literature available to the designer and as such, should represent a very valuable aid in years to come. The analysis of these variations presented in this report will also hopefully become a worthwhile design aid.

Comparison of the overall performance of the two configuration concepts showed the E205 configuration to be superior.

The major limitation of the E205 concept has been uncovered and several suggestions for future research have been recommended to resolve the limitation and check the effect of the required configuration changes on the effects of the geometry variations described above.

This document is presented in four volumes - Volume I - Study Overview, Volume II - Evaluation of Prediction Methodologies, Volume III - Effects of Configuration Variations from Baseline E205 Configuration on Aerodynamic Characteristics, and Volume IV - RALS R104 Aerodynamic Characteristics and Comparisons with E205 Configuration Aerodynamic Characteristics. The figures are placed at the end of each volume for the reader's convenience while the tables are integrated into the text as they occur.

2. INTRODUCTION

Many potential advantages for incorporating VSTOL capability into future Navy fighter/attack aircraft have been perceived by both the government and the aerospace industry. Among the advantages are tactical benefits resulting from dispersal of air strength through operation from ships smaller than aircraft carriers, improved combat tactics via in-flight use of vertical-lift propulsive systems, reduced costs from requirments for construction of smaller ships, and improved close support through short takeoff and landing. Presently, the integration of a vertical-lift propulsive system penalizes subsonic cruise performance and supersonic dash capability, degrades the ship-board deck environment, and imposes additional operational requirements. However, innovative aircraft design, including advances in propulsive system, flight control, structural, and aerodynamic technologies projected to the 1990 time period, has led to the emergence of VSTOL concepts with significant transonic maneuver and supersonic performance potential. Nevertheless, detailed configuration design of these VSTOL aircraft concepts is generally lacking, and only limited experimental data to define the aerodynamic/propulsive characteristics of such vehicles are available. Therefore, studies were commissioned jointly by the Navy (David Taylor Naval Ship Research and Development Center and Naval Air Systems Command) and NASA Ames to investigate the aerodynamic technology associated with various VSTOL fighter/attack aircraft concepts.

In Phase I of the contracted program, (Reference 1) four contractors provided conceptual designs, estimated the aerodynamics of the designs, identified aerodynamic uncertainties of the concepts and proposed a wind-tunnel program to explore these uncertainties. In Phase II of the contracted program, two contractors designed and built wind-tunnel models for tests in the Ames Unitary and 12-Foot Wind Tunnels covering a Mach number range of 0.2 to 2.0.

This report presents the analysis of the testing accomplished with two models designed and built in Phase II of the contracted program by the General Dynamics Corporation (Reference 1 and 2). This analysis was conducted by General Dynamics under a separate contract to NASA Ames under Contract No. NAS2-10344. The two wind-tunnel models investigated in this report represent horizontal attitude takeoff and landing VSTOL fighter attack aircraft derivatives of General Dynamics' Vectored-Engine-Over-Wing (VEO-Wing) concept. This concept (see Figure 2-1) achieves improved

3

transonic maneuvering and short takeoff and landing (STOL) performance by utilizing the full engine momentum from over-wing-mounted engines to augment the external aero-dynamics through a jet-flap effect and vortex augmentation. The major difference between the two configurations is the propulsive system utilized for vertical lift. These propul-sive systems are the jet-diffuser ejector and the General Electric developed Remote Augmentation Lift System (RALS). These systems represent the range of cold-vs-hot deck en-vironments currently being considered for vertical propul-sion concepts. Both systems afford thrust/lift augmenta-tion, which allows reduced vehicle size for a given payload capability. The aerodynamic lift augmentation achieved from the VEO-Wing nozzles through upper circulation also leads to reduced vehicle size. Three-view drawings and artist con-cept drawings of the E205 and R104 airplane configurations are shown in Figures 2-2 through 2-5. The models repre-senting these configurations are described in Section 3.4.

The primary objectives of this analysis effort are:

1. To evaluate the ability of current methodologies to accurately predict the aerodynamic characteristics identified as uncertainties for the two aircraft con-figurations developed in the Phase I study program described above.

2. To analyze the results of the three test entries to determine the effects of configuration variations with the baseline ejector and RALS configurations.

3. To analyze the results of the three test entries to determine the differences in the aerodynamic characteristics of the ejector and RALS baseline configurations.

These objectives are accomplished in this report by tracing the development of the airplane configurations through the design process and noting the predicted aerodynamic characteristics used in the sizing studies for the E205 configuration and the resulting aerodynamic uncertainties that evolved. Following a description of the wind tunnel models and tests that were accomplished, an analysis of the test data yields an appraisal of current prediction methodo-logies to resolve the aerodynamic uncertainties. The analy-ses also aptly demonstrate the variation in aerodynamic characteristics resulting from the wide variations in configuration variables as well as the differences that result from variations in the vertical propulsion concept, i.e., RALS vs ejectors.

Comparisons of predicted and wind tunnel aerodynamic characteristics are limited to the E205 configuration only because (1) either one of the configurations could serve as a sufficient test case to determine the capabilities the prediction methods for this generic class of VEO configurations and (2) the E205 wind tunnel model more closely represents the full scale E205 airplane configuration than does the wind tunnel model of the RALS R104 airplane configuration (see Section 3.4).

3. REVIEW OF AIRPLANE CONFIGURATION DEVELOPMENT STUDY

The E205 and R104 airplane configurations (Figures 2-2 and 2-3) were developed during the Reference 1, Phase I, contracted study effort. This contracted study limited the scope of the analysis to only one concept, the jet-diffuser ejector concept, E205. This configuration concept was selected because it offered more potential shipboard operational benefits due to its benign footprint that other members of the VEO-generic class of VSTOL fighter concepts. Further, the ejector configuration exhibits more aerodynamic uncertainties and differs more from the existing data base than does the RALS. The RALS configuration more closely resembles the VEO-Wing fighter for which an unpowered experimental data base already exists. General Dynamics continued to pursue the RALS configuration through in-house funding in a somewhat parallel study program; in fact, the RALS and ejector configuration were first compared using NAVAIR-supplied ground rules in Reference 3.

However, the E205 and R104 configurations were further developed using the sizing ground rules of Reference 1. The Reference 1 study was structured to assess the importance of the various aerodynamic uncertainties involved in the concepts by actually designing and sizing the airplanes to a set of requirements suggested by the NASA contract guidelines and by General Dynamics' experience in previous Navy VSTOL fighter studies. The requirements shown below, reflect the desire for the aircraft to have good supersonic fighter combat performance (with reasonable mission "legs") when operating in VTO and good attack-support capability when operating in STOL:

Mission: VTO Deck Launch Intercept (DLI) with
(Standard Day)   radius of action = 150 n.mi and design
                        dash M = 1.6 (See Figure 3-1 for
                        detailed mission profile definition).

Combat Performance: Sustained load factor of 6.2 at Mach
(Standard Day)   0.6, 10,000 ft of altitude at 88% VTOL
                        gross weight

                        Specific excess power of 900 fps at 1g,
                        Mach 0.9, 10,000 ft of altitude at 88%
                        VTOL gross weight.

6

VTOL: (Tropical Day)	Vertical acceleration = 1.05 g (IGE) while achieving maximum design control rates simultaneously in all axes, where maximum design control acceleration rates are:

$$Roll = .96 \text{ rad/sec}$$

$$Pitch = .28 \text{ rad/sec}$$

$$Yaw = .40 \text{ rad/sec}$$

STOL	Operational from land and from ships smaller than CV's without catapults and arresting gear; sea-based gross weight = VTO maximum gross weight + 10,000 lb; sea-based WOD = 20 kt for overload.
VTO Takeoff Gross Weight	Maximum = 35,000 lb.
Fuel Flow Conservatism	Use minimum engine without 5% fuel flow conservatism (approximately same as using average engine with 5% fuel flow conservatism).

It should be noted that the RALS 104 configuration, as drawn in Figure 2-3, does not represent an aircraft exactly sized to meet all of the ground rules described above but, instead, served as a sizing baseline configuration for synthesis studies. Comparisons between the ejector and RALS configurations sized to these ground rules are shown in Reference 1 based on synthesis studies.

The VEO-Wing Ejector and RALS fighter/attack configuration layouts have been influenced heavily by the necessity to meet the following three criteria simultaneously:

1. <u>Static margin variation (center of gravity/aerody-namic center) with Mach number from approximately -18% (unstable) subsonically to + 10% (stable) supersonically.</u> The maximum allowble instability of -18% static margin subsonically is a value set by the aerodynamic control and control-system-response capability expected in the 1990 time period.

2. <u>Center-of-gravity, wing, nozzle, and canard-location relationships (as well as static margin) to achieve the supercirculation benefits of the VEO-Wing concept for cruise maneuvering and STOL.</u> To achieve the benefits of the VEO-Wing concept re-

quires the c.g. to be as far aft as possible (with static margin as in Criterion 1). This has a large impact on the configuration design; it is difficult to achieve the desired c.g. location without getting so much "real estate" ahead of the c.g. that the resulting forward-located aerodynamic center produces more instability than can be tolerated.

3. <u>Center-of-Gravity, aircraft-inertias, and thruster locations that meet the hover requirements.</u>

3.1 Airplane Configuration Descriptions

This section provides a brief description of the physical characteristics and design features of the E205 and R104 airplane configurations. For a more detailed description of these configurations, the reader is referred to References 1 and 3 which deal with the following design features in some detail and which are omitted from this report: geometry, propulsion systems, mass properties, structural design, flight controls and the major subsystems such as avionics, crew station equipment, secondary power generation and weapons, electrical, hydraulic, ECS, oxygen and fuel systems, etc.

Both the E205 and R104 supersonic fighter designs are configured to provide propulsive enhancement of external aerodynamics. This unique integrated airframe/propulsion system, known as VEO-Wing (Vectored Engine Over Wing, see Figure 2-1) utilizes the full engine momentum from the over-wing-mounted engines to augment the external aerodynamics through a jet-flap effect. The VEO-Wing feature is combined with spanwise blowing in which a portion of the engine exhaust is used at high angles of attack to produce leading-edge vortex augmentation. This unique system is thus capable of providing lift/drag polar improvements in the full angle of attack range, resulting in improved maneuverability and STOL performance.

3.1.1 Ejector E205 Airplane Configuration

The three view drawing of the jet-diffuser ejector VSTOL fighter/attack conceptual design (E205) sized to meet the mission, hover and combat performance requirements described in Section 3.0 is presented in Figure 2-2.

The concept utilizes a high-canard, low-wing arrangement with podded engines located for over-the-wing blowing. Four chord-wise bays between the center body and nacelles (two forward and two aft) are provided for location of the jet diffuser ejectors.

Unique features of this configuration approach are the incorporation of movable doors to form the ejector nozzle and the stowable primary nozzles, which result in a relatively compact arrangement when the ejectors are not in use. A strake is extended forward and a beaver tail aft to fair off the depth of the ejectors when folded into their cruise position. The ejector design is based on application of the research discussed in detail in Reference 1. The ejectors are sized to be operated with intermediate power airflow from P&WA .35-25-2800 parametric engines. Air is diverted to the ejector primary and throat nozzles through the ducting arrangement shown in Figure 2-2. The augmentation ratio is 1.98 in free air and 1.70 at lift off. Thrust modulation at the forward and aft ejectors, by varying airflow at the ejector primary nozzles, is used for pitch control during hover and transition. Yaw control is achieved by vectoring the ejector flow. Engine exhaust air is ducted to upward and downward firing thrusters for roll control. No lift is produced by this reaction control system in hover. The VEO-Wing engine nozzles can be operated in afterburner power setting with the ejectors running.

VTOL transitions are accomplished by diverting the excess thrust required to hover out of ground effect from the ejectors to the vectorable VEO-Wing nozzles. For STOL operations the hover controls are blended with the aerodynamic controls (the canard, elevons, and all-moving vertical tail) to provide control about the pitch, roll, and yaw axes. The reaction controls are fired fore and aft or up and down as required to provide yaw and roll control at very low speeds or high angles of attack to augment the aerodynamic controls.

During conventional flight, control about the three axes is provided with canards, elevons, and the VEO-Wing nozzle for pitch, flaperons for roll, and the vertical tail and flaperon for yaw. The reaction controls are also available at low speeds for augmenting the aerodynamic controls to extend the lateral-directional control capabilities at high angles of attack. Due to the high longitudinal instability levels that result with this type of configuration, the flight control system is used to schedule the canard, VEO-Wing nozzle, and wing flaps as a function of Mach number, angle of attack, and power setting to achieve desired levels of static longitudinal stability and to augment the longitudinal stability to the required frequency and damping levels.

Dimensional and pertinent design data for the E205 configuration are presented in Table 3-1. The wetted area component buildup is included. The cross sectional area

TABLE 3-1   DIMENSIONAL AND DESIGN DATA
FOR EJECTOR E205 CONFIGURATION

WING

Area (Ref)	384 ft^2	(35.67 m^2)
Aspect Ratio	3.62	
Taper Ratio	.19	
b	37.28 ft	(11.36 m) ·
b/2	223.70 in.	(5.682 m)
CR	207.72 in.	(5.276 m)
CT	39.47 in.	(1.003 m)
c	142.680 in.	(3.624 m)
Y	86.473 in.	(2.196 m)
Airfoil Root & Tip	NACA 64A204	
Sweep-Leading-Edge	40°	
Sweep - c/4	32°	
Incidence	-0°	
Dihedral	0°	

CANARD

Area (Exp)	76.9 ft^2	(7.14 m^2)
Aspect Ratio	2.16	
Taper Ratio	.37	
b (Tip to Tip)	28.6 ft	(8.72 m)
b/2 (Exp)	77.33 in.	(1.96 m)
CR (Exp)	104.58 in.	(2.655 m)
CT	38.67 in.	(.982 m)
c	76.65 in.	(1.947 m)
Y	32.74 in.	(.832 m)
Airfoil Root	NACA 64A005	
Airfoil Tip	NACA 64A003	
Sweep-Leading-Edge	45°	
Sweep - c/4	37°	
Incidence & Dihedral	0°	
Lc (LE c̄ Wing to c̄/4 Canard)	6.7 ft	(2.04 m)
Vc (Volume)	514.3 ft^3	(14.565 m^3)

TABLE 3-1   DIMENSIONAL AND DESIGN DATA
FOR EJECTOR E205 CONFIGURATION
(Continued)

VERTICAL TAIL

Area (Exp)	47.5 ft^2	(4.41 m^2)
Aspect Ratio	1.27	
Taper Ratio	.43	
b	7.8 ft	(2.38 m)
CR	102.6 in.	(2.606 m)
CT	44.1 in.	(1.120 m)
c	77.3 in.	(1.963 m)
Y	40 in.	(1.016 m)
Airfoil Root	5.3% Biconvex	
Airfoil Tip	4% Biconvex	
Sweep - Leading-Edge	47.5°	
LVT (LE c Wing to c/4 VT	17.8 ft	(5.43 m)
VVT (Volume)	845.1 ft^3	(23.933 m^3)

WETTED AREAS

Fuselage	451 ft^2	(41.90 m^2)
Canopy	33 ft^2	(3.07 m^2)
Nacelle	461 ft^2	(42.83 m^2)
Wing	919.5 ft^2	(85.42 m^2)
Canard	153.8 ft^2	(14.29 m^2)
Vertical Tail	95 ft^2	(8.83 m^2)
Dorsal	8 ft^2	(.74 m^2)
Wing Aft of Nac	27.7 ft^2	(2.57 m^2)
TOTAL	2159 ft^2	(199.64 m^2)

Fineness Ratio (l/de)	7.66	
Fuel Fraction	27.2%	
Structural Fraction (w/o Ejectors)	32.4%	
Composites (% of Struct Wt) (w/o Landing Gear)	23.1%	
Advanced Metallics (Incl Ejectors) (% of Struc Wt w/o Landing Gear)	72.8%	
C G Location (% c)	3.0%	

VTO TOGW/Max TOGW	34987/44987	(15853/20384 kg)
Combat Wt (88% VTOGW)	30789 lb	(13950 kg)
Flight Design Wt (88% VTOGW)	30789 lb	(13950 kg)
Empty Wt	23402 lb	(10603 kg)
Payload (VTO/Max Overlead)	1146/11,146 lb	(520/5055 kg)
Installed Gun Sys. Weight/Ammo	521/500 lb	(236/227 kg)
Avionic Wt (Installed/ Uninstalled)	1057/846 lb	(479/384 kg)

TABLE 3-1 DIMENSIONAL AND DESIGN DATA FOR EJECTOR E205 CONFIGURATION (Continued)

Internal Fuel Volume		
Fuselage (Bladder)	877 lb	(3974 kg)
Wing (Integral, Halon		
Inerted)	750 lb	(340 kg)
Total	9521 lb	(4314 kg)
Design Mission Fuel	9521 lb	(4314 kg)
Number of Engines & Types	(2) P&W Parametric	
	Eng FB ABTF	
	BPR=.362 OPR=25	
	TIT=2800°F	(1537.8°C)
Thrust (Max A/B SLS-		
Unistalled Each)	22,718 lb	(10,294 kg)
Inlet Type	Axisymmetric Normal Shock	
	Shock	
Al Per Engine	4.86 ft^2	(.451 m^2)
W/S At VTOGW	91 lb/ft^2	(444 kg/m^2)
T/W At VTOGW (Max A/B SLS		
Uninstalled Thrust)	1.3	
Max Cross Section Area		
Minus Al	33.2 ft^2	(3.084 m^2)
Airplane Overall Dimensions		
Overall Length	53.3 ft	(16.25 m)
Overall Span (Including		
Missiles)	39.4 ft	(12.0 m)
Overall Height	15.4 ft	(4.69 m)
Flight Design Limit Load		
Factor	7.5 g	
Design Rate of Sink	15 fps	(4.57 mps)

distribution is shown in Figure 3-2. The c.g. is maintained by fuel burn sequencing at +.03c (F.S. 308.86) as long as possible to achieve the VEO benefits for combat (until about 3000 of the 9521 lb of fuel for the DLI mission remains).

The control devices and deflection limits are as follows:

		Max deflection
1.	VEO-Wing nozzle	$-10°$ to $+30°$
2.	Flaperon (outboard of VEO-Wing nozzle)	$-20°$ to $+30°$
3.	Canard	$-25°$ to $+25°$
4.	Reaction controls	$-90°$ and $+90°$
5.	All-moving vertical tail	$-25°$ to $+25°$

The flaperon acts with the VEO-Wing nozzle for high lift but also acts as an aileron from the deflected flap position to provide roll control.

3.1.2 RALS R104 Airplane Configuration

The RALS R104 configuration (Figure 2-3) utilizes a high-canard, low-wing arrangement with podded engines located for over-the-wing blowing like the E205 configuration. The RALS concept provides a vectorable force forward of the aircraft c.g. by augmenting fan-discharge air (with a burner) from the GE 16/VF19-D1 (.6 bypass ratio) variable-cycle engine in a remote duct buring system. A "three poster" configuration is thus achieved for vertical flight by vectoring the reheated VEO Wing exhaust nozzles 90 degrees downward (in conjunction with the RALS nozzles). The nominal exhaust tempertaure of both the remote and primary nozzles is 2800°F. Thrust modulation of the RALS and VEO-Wing nozzle burner is used for pitch control during hover and transition which results in temperatures up to 3200°F. Yaw control is provided by vectoring of the VEO-Wing nozzle. Roll control is achieved with downward-firing reaction control thrusters, which are located in the wing tips and always contribute to lift. Transition from hover to wingborne flight is accomplished by gradually diverting the thrust from the forward RALS to the aft VEO-Wing nozzles as wingborne flight is approached. To achieve the VEO-Wing benefits for up-and-away flight, the c.g. is held as far aft as possible (c.g. = +1.1%c).

This configuration (like E205) also features spanwise blowing louvers (upstream of the VEO-Wing nozzle burner rings), which exhaust engine thrust out over the wing (Figure 2-3) to augment the leading vortex, thus delaying stall to higher angles of attack and producing excellent STOL performance (although the effects of spanwise blowing are not incorporated in this report).

For operations at low speeds, the configuration features an all-moving verticl tail.

The RALS nozzles are gimballed to provide 15 degrees of deflection from 90 degrees downward and 360 degrees in the planform view, except straight aft, where a maximum deflection of 30 degrees is possible. These RALS nozzles not only are used to achieve vertical transitions or hover by providing pitch and yaw control, but also are used as forward thrusters to achieve nose-wheel rotation at very low flight speeds to provide excellent STOL performance.

The control devices for up-and-away flight and their deflection limits are as follows:

		Max Deflection
1.	VEO-Wing nozzles	$-10°$ to $+90°$
2.	Flaperon (outboard of VEO-Wing nozzle)	$-20°$ to $+30°$
3.	Canard	$-25°$ to $+25°$
4.	Reaction controls	$-90°$ and $+90°$
5.	All-moving vertical tail	$-25°$ to $+25°$

Just as on the E205, the flaperon not only acts with the VEO-Wing nozzle for high lift, but also acts as an aileron from the deflected flap position to provide roll control in the transition, STOL or conventional flight modes.

Like E205, IR-guided missiles are carried on the wing tip; all other payload on R104 is carried on the nacelles and the wide flat fuselage between the nacelles. Dimensional and pertinent design data for the R104 configuration are presented in Table 3-2. A cross-sectional area distribution is shown in Figure 3-3; the large volumes (and consequently large cross-sectional areas) required to install the RALS ducts in the fuselage plus the large engines required for V/STOL operation result in the high peak in the are distribution. The wetted area component build-up is also shown in Table 3-2.

TABLE 3-2   R104 DIMENSIONAL AND DESIGN DATA

WING

Area (Ref)	300 Ft^2	(27.867m^2)
Aspect Ratio	3.6	
Taper Ratio	.20	
b	32.9 Ft	(10.028m)
b/2	197.2 In	(5.009m)
CR	182.5 In	(4636m)
Ct	36.5 In	(.927m)
c	126 In	(3.200m)
Y	75.7 In	(1.923m)
t/c Root & Tip	NACA 64A204	
Sweep-Leading-Edge	40°	
Sweep – c/4	33°	
Incidence & Dihedral	0°	

CANARD

Area (Exp)	66 Ft^2	(6.131m^2)
Aspect Ratio	2.16	
Taper Ratio	.37	
b (Tip to Tip)	25.4 Ft	(7.742m)
b/2 (Exp)	71.7 In	(1.821m)
CR (Exp)	96.5 In	(2.451m)
CT	36 In	(.914m)
c	71 In	(1.803m)
Y	32 In	(.813m)
t/C Root	NACA 64A005	
t/C Tip	NACA 64A003	
Sweep-Leading-Edge	45°	
Sweep – c/4	37°	
Incidence & Dihedral	0°	
Lc (LE c/4 Wing to c/4 Canard)	6.5 Ft	(1.981m)
Vc	429 Ft^3	(12.148m^3)

VERTICAL TAIL

Area (Exp)	43 Ft^2	(3.995m^2)
Aspect Ratio	1.25	
Taper Ratio	.43	
b	7.3 ft	(2.225m)
CR	98.5 Ft	(30.023m)
CT	42.34 In	(12.91m)
c	74.7 In	(22.769m)
Y	38 In	(.965m)
t/c Root	5.3% Biconvex	
t/c Tip	4% Biconvex	
Sweep – Leading Edge	47.5°	

TABLE 3-2   R104 DIMENSIONAL AND DESIGN DATA

(Continued)

LVT (LE $\bar{c}$ Wing to $\bar{c}$/4 VT)	16.08 Ft	(4.901m)
VVT	691.6 Ft^3	(19.584m^3)

WETTED AREAS

Fuselage	479 Ft^2	(44.5m^2)
Canopy	42 Ft^2	(3.90m^2)
Nacelle	473 Ft^2	(43.94m^2)
Wing	338 Ft^2	
Canard	132 Ft^2	(12.26m^2)
Vertical Tail	86 Ft^2	(7.99m^2)
Dorsal	6 Ft^2	(.557m^2)
Wing Aft of Nac	28 Ft^2	(2.60m^2)
TOTAL	1584 Ft^2	(147.158m^2)

Fineness Ratio (1/de)	7.12	
Fuel Fraction	34%	
Structural Fraction	28.7%	
Composites (% of Struct Wt) (W/O Landing Gear)	26.1%	
Advanced Metallics (% of Struct Wt W/O Landing Gear)	64.3%	
C.G. Location (% c)	0.6%	

VTO TOGW/Max TOGW	31,940/41,940	(14,485 Kg/19020.
Combat Wt (TOGW-40% WF)	27,590 Lb	(12512 Kg)
Flight Design Wt (TOGW-40% WF)	27,590 Lb	(12512 Kg)
Empty Wt	19,000 Lb	
Payload (VTO/Max Overload)	1146/11,146 Lb	(520 Kg/5055 Kg)
Installed Gun Sys. Weight/ Ammo	521/500 Lb	(236 Kg/226 Kg)
Avionic Wt (Installed/ Uninstalled)	1057/846 Lb	(479 Kg)
Internal Fuel Volume Fuselage (Bladder)	10,315 Lb	(4678 Kg)
Wing (Integtral, Halon Inerted)	560 Lb	(254 Kg)
Total	10,875 Lb	(4932 Kg)
Number of Engines & Types	(2) GE16/VVCE 5 Study D$_2$ Engines With Remote Aug Lift Sys.	
Thrust (SLS-Uninstalled Each)	21,747 Lbs	(9863 Kg)

TABLE 3-2   R104 DIMENSIONAL AND DESIGN DATA

(Continued)

Inlet Type	Axi-Symmetgric Normal Shock	
Al Per Engine	4.55 Ft^2	(1.387m^2)
W/S At TOGW	106.5 Lb/Ft^2	(520 Kg/m^2)
T/W At TOGW (SLS Uninstalled)	1.36	
Max Cross Section Area	38 Ft^2	(3.530m^2)
Airplane Overall Dimensions		
Overall Length	48.8 Ft	(14.874m)
Overall Span	32.9 Ft	(10.028m)
Overall Height	11.54 Ft	(3.517m)
Flight Design Limit Load Factor	7.5 g	
Design Rate of Sink	15 fps	(4.572m/sec)

Like the E205 configuration, the structure of the R104
configuration is designed for a limit load factor of 7.5 g's
and a design sink speed of 15 ft/sec. Both aircraft employ
advanced metals and composites as well as advances in
avionics to achieve weight savings considered feasible by
the 1995 time period.

3.2 Predicted Aerodynamic Characteristics

One of the primary objectives of this analysis effort
is to determine the capabilities of current prediction
methodologies to predict the aerodynamic characteristics of
the E205 type of configuration. In Reference 1 predictions
of the longitudinal and lateral-directional aerodynamic
characteristics of the full-scale E205 airplane configur-
ation were presented for the subsonic (STOL/VTOL, M <.3) and
transonic (cruise/maneuver, .3 <M <1.0) and supersonic
(dash, M >1.0) flight regimes of the design DLI mission (de-
fined in Section 3.0). These full scale aerodynamic predi-
ctions are briefly reviewed in this section because they
form the basis for developing the predicted model-scale
wind-tunnel aerodynamic characteristics that are compared in
Volume II with the actual wind-tunnel data to determine the
prediction-methodology capabilities for the E205 type of
configuration. Predictions of the full-scale E205 longi-
tudinal aerodynamic characteristics including the lift,
drag, and pitching moment curves, aerodynamic center travel
and buffet onset angle of attack are presented in this sec-
tion as well as estimates of some of the lateral-directional
characteristics including the rigid sideslip derivatives,
vertical tail effectiveness and aileron effectiveness.

The predicted longitudinal aerodynamics of the
full-scale E205 aircraft configuration are based on
estimated values of minimum drag while the lift, pitching
moment, and drag due-to-lift rely heavily on the
experimental data base developed from wind-tunnel tests of
the powered General Dynamics Research Model (Ref. 4) and the
unpowered VEO-Wing fighter model (Figure 3-4) (Ref. 5). Figure
3-5 illustrates the forces and moments considered in
predicting the full scale E205 aircraft aerodynamic
characteristics. Table 3-3 provides a summary of analysis
schemes with other pertinent data included for each flight
regime. Three types of data coefficients were developed in
Reference 1 for analyzing the configuration in these flight
regimes and are defined by the following equations:

1. Total Coefficients (Subscript t): All aerodynamic
    plus thrust forces included

$$C_{L_t} = C_{L_{Aero}} + C_{T_{V.N.}} \sin(\delta_F + \alpha) + C_{T_{EJ}} \cos\alpha - C_{D_{ram} \atop Ejector} \sin\alpha$$

$$C_{D_t} = C_{D_{Aero}} \quad C_T \cos\alpha(\delta_F + \alpha) + C_{T_{EJ}} \sin\alpha + C_{D_{Eng\text{-}Inlet \atop Ram\ Drag}} + C_{D_{ram} \atop Ejector} \cos\alpha$$

19

Table 3-3 Methods Summary

FLIGHT REGIME	PROPULSION SYSTEM EMPLOYED	VEO NOZZLE THRUST		BOOKKEEPING AND TRIM METHODS	DATA TYPE PRESENTED
		ANGLE	MAGNITUDE		
STOL, VTOL $M \simeq .3$	THRUST VECT FROM VEO NOZZLE + EJECTOR THRUST + SPANWISE BLOWING (NOT USED IN REPORTED ANALYSIS BUT POSSIBLE)	$\delta_{TE} = 30^{\circ}$	$C_T \leq 7.4$	GROSS THRUST APPLIED/REMOVED IN (+δ_{TE}) DIRECTION, NOZZLE & INLET FORCES APPLIED EXTERNALLY TRIM w FLAPERON, CANARD, EJECTORS, VEO WING NOZZLE	AERO EQUIVALENT TOTAL
CRUISE/ MANEUVER $.3 \leq M \leq 1.0$	THRUST VECT FROM VEO NOZZLE	$\delta_{TE} = 15^{\circ}$	$C_T \leq .2$	NET THRUST APPLIED/REMOVED IN DIRECTION INDUCED & VECTORING EFFECTS INCLUDED IN "EQUIVALENT" POLAR NOZZLE & INLET FORCES IN PROP. TRIM WITH FLAPERON, CANARD, VEO WING NOZZLE	EQUIVALENT
DASH $M > 1.0$	NO THRUST VECTORING NO SPANWISE BLOWING	$\delta_{TE} = 0^{\circ}$	$C_T < .15$	CONVENTIONAL A/C METHODS (USE UNPOWERED DATA) TRIM WITH CANARD	EQUIVALENT

$$C_{M_t} = C_{M_{Aero}} + C_T \cos \delta_F \left(\frac{C.G.W.L. - V.N.W.L.}{\bar{c}}\right)$$

$$+ C_{T_{V.N.}} \sin \delta_F \left(\frac{C.G.F.S. - V.N.F.S.}{\bar{c}}\right)$$

$$+ C_{T_{EJ}} \left(\frac{C.G.F.S. - EJ.F.S.}{\bar{c}}\right) + C_{D_{Eng-Inlet}} \cdot \sin\alpha \left(\frac{C.G.F.S. - Inlet\ F.S.}{\bar{c}}\right)$$

Where C.G.W.L. = waterline for center-of-gravity location

V.N.W.L. = waterline of VEO-Wing nozzle thrust vector

C.G.F.S. = fuselage station for center-of-gravity location

V.N.F.S. = fuselage station of VEO-Wing nozzle thrust vector

EJ.F.S. = fuselage station of ejector thrust vector.

Assuming ejector thrust always 90° to W.L., i.e. no thrust recovery.

2. Equivalent Coefficients (Subscript E): Aerodynamic plus thrust forces with thrust angle-of-attack effects removed are:

$$C_{L_E} = C_{L_T} - C_{T_{V.N.}} \sin\alpha - C_{T_{EJ}} \cos\alpha + C_{D_{ram\ Ejector}} \sin\alpha$$

$$C_{D_E} = C_{D_T} + C_{T_{V.N.}} \cos\alpha - C_{T_{EJ}} \sin\alpha - C_{D_{ram\ Ejector}} \cos\alpha$$

$$C_{M_E} = C_{M_T} - C_{T_{V.N.}} \left(\frac{C.G.W.L. - V.N.W.L.}{\bar{c}}\right) - C_{T_{EJ}} \left(\frac{C.G.F.S. - EJ.F.S.}{\bar{c}}\right)$$

3. <u>Aerodynamic-Only Coefficients</u> (Subscript Aero):
Longitudinal force and moment coefficients with all
thrust effects removed:
$C_{L_{Aero}}$, $C_{D_{Aero}}$, $C_{M_{Aero}}$. The coefficients were de-
veloped by applying corrections (for super-circulation,
VEO-Wing nozzle deflection, and canard deflections,
dreived from the General Dynamics Research model plus
differences between the AFFDL VEO-Wing fighter model
and E205 geometry) to the unpowered VEO-Wing fighter
model wing-body data of Reference 4.

A detailed set of equations for developing the
aero-only coefficients for the E205 configuration in
the STO/VTO flight regime is presented in Figure 3-6.

The predicted trimmed lift, drag and pitching moment
curves for the subsonic, transonic and supersonic flight
regimes for the full scale E205 aircraft are presented from
Reference 1 in Figures 3-12 through 3-17 ; power
effects are included where appropriate. In the subsonic
regime, the trimmed lift and drag curves differ from those
published in Reference 1 due to an error discovered in
previous calculations.

Table 3-4 presents the estimated minimum trimmed drag
component-buildup for the full scale E205 configuration from
.2 $\leq$M $\leq$2.0 with canard, VEO-Wing nozzle, and flaperons at a
zero degrees deflection. Estimated trimmed minimum drag is
plotted versus Mach number in Figure 3-7. The subsonic and
supersonic friction, form, wing camber, and interference
drag were estimated by an empirical aircraft aerodynamic
prediction method developed by General Dynamics for AFFDL
(Reference 6). The supersonic wave drag was estimated by a
modified version of the Harris area rule procedure. The
roughness + protuberance drag was estimated at 18% of the
friction plus form drag subsonically and 28% of friction
drag supersonically based on F-16 flight test experience.
This trimmed drag also includes increments for flap scrub
drag, and installed missiles and launchers for the DLI
mission (2 Low-Cost Lightweight missiles and 2 Advanced
Medium Range Air-to-Air Missiles + Launchers).

The STOL/VTOL longitudinal aerodynamics were estimated
by adding increments in lift, drag, and pitching moment to
the wing-body fighter model data of Reference 4 (Figure 3-8)
according to the equations described above and in Figure
3-6. These increments, derived from the powered research
model of Reference 2 (for canard deflection, wing trailing
edge flap and VEO-Wing nozzle deflection as well as thrust
level), were corrected, where applicable, for geometry
differences between the powered research and fighter

22

Table 3-4   E 205 MINIMUM DRAG BUILDUP

S_{ref} = 384 ft^2

DRAG COMPONENT	MACH NUMBER							
	.2	.4	.6	.8	.9	1.2	1.6	2.0
	(Drag in Counts)							
Friction	166.5	149.3	139.0	130.4	126.5	116.0	103.0	90.8
Form	17.2	15.5	14.2	13.4	13.1	-	-	-
Interference	8.2	6.9	10.9	21.0	22.2	-	-	-
Wing Camber	2.1	2.1	2.1	2.1	6.3	9.4	10.4	14.6
Roughness + Protuberance	25.9	25.9	25.9	25.9	25.9	32.5	28.8	25.4
Flap Scrub	32.7	10.9	5.5	4.4	4.4	2.2	1.1	1.1
Wave	-	-	-	-	-	292.3	289.4	281.4
Missiles + Launchers								
(2) Wing-Tip LCLM	7.7	7.7	7.7	7.9	8.7	16.1	14.3	12.2
(2) NAC-MT'D AMRRAM	7.7	7.7	7.7	7.9	8.9	13.5	11.0	7.5
Trim	0	0	0	0	0	0	8	8
Total $C_{D_{min}}$	268	226	213	213	216	482	466	441

models and the E205 configuration. Similar corrections were also made to the wing-body fighter model data to account for geometry differences with the E205 configuration. Figures 3-9 through 3-12 present the resulting predicted full scale E205 STOL/VTOL power-off and power-on lift, drag, and pitching moment curves. Figures 3-9, 3-10, and 3-11 have been lifted from Volume II to illustrate the predicted wind tunnel-model low speed (M=.2) lift, drag and pitching moment characteristics for variations in canard and wing trailing-edge flap deflection. The full scale airplane predictions (power-off) would differ from these curves only by a scale effects correction to minimum drag. Figure 3-12 illustrates the envelope of trimmed lift curves and drag polars that are obtained when the power effects are included with the un-powered data of Figures 3-9 through 3-11 (corrected to full scale airplane). Figure 3-12 demonstrates that by using the forward ejectors in conjunction with the vectored VEO-Wing nozzles, virtually any reasonable angle-of-attack range can be achieved for STO/VTOL operations. This is discussed in more detail in Volume II.

The full-scale airplane cruise/maneuver (transonic) aero data estimates presented in Figure 3-13 required an alternate approach from the STOL/VTOL data estimates. The limited existing data base prevented the development of aerodynamic estimates for variations in all of the desired parameter combinations (canard deflection, VEO-Wing nozzle deflection, flaperon deflection, C_μ, and Mach number). Out of necessity an alternate approach was sought, which led directly to representative estimates of the trimmed cruise maneuver drag polars without developing the untrimmed data as follows. Figure 3-14 schematically illustrates how a set of equivalent trimmed, optimum-span-efficiency (e) envelopes (vs C_μ and Mach number) were developed from the powered VEO-Wing nozzle only for trim with a zero-degree canard deflection, maximum negative static margin = -18% at M = .2, and c.g. = +.03c (like Configuration E205).

For a given Mach No., VEO-Wing nozzle C_μ, and with canard undeflected, the equivalent wing span efficiency is derived and plotted as a function VEO-Wing nozzle deflection, δTE, and equivalent lift coefficient in Figure 3-15. The δTE required to trim (with undeflected canard) at various angles of attack and equivalent lift coefficient is determined from the equivalent lift and pitching moment curves and allows the determination of the optimum trimmed span efficiency envelope as a function of equivalent lift coefficient.

However, since the estimated static margin for δc = 0° is more unstable than allowable for the E205 configuration (as explained in subsequent paragraphs), the flight control computer schedules the canard with Mach No. and angle of attack to achieve the desired stability level. Therefore, a

reoptimization of the canard/VEO-wing-nozzle deflections would be required at each Mach No. and blowing-momentum-coefficient combination to achieve the maximum obtainable e-envelopes. Since the existing data base was inadequate for developing these max-obtainable e-envelopes, the e-envelopes using the VEO-Wing nozzle only for trim were used in making these predictions. Although the e's are not necessarily the optimum achievable with the canard/VEO-Wing nozzle trim, they are considered representative of what can be achieved with canard/nozzle deflection combinations given enough experimental data.

The C_L at C_{Dmin} is a fallout of the way the e's are derived; these e's are used directly with the estimated minimum drags to produce the resulting cruise/maneuver equivalent trimmed drag polars shown in Figure 3-13. (The minimum-drag trim penalty was negligible based on the powered model data.) This approach does not afford the development and visibility of the untrimmed lift, drag, and pitching moment curves directly because this would require enough experimental data to determine the canard/VEO-Wing nozzle deflection schedule with angle of attack, Mach No., and C_T (or C_μ).

The estimated supersonic (M = 1.2 and 1.6) lift, drag, and pitching moment curves were developed for the E205 configuration by correcting the unpowered VEO-Wing fighter model data (zero degrees VEO-Wing nozzle deflection) of Reference 4 for changes in C_{M_O}, canard arm, and reference areas. These data are presented in Figures 3-15 and 3-17 along with the trimmed lift curves and drag polars which are developed from these data and shown in Figure 3-13.

Aerodynamic Center

As discussed in Reference 1, the aerodynamic center travel with Mach number plays a major role in the design of the VEO-Wing configurations.

Estimates of the E205 configuration aerodynamic-center travel with Mach no. have been made by use of the Carmichael Procedure (Reference 7) and the Datcom method (Reference 8). Figure 3-19 presents a General Dynamics a.c. prediction accuracy correlation for the Carmichael procedure for various configurations, including the VEO-Wing fighter model of Reference 5. The correction vs Mach no. (Figure 3-19) indicated for the VEO-Wing fighter model was applied to the Carmichael predictions for the E205 configuration (a similar configuration) to produce the corrected Carmichael estimates, shown in Figure 3-18, for a zero-degree canard deflection and with canard off. The Datcom estimate for canard at a zero-degree deflection for M = .4 is also shown

25

for reference and shows a significant disparity between the prediction methods.

It was thought to be very difficult to predict the E205 a.c. with either of these existing methods because of the unusual aspects of the configuration: the wide, flat body with separated nacelles, the relatively blunt forward strake, etc. The methods do not lend themselves to this type of configuration. The configuration is being driven hard by the predicted instability levels. This is a major aerodynamic uncertainty that must be resolved with an experimental test program. The methods above predict the a.c. in the linear attached flow (low α) regions only; as non-linear effects are experienced at high α's, the a.c.-variation prediction methods are less reliable and experimental data must be used as a guide. So many aspects of the design are dependent on these high-α stability characteristics; a wind tunnel program must be conducted to develop and tune the E205 configuration with any confidence.

The E205 configuration is longitudinally statically un-stable to achieve the VEO-Wing nozzle benefits. As noted above, the predicted instability levels are greater than can be presently tolerated. The maximum-allowable instability dictated by control system limitations is approximately 15-18% MAC. Therefore, the Flight Control System (FCS) will be used to augment the stability to the required level of frequency and damping. As part of this augmentation the flight control computer will be used to schedule the canard as a function of Mach number and angle of attack to achieve the desired level of static longitudinal stability.

Buffet Onset

The estimated buffet onset angle of attack variation with Mach no., canard deflection and wing trailing-edge flap deflection are presented in Figure 3-20; these estimates do not include the effects of thrust deflection which are as yet unknown but are expected to be favorable. These estimates were determined from analysis of the axial force data of the VEO-Wing fighter configuration force model of Reference 5 using the methods of Reference 9.

Lateral-Directional Characteristics

Figures 3-21a through 3-21e present the estimated static lateral-directional characteristics for the E205 configuration. The variation in the rigid sideslip deriva-tions, C_{Y_β} , C_{n_β}, and C_{l_β} , with angle of attack and Mach no. have been estimated using Datcom procedures. The derivatives are determined for α's from -2° to +2°. It should be noted that the wide forward fuselage fairing and

26

nacelles contribute to the uncertainties in predicting the static lateral-directional instability and the effects on sidewash. The variation of the directional characteristics is largely dependent on this unorthodox forebody loading, which is not easily predicted by standard methods. The dihedral effect, which is dependent on C_μ, will be greatly affected by the induced super-circulation lift. The lateral characteristics were also expected to be affected by the canard and canard deflections. Data in these figures has been predicted for the zero-canard-deflection case.

Directional control for configuration E205 is obtained with an all-movable vertical tail. Control effectiveness of this surface is presented in Figure 3-21d. Standard DATCOM methods for these predictions were used.

Lateral control for configuration E205 is obtained with ailerons located from immediately outboard of the VEO-Wing nozzle to approximately 85% semi-span. The predicted values of roll-control effectiveness are presented in Figure 3-21e.

The augmentation in rolling moment due to the VEO-Wing has not been included because of lack of available data. Side force and yawing moments due to aileron deflection were not predicted. The yawing moment is caused by the pressure gradient against the side of the fuselage. There was not enough experimental data available for correlation to any reliable prediction method.

3.3 Resulting Aerodynamic Uncertainties

In Reference 1, the critical aerodynamic uncertainties were identified as those aerodynamic parameters which had the greatest effect on the E205 design and performance and which could not be accurately predicted with confidence. The power-off aerodynamic uncertainties identified were the prime targets for experimental investigation in the wind tunnel tests described in Section 3.4.

Both the ejector and RALS configurations have large, wide, flat fuselage/strake areas end-plated by nacelles with the primary lifting surfaces located outboard. The aerodynamics for this type of configuration are difficult to predict with existing tools. The unpowered-aerodynamic-test data base approximates the RALS much better than the ejector configuration, but no powered data exists for this separated nacelle type configuration.

A reiteration follows of how these aerodynamic uncertainties are related to the VEO-Wing/ejector design. While the following discussion focuses primarily on the ejector configuration, E205, many of the comments apply to the in-house RALS configuration due to the similarity in external arrangements.

27

° $\underline{e}$ - The optimum e envelopes that can be obtained
with canard/VEO-Wing nozzle combinations for trim
must be confirmed since the experimental data base
does not exist to allow optimizing the canard/VEO-
Wing nozzle dfelctions (especially at transonic
speeds). The transonic maneuver performance (and
subsequent aircraft sizing) presented in this study
are predicated on the assumption that the envelope
e's developed for the more stable VEO-Wing fighter
configuration (Reference 4) with trim provided by
the VEO-Wing nozzle only (i.e., canard fixed) can be
duplicated with the canard/VEO-Wing nozzle deflec-
tions, which also provide effective augmented in-
stability levels of -18%. The effect of canard
location will be examined in this effort as well as
the influence of the strake/inner-body region on
aerodynamic center and the resulting trimmed e.

° <u>Minimum Drag</u> - Large volumes are required for inst-
allation of the vertical-lift ejector system
(ejector bays and ducting). As a result, increases
in wave drag and friction drag are incurred compared
to a conventional takeoff-and-landing (CTOL)
configuration. Minimizing the impact of increased
cross-sectional area on supersonic wave drag
requires considerable experimental configuration
tailoring. Integration of the wing/nacelle/strake
must be examined experimentally to minimize
interference drag at transonic speeds because it is
very difficult to predict the flow field and
subsequent interference drag between the fuselage
body and the nacelles.

° <u>Trim Drag</u> - Trim-drag penalty is critical for
transonic maneuvering and the supersonic dash. The
effect of canard location and schedule optimization
will be investigated, as well as the effect of a.c.
on trim drag.

° $C_{L\ max}$ - Maximum lift coefficient is critical for
transonic maneuvering, STOL, and VTOL transitions.
The usable C_{Lmax} is determined by both longitudinal
pitching moment and lateral-directional control
characteristics at high α, which are virtually
impossible to predict with the wide-bodied
configuration being studied with power effects.

° <u>Body/Wing Design for C_{mo}</u> - During maneuver at
transonic speeds, it is desirable to camber the
body/wing for a positive C_{mo} contribution to
alleviate the nose-down pitching moments induced by
the vectored over-wing nozzles. Without this Cmo

28

contribution, the (larger) positive canard deflections required to trim degrade the configuration transonic maneuver capability. Unfortunately, the E205 configuration, with jet diffuser ejectors installed in the fuselage, precludes the use of a design body camber. (This restriction does not exist for the RALS configuration, which has body camber incorporated.) One possible approach to obtain the desired positive C_{m_0} shift for the ejector configuration is to employ a fuselage beaver tail deflected upward during maneuvers.

° Aerodynamic Center Location - Power-off aerodynamic-center predictions versus Mach number were shown in for the ejector configuration (canard off and zero canard deflection). The estimates are based on the Carmichael method (Reference 7), with a comparison point against the DATCOM method (Reference 8.) at Mach 0.4 and zero canard deflection. There is a significant disparity between the predicted values for the two methods, which must be resolved during the testing.

It is very difficult to predict the aerodynamic center with either of these methods because of the unusual aspects of the configuration, the wide flat body with separated nacelles, and the relatively blunt forward strake. Also, the variation of aerodynamic center with power setting, angle of attack, and trailing-edge flap deflection is difficult to estimate with conventional methods.

° Buffet Characteristics - The close-coupled canard of the E205 configuration is expected to delay the buffet onset to higher angles of attack in much the same way as does the forebody strake on the F-16 aircraft. However, data to substantiate this favorable effect is lacking for canard/wing configurations. An additional increase in angle of attack for buffet onset should result from power-on supercirculation effects. It is desirable to obtain root-bending-moment (C_{RMS}) strain-gage data during the wind tunnel tests to verify the estimated configuration buffet characteristics.

° Lateral-Directional Characteristics - Lateral-directional characteristics determine the α_{max} and resulting usable $C_{L_{max}}$, which contributes to airplane sizing for transonic maneuvering STO, and VTOL operations. The effectiveness of the all-moving vertical tail in preserving lateral-directional control at high angles of attack when influenced by

29

the large flat body and strake of the E205 (or RALS)
configurations is difficult to estimate.

3.4 Description of Wind Tunnel Models

The 0.0939 scale wind tunnel model representing the
E205 aircraft configuration is defined in Figures 3-22 and
3-23, and was constructed by General Dynamics and tested at AMES
Research Center. The overall dimensions of the model are
illustrated in the three view drawing in Figure 3-22 and
Table 3-5 while the cross-sectional area distribution of the
model is shown in Figure 3-24; note that the model
cross-sectional area distribution differs somewhat from that
of the airplane (Figure 3-2). The model scale was dictated
by the Ames requirement that the model be sized to match the
airplane engine maximum inlet airflow with that of the
XM2R/CMAPS engine simulator being developed for future Ames
investigations into propulsion/airframe interactions. The
model is defined in detail in Reference 2.

A second wind tunnel model was constructed to investi-
gate some aspects of the RALS R104 configuration. The three
view drawing of the RALS model is shown in Figure 3-25
while the cross sectional area distribution and photographs
of the model are shown in Figures 3-26 and 3-27. This model
was constructed by building a new center fuselage section
(simulating the RALS fuselage lines aft of the canopy/nose
area); (the transition in lines from the E205 nose and
canopy to the RALS fuselage lines resulted in an
aerodynamically unfavorable concave depression which may be
faired-out in future investigations). The E205 model wings,
canards, vertical tail, nacelles, nose and canopy were used
on the RALS model; the major changes are a narrower fuselage
resulting in more closely spaced nacelles and a thicker
strake, and a deeper, narrower vertical channel between the
nacelles and fuselage sides. Fairings on the E205 nacelles
were removed to more closely simulate the nacelle shape of
th RALS configuration. The use of the wing panels outboard
of the nacelles on the R104 configuration resulted in a
theoretical wing area of 357 ft^2 instead of the 300 ft^2 of
the R104 aircraft.

Both the E205 and R104 model configurations have
several very useful geometric variables which allow tailor-
ing the aerodynamic performance of the configurations and
provide real insight into the mechanisms of the uncer-
tainties described above. Table 3-6 lists these geometric
variables and the ranges of associated deflections or
locations for each. Both models allowed three longitudinal
canard locations (baseline (C_1), forward (C_2), and aft (C_3)
Figure 3-28a); the canards have leading and trailing-edge

30

Table 3-5
SUMMARY OF CONSTANTS

PARAMETER	E-205	R-104
Fuselage Base Area, A_b ----------------------	9.5991 in^2	9.2941 in^2
Nacelle Exit Area, A_e(per side)-------------	4.8982 in^2	4.8982 in^2
Nacelle Inlet Area, A_i(per side)-------------	6.1685 in^2	6.1685 in^2
Nacelle Plug Base Area, A_p(per side)---------	3.2484 in^2	3.2484 in^2
Wing Reference Area, S ---------------------	3.3858 ft^2	3.1541 ft^2
Wing Reference Span, b ---------------------	42.010 in	40.270 in
Wing Reference Mean Aerodynamic Chord, $\bar{c}$ ----	13.398 in	12.973 in
Longitudinal Transfer Distance, X ----------	1.002 in	1.479 in
Lateral Transfer Distance, Y ---------------	0.000 in	0.000 in
Vertical Transfer Distance, Z ---------------	0.700 in	0.419 in
Moment Reference Center @ FS ----------------	29.002	29.463
WL ----------------	13.050	13.050
BL ----------------	0.000	0.000
Balance Incidence Angle, i_m ----------------- (positive incidence airplane nose-up)	0°00'	2°00'

TABLE 3-6
AVAILABLE COMPONENT DEFLECTIONS

Component	Deflection
Wing Outboard Trailing-Edge Flap	$0°00'$
	$10°13'$
	$20°24'$
	$25°29'$
Wing Leading-Edge Flap	$0°$
	$15°$
	$30°$
Wing Inboard Trailing-Edge Flap	$0°$
	$10°$
	$20°$
	$25°$
Canard Leading-Edge Flap	$0°$
	$15°$
Canard Trailing-Edge Flap	$0°$
	$20°$
All Moveable Horizontal Canard	$0°$
	$\pm10°$
	$\pm20°$
All Moveable Vertical Tail	$0°$
	$5°$
	$15°$

32

flaps (inboard and outboard segments); the vertical tail is all moving to several deflections. The E205 model has three strake variations (baseline S_1) mid sweep (S_2) and, low sweep (S_3), as shown in Figure 3-28b.

Both models are sting mounted through the base of the fuselage with forces and moments measured with a 2.5in. Task MK-XXA six component strain gage balance. The moment reference center for both models was located longitudinally at 3-percent of the mean aerodynamic chord which represents fuselage station 29.002 on the E205 model and fuselage station 29.463 on the R104 model along waterline 13.050. The model angle of attack is referenced to the wing reference chord plane which is along a waterline. Fuselage-sting cavity pressure from three static orifices (two located immediately aft of the balance and one located 0.5 inches forward of the fuselage base) and nacelle nozzle exit plug base pressure from static orifices located in each nozzle plug base were measured concurrently with the force data. Nacelle nozzle exit static and total pressures were recorded during internal drag runs. Two pressure rakes, each containing 20 total pressure orifices were calibrated prior to the wind tunnel tests against known mass flows measured by ASME nozzles; these rakes were used to gather the total pressure data for the internal drag calculations while the static pressures were obtained from the manifolded orifices located in the nozzle exit plug walls. Fluctuating wing bending moments are measured as a buffet indicator (RMS value) using Kulite diffused semiconductor four-arm strain gage sensor, type 5B-3-350-300-4, locatged at 40% chord and span station 9.600 on the E205 and 8.73 on the R104 models.

3.5 Wind Tunnel Test Programs

The wind tunnel models described in the previous section were tested once in each of the following NASA Ames Research Center wind tunnels: the 12-foot pressure tunnel, the 11x11 foot transonic tunnel, and the 9x7 foot supersonic tunnel. These are single return tunnels with controls that allow independent variation of Mach number, density, temperature and humidity. Tests were conducted at Mach numbers ranging from .2 to 2.0 at a constant Reynolds number of 9.84 x 10^6/M (3.0 x 10^6/ft). To evaluate Reynolds number effects, selected configurations were tested at additional Reynolds numbers for several Mach numbers. The angle of attack range was -5° to 90° in the 12-foot, -5° to 27° (maximum allowable loading) in the 11x11 foot, and -5 to 15° in the 9x7 foot tunnel. The angle of sideslip ranged from -4 to +8°.

33

The measured angles of attack and sideslip were corrected for wind-tunnel-flow misalignment and for balance and sting deflections caused by aerodynamic loads.

The measured axial forces have been adjusted to a condition corresponding to that of having free-stream static pressure acting on the fuselage cavity and on the base areas of the two nacelle choke plugs. The data in this report has also been adjusted for internal forces acting in the flow-through nacelles using the internal and normal forces derived from the series of runs employing the duct exits rakes in each nacelle.

To assure a turbulent boundary layer, transition grit strips were placed near the leading-edges of the wing, canard and vertical tail, around the fuselage nose and around the nacelle leading-edges.

4.0 CONCLUSIONS AND RECOMMENDATIONS

The initial objectives of this research effort have
been accomplished. The capabilities of current prediction
methodologies to evaluate configurations of the VEO-Wing-
VSTOL generic family have been evaluated, the effects of
geometry variations have been examined, and two versions of
this generic family, the E205 and R104 configurations, have
been aerodynamically evaluated and compared. As a result of
these evaluations and analysis additional research is
recommended.

CAPABILITIES OF PREDICTION METHODS

Because of the unusual geometry involved with the E205
and R104 configurations there was substantial concern that
current prediction methods would not do an adequate job on
predicting many of the areas of "aerodynamic uncertainty"
for the E205 configuration.

In summary, the minimum drag is predicted reasonably
well in the subsonic and transonic speed regimes with
existing methods; there are some substantial problems with
the predictions supersonically where the actual drag is
substantially higher than predicted. Part of this discrep-
ancy many be due to a failure to accurately predict the
model sting interference effects and the excess interference
suspected due to the model components.

The aerodynamic center variation with Mach number was
reasonably well predicted for the E205 configuration with
the Carmichael Woodward procedure. However, a failure to
consult the Carmichael Woodward results regarding the ef-
fective camber of the configuration resulted in the error in
predicting C_{m_0} which in turn resulted in larger trim penal-
ties than anticipated as some speeds.

In fact, the agreement between the predicted and test
untrimmed lift, drag, and pitching moment curves is rather
good (except for the error in C_{m_0}) with the canard and flap
undeflected at most speeds. The canard is a little more
effective than predicted because of the higher upwash than
expected caused by the E205 wing-body. The wing trailing-
edge flaps were also found to be slightly more effective
than predicted ; the flap effectiveness was also found to
vary with canard deflection which was not accounted for in
the original predictions. However, the flap effectiveness
was predicted by ratioing data from a similar configuration
using appropriate parameters. This continues to be a
basically reliable method of predicting the flap effects.

Trimming at low speeds was accomplished using combinations of wing trailing-edge flaps and deflected thrust from the VEO-Wing nozzles balanced by the modulated thrust from the forward ejectors. The canard was not used for trim but could be deflected for maneuvering from trim (gust response, etc.). Transonically and supersonically, leaving the canard undeflected and varying the wing trailing-edge flap deflection yielded trimmed drag polars that were almost as good as with an optimum combination of canard and flap indicating that it may be possible to justify fixing the canard and using only a canard trailing-edge flap for aiding maneuvering from trim. The trimmed wind tunnel data corrected to full scale and including the power effects (super-circulation and deflected thrust) of Reference 1 were compared with the predicted power-on trimmed full scale aircraft characteristics of Reference 1 on which the E205 performance was evaluated. In general the test results indicate better characteristics than predicted except for C_{m_0} at some transonic and supersonic speeds, which can largely be traced back to a failure to accurately predict C_{m_0}, resulting in substantial trim penalties. The polar shapes are, for the most part, better than predicted indicated that the maneuvering cruise, and dash performance which played a substantial role in sizing the aircraft to the ground rules described in Section 2.0 can be achieved, especially if some redesign to provide a more acceptable C_{m_0} variation is employed.

The buffet-onset angle of attack variation with Mach number developed from the test data (using the RMS value of the wing-root bending-moment strain gage output) indicates that the E205 buffet characteristics are better than predicted but do agree in trend with the predictions.

The Datcom prediction techniques for the lateral-directional characteristics appear to adequately account for the configuration effects except for sidewash generated at angles of attack. Most prediction techniques are only concerned with the linear range of the parameters involved. The sidewash determined from these tests indicates a need to examine the configuration to at least determine what components effect the sidewash using a procedure such as Carmichael Woodward since Datcom does not adequately handle the sidewash prediction at angle of attack.

EFFECTS OF GEOMETRY VARIATIONS

A matrix of combinations of canard longitudinal location and strake shape were investigated for the E205 configuration. This investigation indicated that there are major "first order" effects for varying either canard location or strake shape, but the influence of the strake shape on the canard effectiveness or the canard location

36

on the changes produced by varying strake shape are "second order" for this type of configuration; i.e., in the preliminary design stage the effects of canard location and strake shape must be considered, but the mutual interference of the canard and strake is not that important to the type of nacelle-strake-canard arrangement exhibited on E205.

Canard location produced the expected changes with the most dramatic change being the substantial variation in a.c. caused largely by changes in the canard/wing interaction. Also of major importance is the change in effective configuration camber produced by changing canard location resulting in C and subsequent trim variations. The mid-canard location of the baseline E205 configuration offered the best overall trimmed characteristics across the Mach range as well as the best lateral-directional characteristics.

Variations in strake shape were found to be a very effective means of tailoring the pitching moment curve at high angles of attack to avoid pitch-up. Strake effects become more pronounced with increasing angles of attack and Mach number. The S1 C1 combination offers the best overall pitch-trimmed characteristics over the Mach range tested. At low speeds, the S1 C1 combination also exhibits the best overall lateral-directional characteristics; at transonic and supersonic Mach numbers, the limited amount of data precluded determining the best canard/strake combination for lateral-directional characteristics.

COMPARISON OF E205 AND R104 CHARACTERISTICS

The configuration body-nacelle-strake arrangement does influence the performance of the canard and wing. Comparison of the E205 and R104 wind tunnel model results indicate that the wide, flat strake arrangement of the E205 configuration acts as an effective lifting surface inducing a substantial upwash on the canard and wing. This results in the E205 wing and canard each performing better (alone and in the presence of each other) on the E205 configuration than with the narrow strake arrangement on the R104 configuration.

The untrimmed minimum drag of the E205 and R104 configurations is about the same subsonically; the R104 transonic drag rise is much more severe, followed by substantially higher supersonic drag. This increased drag of the R104 is due to its larger maximum cross-sectional area, the higher interference drag due to the

37

narrow channel between the nacelle and fuselage, and the adverse effects of the concavity formed by using the E205 nose and canopy with the R104 fuselage.

The aerodynamic center variation with Mach number for the two configurations are similar. The addition of the canard makes approximately the same a.c. shift for both vehicles.

The flap effectiveness for the two configurations is almost identical.

Comparisons between the E205 and R104 wind tunnel model (unpowered) trimmed polars indicate that at transonic Mach numbers the E205 has a better trimmed drag polar than the R104 for C_L's > .35, so for combat maneuvering the E205 looks superior; the R104 appears slightly superior for transonic cruise at low C_L's. At M = 1.2 the E205 is superior at all C_L's primarily because of the lower minimum drag. Although the untrimmed minimum drag of the R104 is higher than that of the E205 at all supersonic Mach numbers, the trimmed minimum drag however is less for the R104 at Mach numbers < 2.0 primarily because of differences in C_{m_O} of the two configurations.

The lateral-directional characteristics of the two configurations are very similar except at M = 1.2 where there is apparently a more favorable flow at the vertical tail for the R104 than the E205.

The major deficiency of both the E205 and R104 configurations appears to be the inability to trim to angles of attack higher than 6 to 8 degrees at low speeds with either the canard or wing trailing-edge flap with the power off. The large configuration instabilities at low speed require large negative canard deflections to trim with the power off; $\delta_c = -20°$ was the largest negative deflection tested and this was not adequate to trim over a reasonable α - range. The canard appears stalled at a canard-local angle of attack of near -20° (in the presence of the wing), so that the resulting trim limit appears to be about 8° model angle of attack. Part of the problem is, of course, the fact that the wing itself is stalling at about $\alpha = 8°$ because it has been provided no leading-edge protection, the leading-edge flaps not being employed due to a lack of test time.

The airplanes could be said to be balanced at the wrong point but movement of the c.g. forward would result in deteriorating canard control power even more. Several areas of additional research are suggested below to investigate the "real" aerodynamic characteristics of the configuration if the wing is working properly and to solve the problem of limited trimmed α- range at low speeds.

1. Test the existing E205 wind tunnel model at low speeds to develop an acceptable trimmed α- range by varying the wing leading flaps across the wing span in combination with the canard at various deflections (deflecting the canard to negative deflections $\delta_c < -20°$) plus varying the strake shape. The objective of this testing would be to allow the wing to work effectively to higher α's; of course, as the pitch-trim limit is raised, the next operational constraint is the α - limit due to deteriorating lateral-directional control ($\alpha \cong 16°$). Hopefully, aiding the wing performance and working on the strake shape will have positive effects on increasing the lateral-directional α- limits. With the configuration working better at low speeds, higher Mach number improvements can be investigated. Also, the effects of the canard location movements and trimmed characteristics should be rechecked from the current tests to see if the magnitudes have substantially changed (trends are expected to be the same but magnitudes will probably substantially change, e.g., "wing-alone" performance or "canard-alone").

2. Remove the canard and develop E205 wing-body characteristics that are acceptable to higher α's at low speed in the same manner described in the preceding paragraph recalling that the strake shape as well as the wing leading-edge flaps are effective means of modifying pitching moment characteristics and avoiding pitch up. When this is accomplished, mount the canards on the top of the vertical tail to be used as horizontal tails and test to develop the trimmed characteristics across the Mach number range using combinations of horizontal tail and wing leading and trailing-edge flaps. Estimates show that the existing canards are an acceptable size and planform for use as horizontal tails on this configuration.

39

3. Based on the results of the data analysis presented in this report, a change in canard and wing planform is suggested for the E205 configuration which should alleviate the problem of low speed, power-off limited trimmed α-range.

General Dynamics has had considerable experience with wind tunnel testing delta planform configurations - with and without horizontal canards. A recent example was the Convair Division's lift-plus-lift-cruise V/STOL program. In general, optimum low-speed and transonic maneuvering performance was obtained with this configuration balanced sufficiently unstable, canard-on, so that trailing-edge-down elevon deflection was required for trim. Pitch recovery control power at high angles of attack was obtained by unloading the canard (high authority actuators are required). Pure tailless configurations do not possess sufficient nose-down control authority through the trailing-edge surfaces to permit maneuvering flight at negative static margins much greater than 1-2%. For modest canard-wing area and span ratios, the size of the canard only determines the center-of-gravity position at which the configuration should be balanced.

Based on this Convair experience, the modifications to the wind tunnel model indicated in Figure 4-1 are recommended as a potential direction toward effecting improvements in Configuration E-205 balance. Specifically, the wing has been enlarged and moved aft, in order to position the wing-body a.c. slightly behind the 3% reference point. The planform selected is based upon previous wind tunnel experience, and is expected to give linear pitching moment characteristics at operational angles of attack. (Some wing leading-edge treatment may be required at extremely high maneuvering angles of attack). At the same time, the canard has been decreased in size and moved forward to the forward pivot location (MS 21.036). Summary geometric data are noted on the figure.

Aerodynamic predictions have been made, utilizing readily available wing-body and canard surface methods, in conjunction with wind-tunnel extracted canard flow fields (E205 data). These data are inset on Figure 4-1. The wind-tunnel C_{m_0} has been included, although a portion of further configuration development efforts would be directed

toward the elimination of this phenomenon. Note that a
nominal static margin of - 8.5% is indicated (M = 0.2),
and that the configuration is significantly more controllable
in the normal range of lift coefficients.

Construction and testing of the new canard and wing
planform arrangement is strongly suggested because (1)
it can be accomplished with minimal cost utilizing the
existing E205 model hardware (only a new canard, canard
deflection bracket, and wing panel outboard of the nacelle
are required) and (2) it would allow the confirmation of
the expected solution to the low speed trim problem.

5.0 REFERENCES

1. Lummus, J. R., <u>Study of Aerodynamic Technology for a VSTOL Fighter/Attack Aircraft</u>, NASA CR-152128, May, 1978.

2. Walker, J. J., <u>Model and Test Information Report, .0939-scale VSTOL Fighter/Attack Aircraft Wind Tunnel Force Model</u>, General Dynamics Rept FZT-344, Dec., 1978.

3. <u>Advanced VSTOL Fighter Attack Aircraft Preconcept Formulation Study</u>, General Dynamics Fort Worth Division Report NAV-GD-006, March, 1978.

4. Woodrey, R. W., et al., <u>An Experimental Investigation of a Vectored-Engine-Over-Wing Powered Lift Concept</u>, AFFDL-TR-76-92, Volumes I and II, September, 1976.

5. Heim, E. R., <u>Basic Aerodynamic Data for a Vectored-Engine-Over-Wing Configuration</u>, AEDC-TR-78-1, February 1978.

6. Schemensky, R. T., <u>Development of an Empirically Based Computer program to Predict the Aerodynamic Characteristics of Aircraft</u>, AFFDL-TR-73-144, Vols. 1 and 2, November, 1973.

7. Carmichael, R. L., Costellano, C. R., and Chen, F. C., "The Use of Finite Element Methods for Predicting the Aerodynamics of Wing-Body Combinations," <u>Analytical Methods in Aircraft Aerodynamics</u>, NASA SP-228, October, 1969.

8. Hoak, D. E., <u>USAF Stability and Control DATCOM</u>, October, 1960.

9. Ray, Edward J., <u>Techniques for Determining Buffet Onset</u>, NASA TMS 2103, November, 1970.
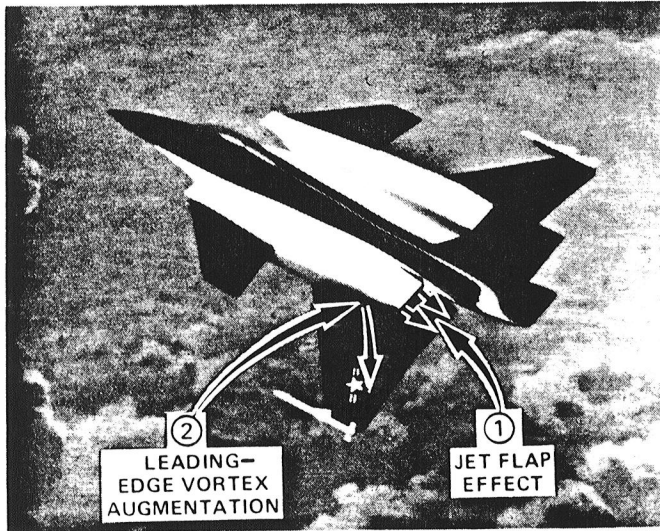
● HIGH LIFT COEFFICIENTS (Low Approach Speeds)
AT TAKE-OFF/LANDING CONDITIONS
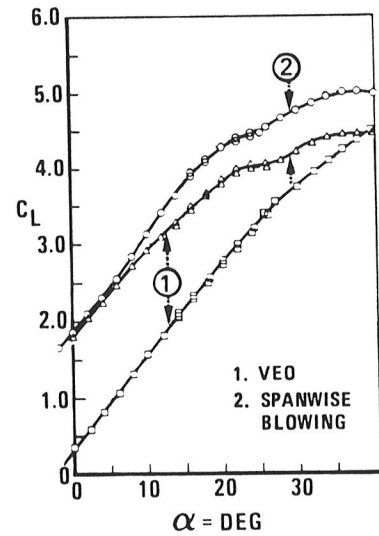
● FULL ANGLE OF ATTACK POLAR IMPROVEMENT
AT TRANSONIC SPEEDS

● COMBINES SUPERCIRCULATION
FROM OVER-WING-MOUNTED
ENGINES WITH LEADING-EDGE
VORTEX AUGMENTATION

● UTILIZES FULL ENGINE
MOMENTUM (No Bleed)
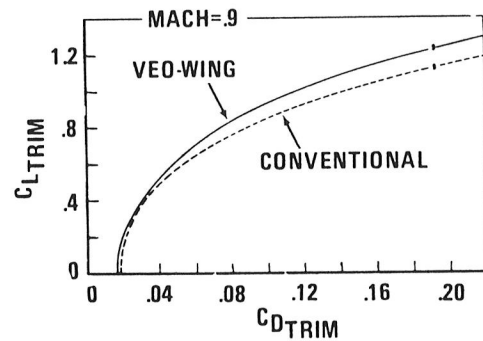
Figure 2-1   VEO-Wing Powered Lift Concept
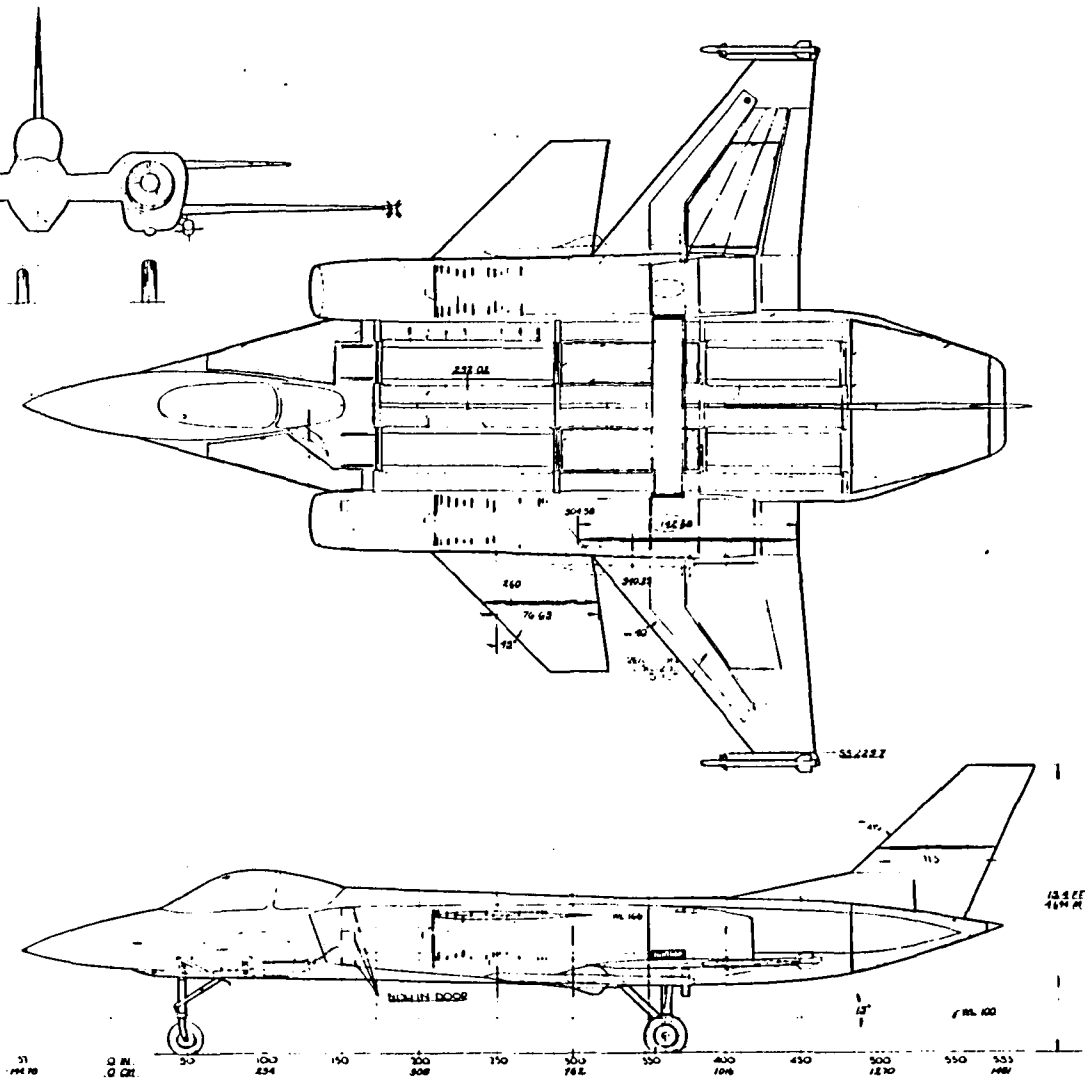
PRELIMINARY DESIGN DRAWING
LINES STUDY
V/STOL B
CONFIG E 205
GENERAL DYNAMICS
Fort Worth Division
FW780G013

Figure 2-2   E205 Three-View Drawing

Figure 2-3   R104 Three-View Drawing

45
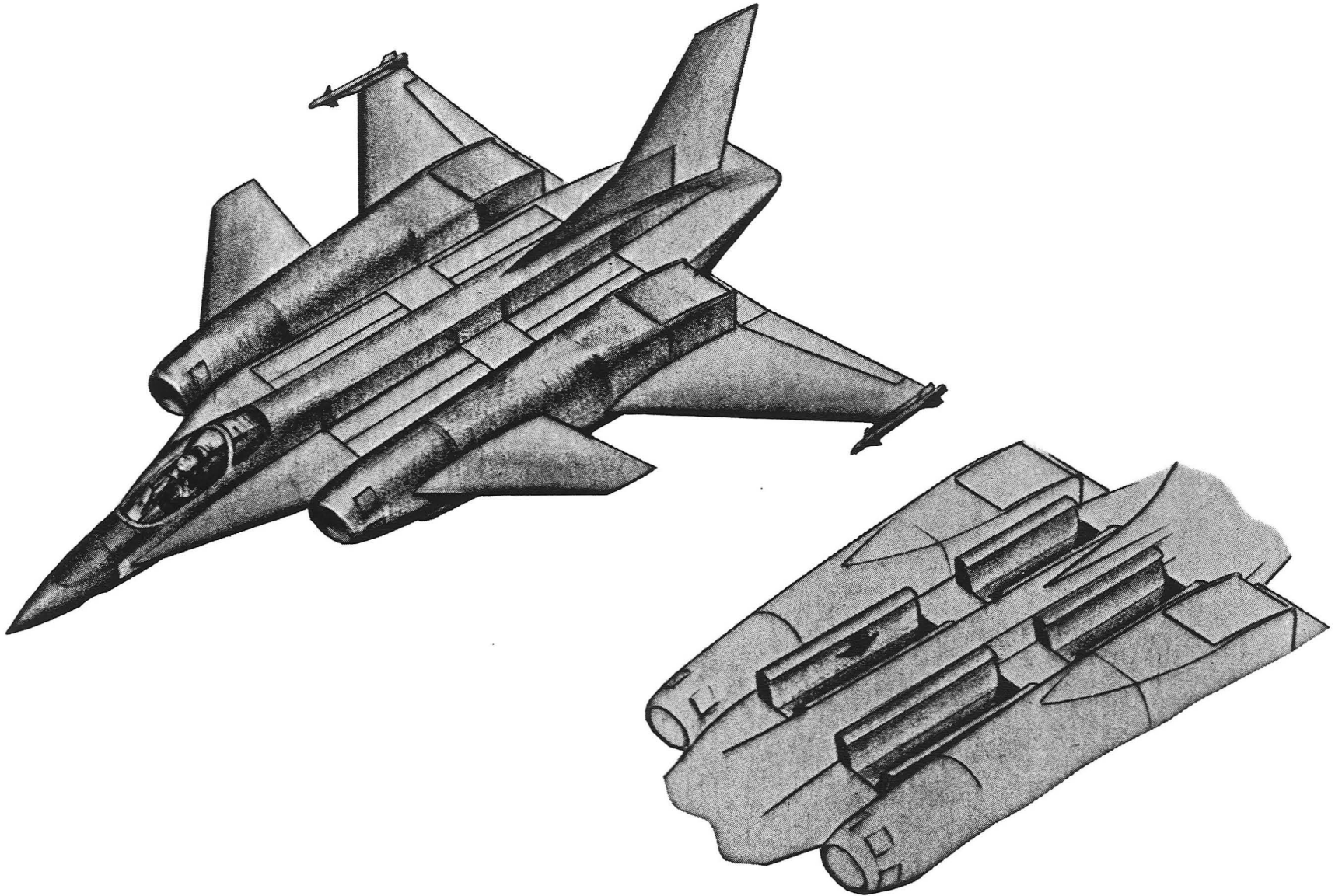
Figure 2-4 Ejector Configuration in Cruise Mode

46
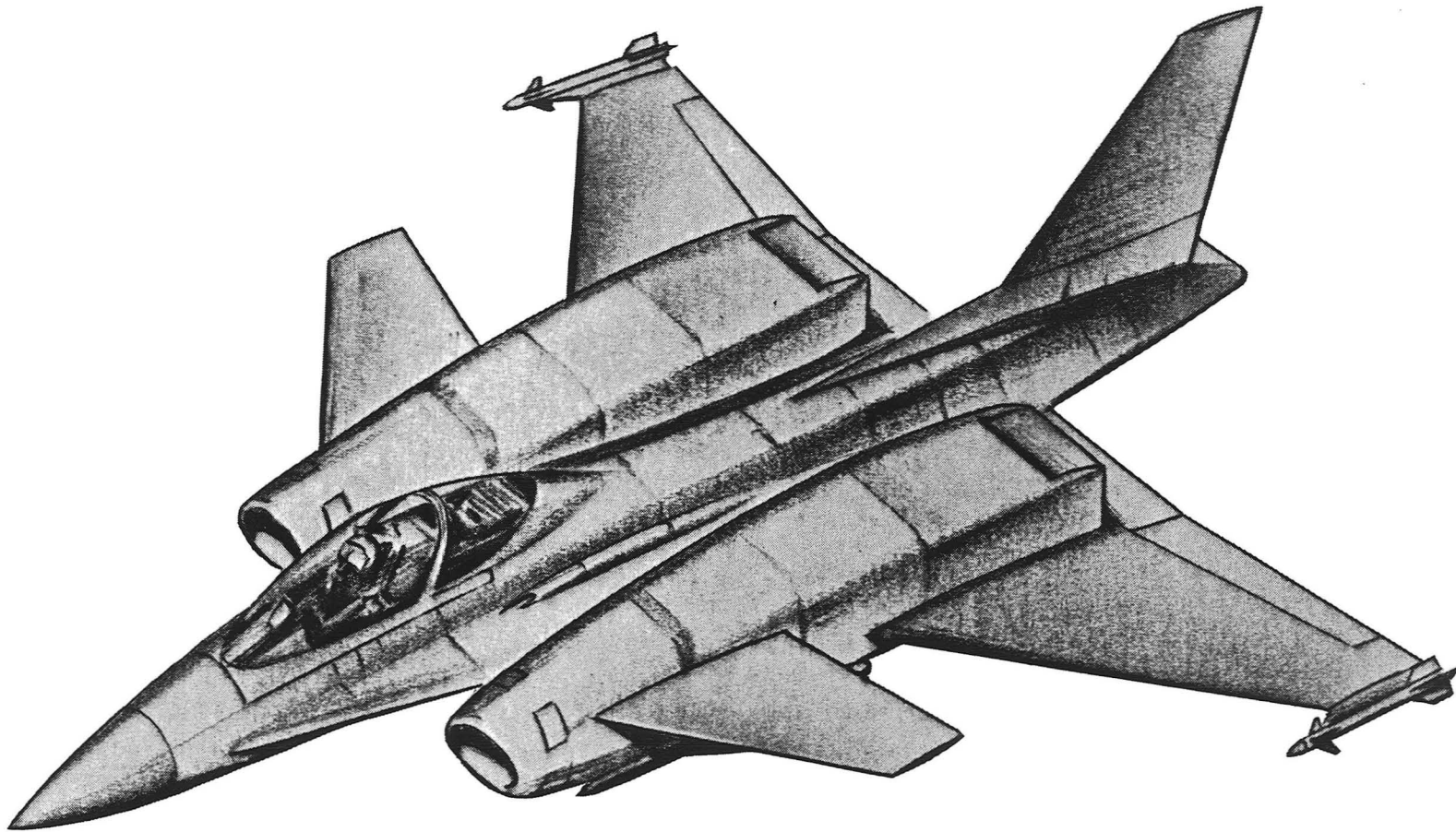
Figure 2-5 Artist Concept of RALS R104 Configuration

MISSION DEFINITION
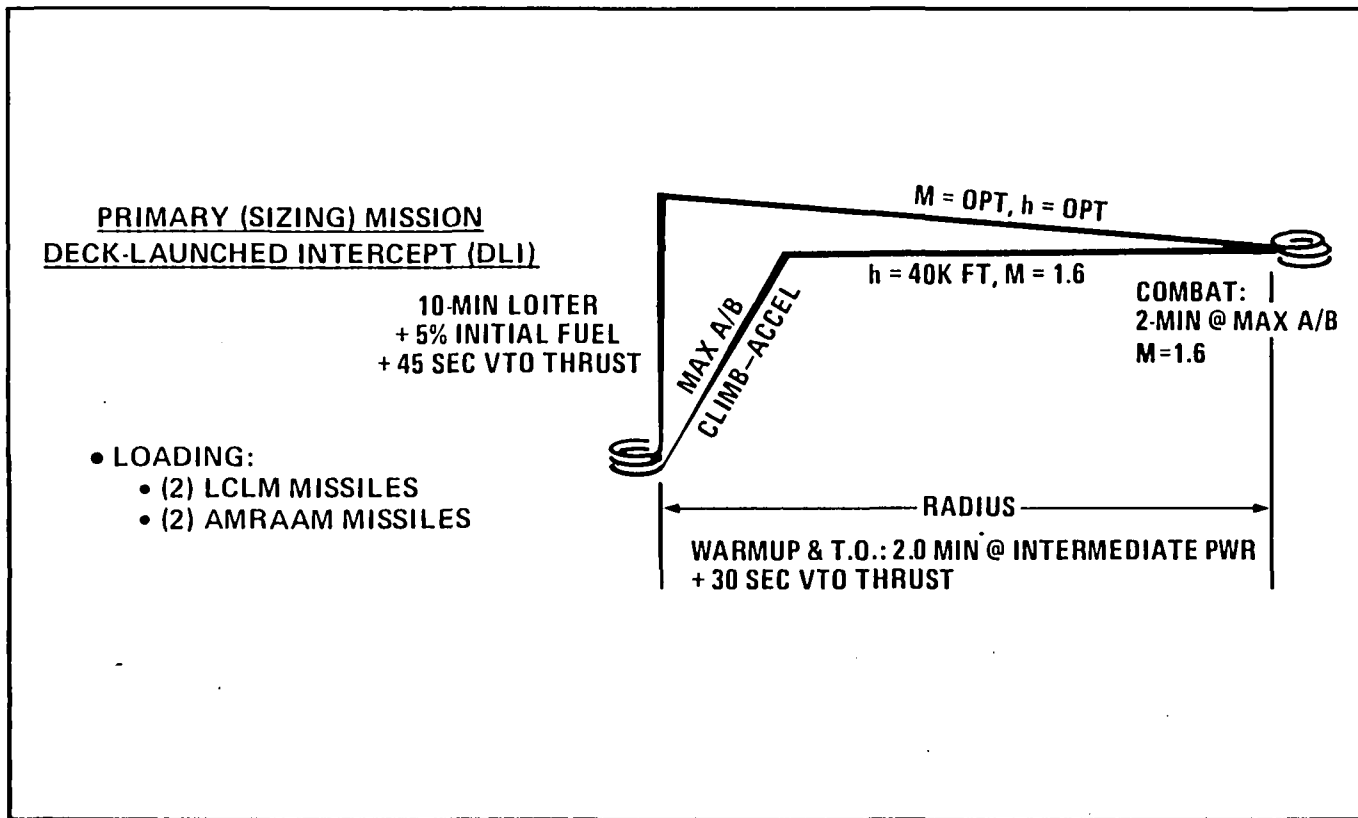
Figure 3-1   DLI Mission Profile
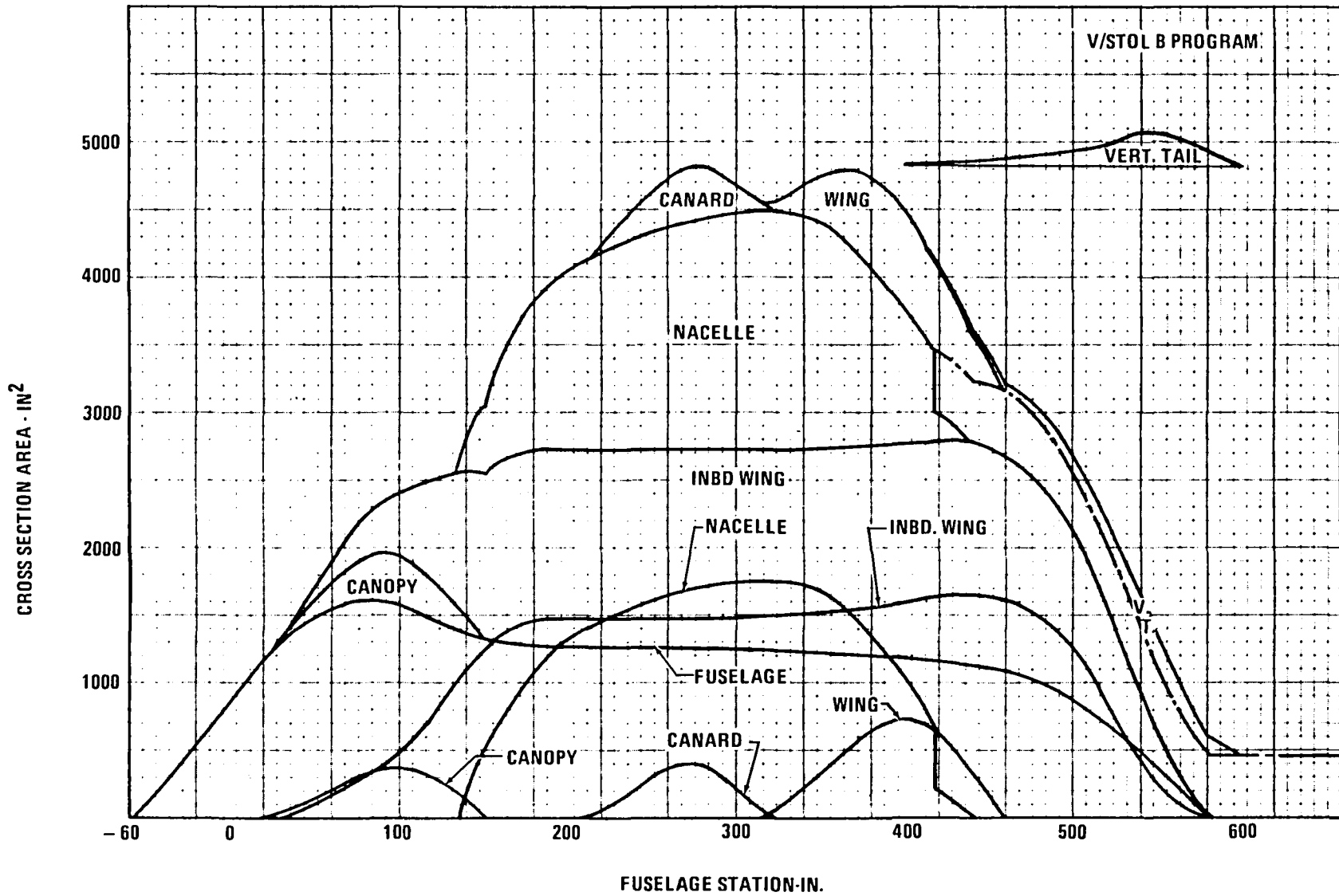
Figure 3-2   E205 Cross-Sectional Area Distribution
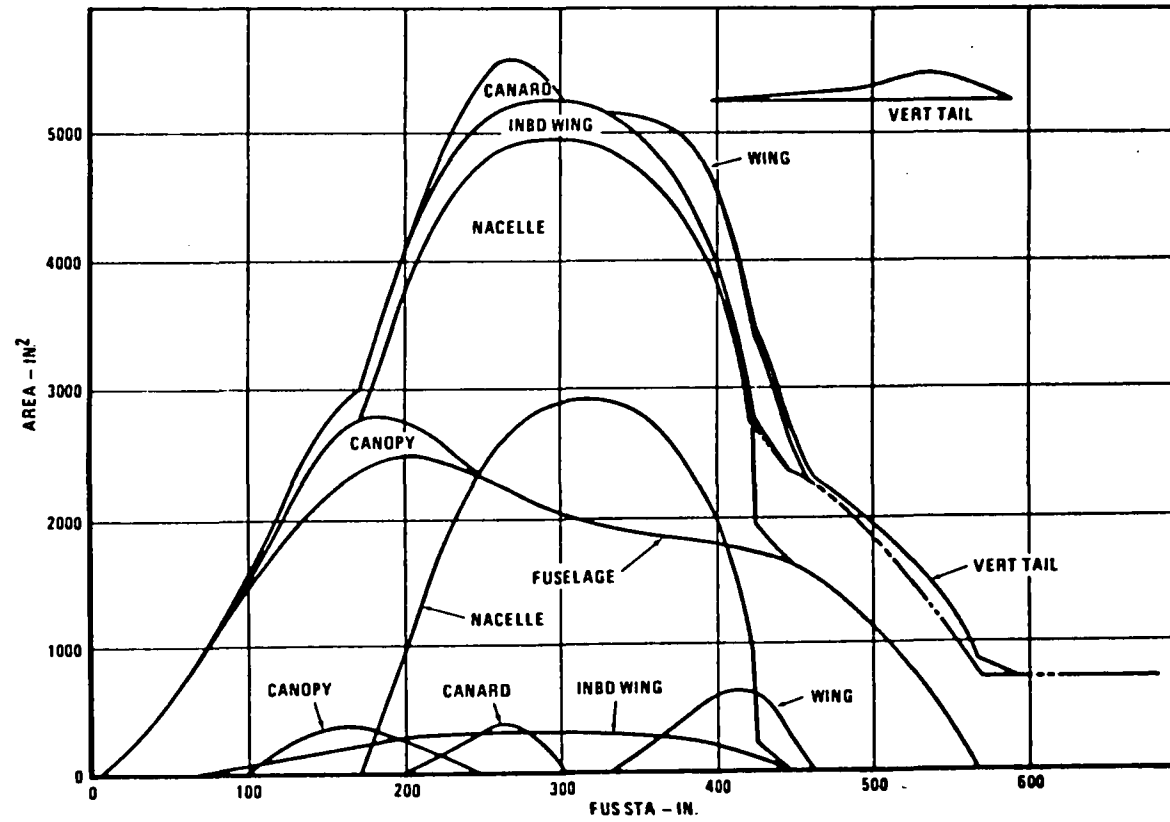
Figure 3-3 Cross-Sectional Area Distribution, R104

GD/NASA/AFFDL RESEARCH MODEL
(Ref. 4)

AFFDL VEO FIGHTER MODEL AEDC TEST
(Ref. 5)
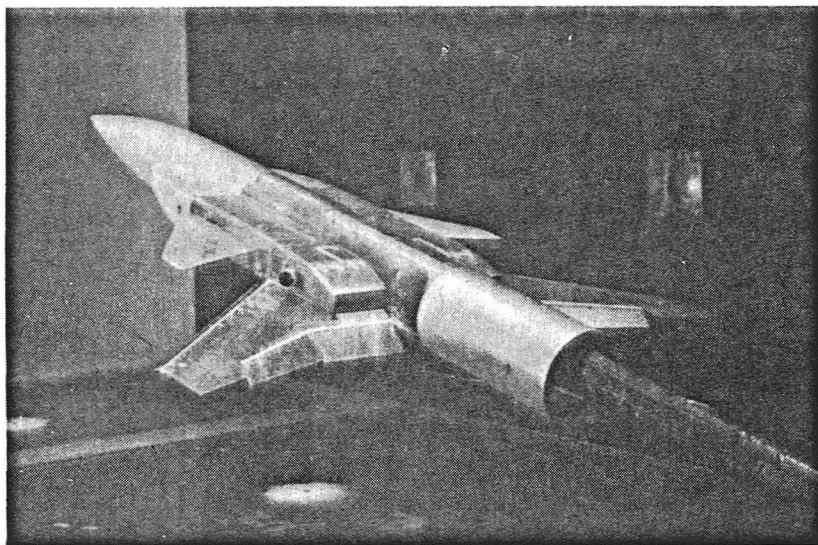
- **POWERED MODEL**
    Tested Subsonic to Supersonic
    α's to 40° Subsonic
- **PROVIDES**—Power Effects
    —Canard Effects
    (Subsonic)
    —Transonic e's
FOR THIS STUDY
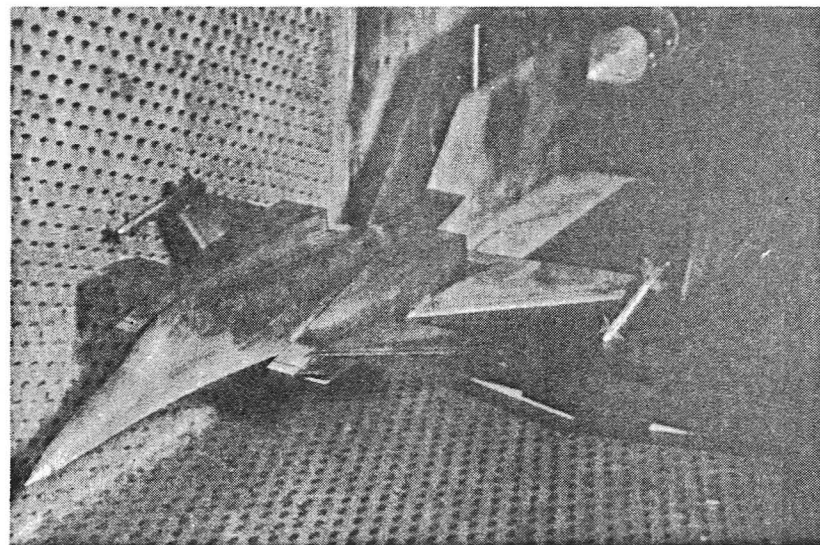
- **UNPOWERED FLOW THROUGH MODEL**

- **PROVIDES**—Power Off Baseline for
    VSTOL Aero Buildup
    —Supersonic Trimmed Polar
    Shapes
FOR THIS STUDY

Figure 3-4   VEO-Wing Experimental Data Base
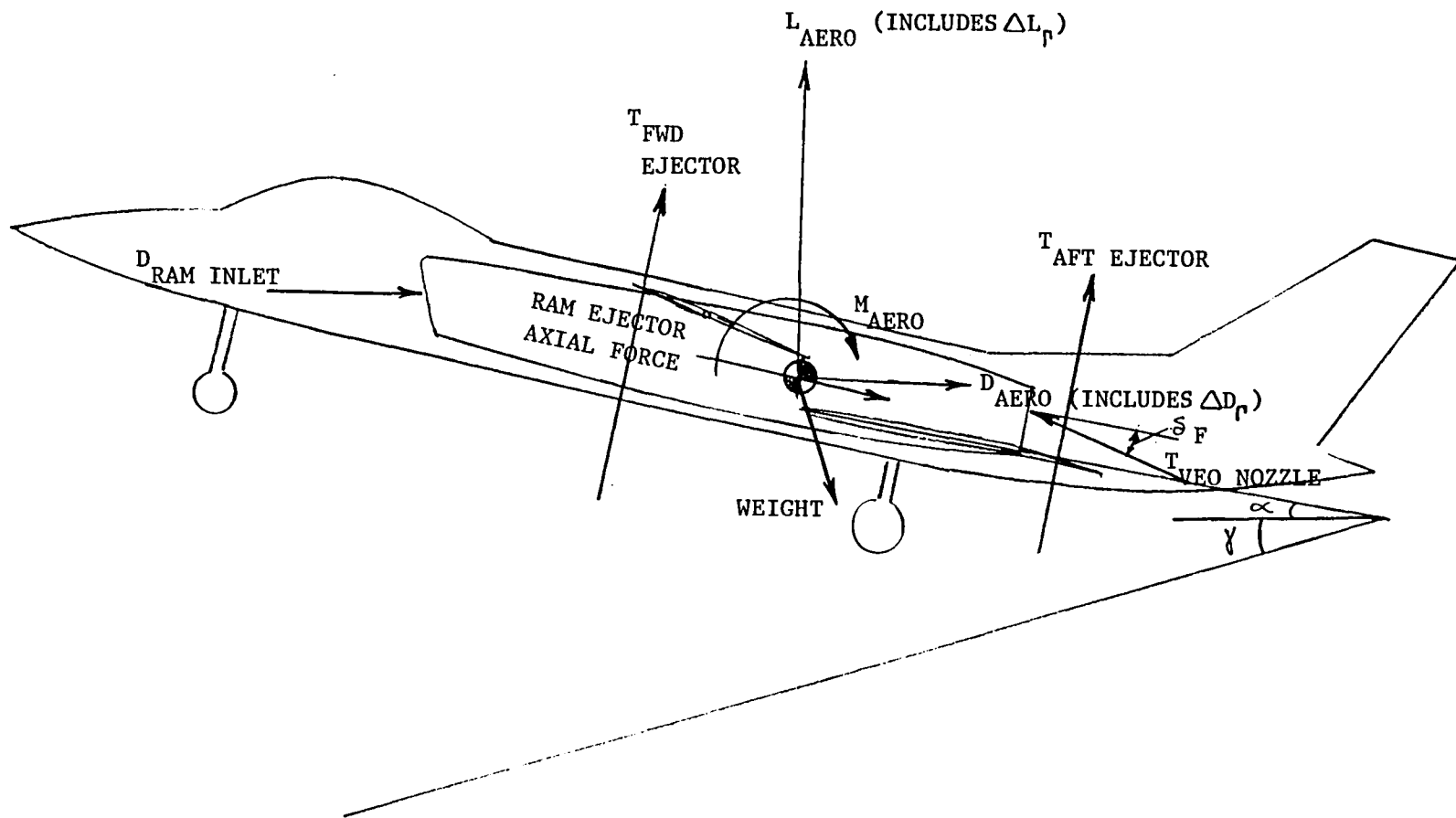
Figure 3-5   Longitudinal Forces Acting on E205

AERO-ONLY COEFFICIENTS BUILDUP

$$C_{L_{AERO}} = C_{L_{WB_{TEST}}} \cdot \frac{S_{W_{E205}}}{S_{W_{TEST}}} \cdot \frac{S_{REF_{TEST}}}{S_{REF_{E205}}} + \Delta C_{L_{CHANGE}} \frac{S_{REF_{TEST}}}{S_{REF_{E205}}} + \Delta C_{L_{CANARD}} \frac{S_{C_{E205}}}{S_{C_{TEST}}} \frac{S_{REF_{TEST}}}{S_{REF_{E205}}} + \Delta C_{L_{FLAP}} \cdot \frac{S_{W_{E205}}}{S_{W_{TEST}}} \cdot \frac{S_{REF_{TEST}}}{S_{REF_{E205}}}$$

$$C_{D_{AERO}} = C_{D_{WB_{TEST}}} \cdot \frac{S_{W_{E205}}}{S_{W_{TEST}}} \cdot \frac{S_{REF_{TEST}}}{S_{REF_{E205}}} + \Delta C_{D_{CHANGE}} \frac{S_{REF_{TEST}}}{S_{REF_{E205}}} + \Delta C_{D_{CANARD}} \frac{S_{C_{E205}}}{S_{C_{TEST}}} \frac{S_{REF_{TEST}}}{S_{REF_{E250}}} + \Delta C_{D_{FLAP}} \frac{S_{W_{E205}}}{S_{W_{TEST}}} \frac{S_{REF_{TEST}}}{S_{REF_{E205}}}$$

$$C_{M_{AERO}} = C_{M_{WB_{TEST}}} \cdot \frac{S_{W_{E205}}}{S_{W_{TEST}}} \cdot \frac{S_{REF_{TEST}} \cdot \bar{c}_{TEST}}{S_{REF_{E205}} \cdot \bar{c}_{E205}} + \Delta C_{M_{CHANGE}} \cdot \frac{S_{REF_{TEST}} \cdot \bar{c}_{TEST}}{S_{REF_{E205}} \cdot \bar{c}_{E205}} + \Delta C_{M_{CANARD}} \frac{S_{C_{E205}}}{S_{C_{TEST}}} \cdot \frac{S_{REF_{TEST}} \cdot \bar{c}_{TEST}}{S_{REF_{E205}} \cdot \bar{c}_{E205}}$$

$$+ \Delta C_{L_{CANARD_{E205}}} \frac{x_{C_{TEST}} - x_{C_{E205}}}{\bar{c}_{REF_{TEST}}} \frac{\bar{c}_{REF_{TEST}}}{\bar{c}_{REF_{E205}}} + \Delta C_{L_{FLAP}} \cdot \frac{x_{CP}}{\bar{c}_{TEST}} \cdot \frac{\bar{c}_{REF_{TEST}}}{\bar{c}_{REF_{E205}}} + C_{L_{AERO}} \cdot \left(c_{g_{E205}} - \text{moment ref.}_{TEST} \right)$$

Figure 3-6   Equations for Building Up Aero-Only Coefficients
for E205 Airplane Configuration
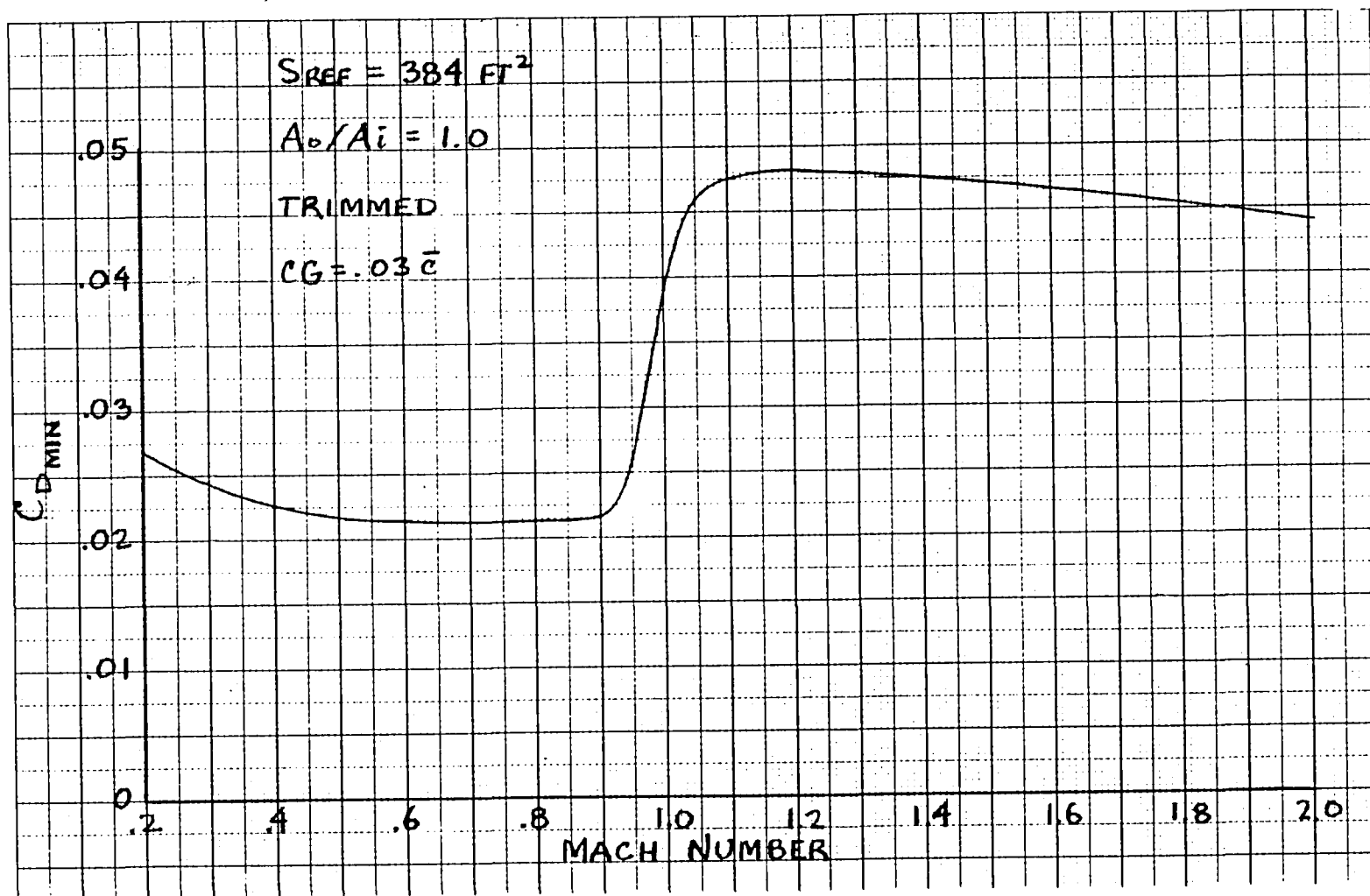
Figure 3-7   E205 Minimum Trimmed Drag Versus Mach Number
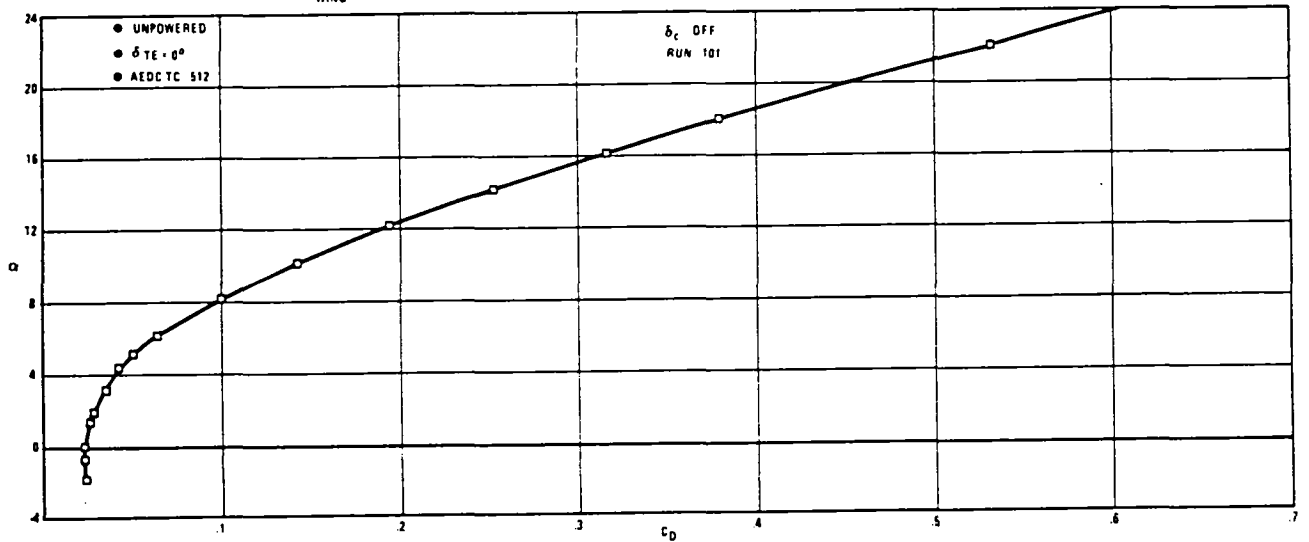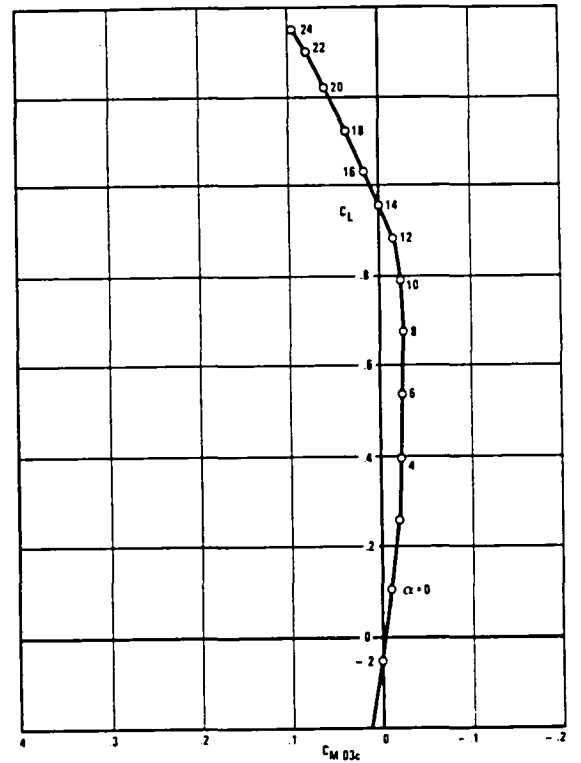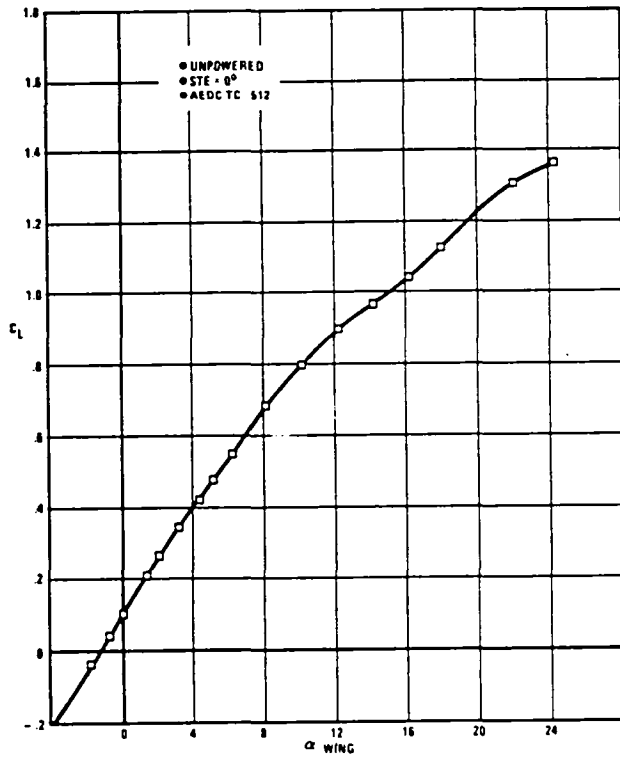
Figure 3-8   Power-Off Wing Body Lift, Drag, and
              Pitching Moment Characteristics
              for the VEO-Wing Fighter Model
              of Reference 4 , Mach = .2

SYM	TEST	RUN	MACH	LEF	TEF	HORIZ.
✗	Predicted		0.20	0.0	0.0	-10.0
☐	Predicted		0.20	0.0	0.0	0.0
△	Predicted		0.20	0.0	0.0	10.0
◇	Predicted		0.20	Wing-Body		
▽	327	43	0.20	0.0	0.0	0.0
▽	327	30	0.20	0.0	0.0	OFF

ARC-12-327
E 205

S_{REF} = 384.00 ft.^{2}
C_{REF} = 142.68 in.
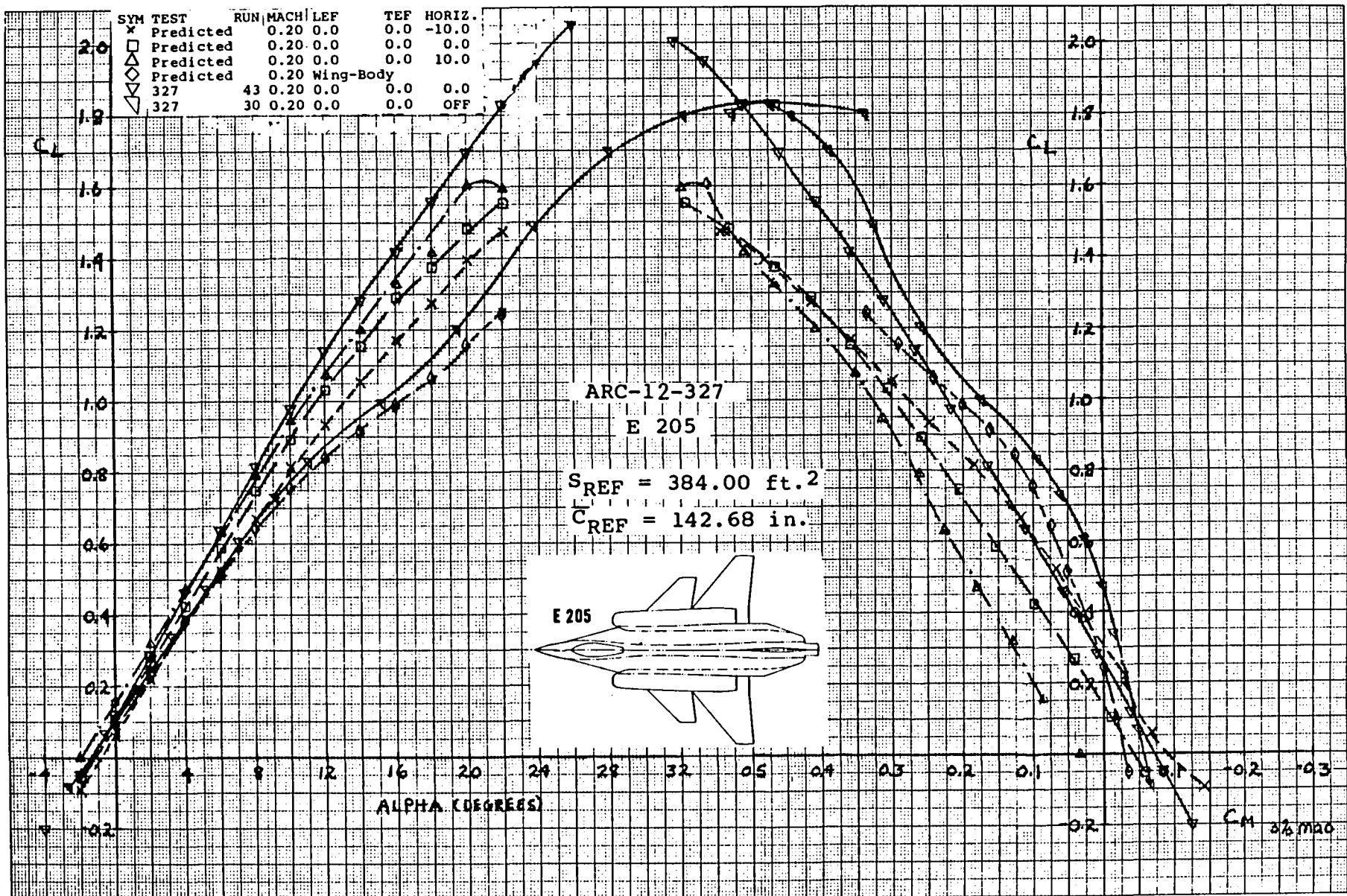
E 205

Figure 3-9a Lift and Moment Comparison of Predicted and Test Longitudinal
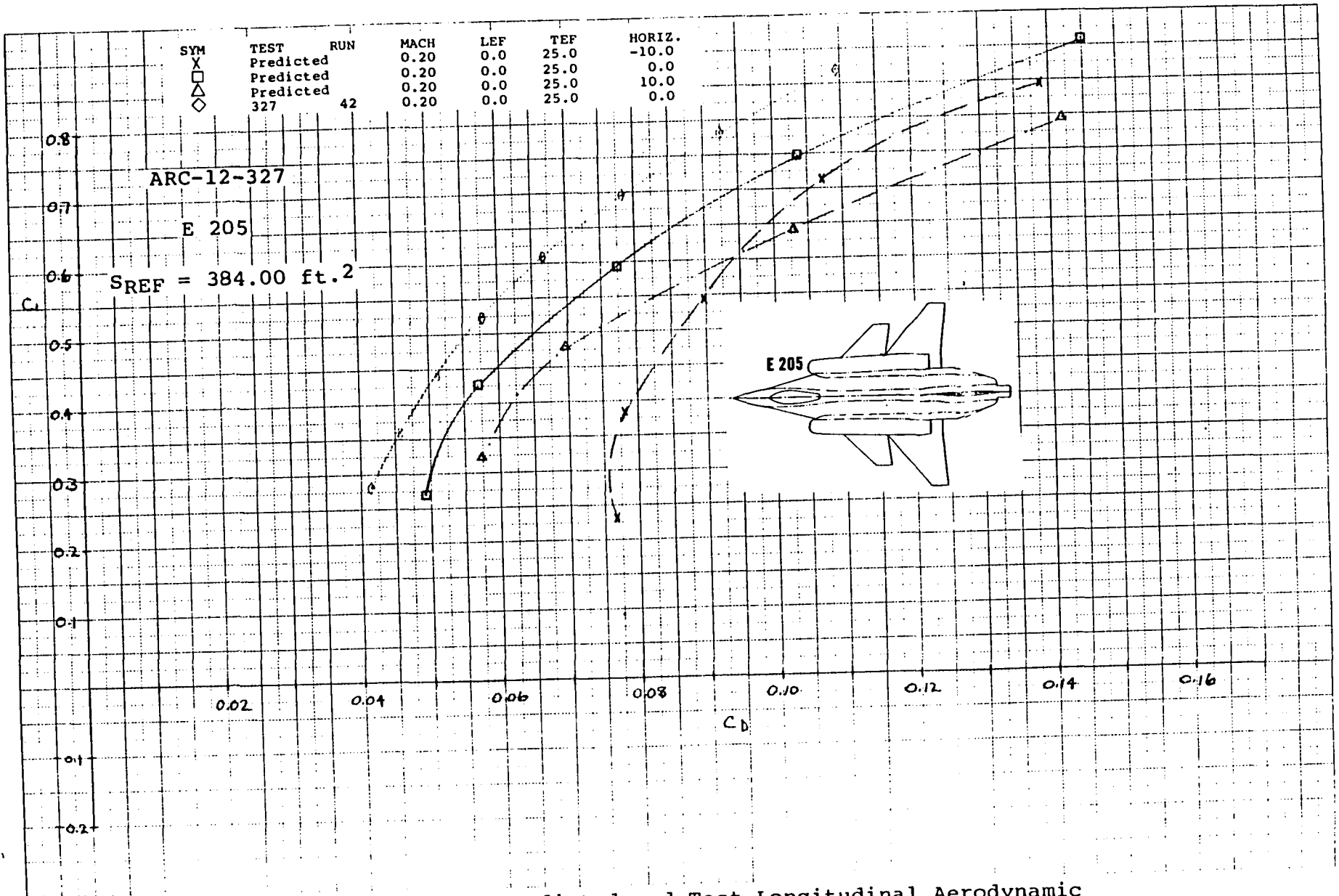Aerodynamic Characteristics of Baseline E 205 Configuration, Power-Off,
Mach = .2
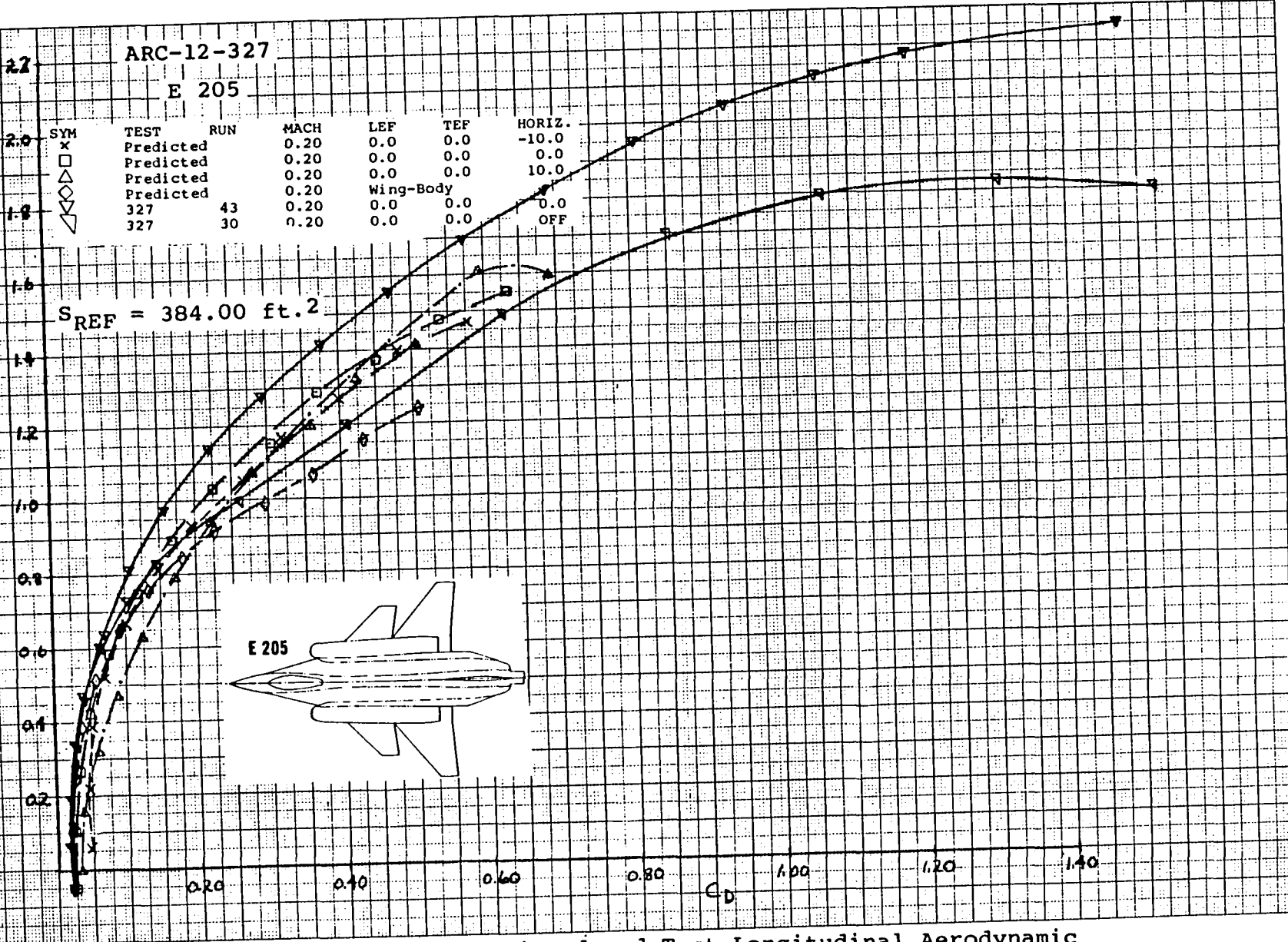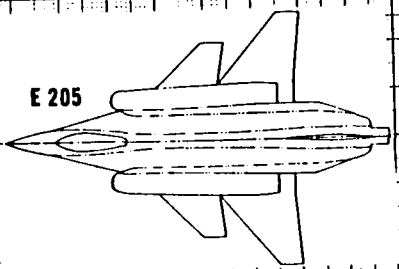
Figure 3-9b Drag Comparison of Predicted and Test Longitudinal Aerodynamic
Characteristics of Baseline E 205 Configuration, (Expanded Drag Scale),
Power-Off, Mach = .2

SYM	TEST	RUN	MACH	LEF	TEF	HORIZ.
X	Predicted		0.20	0.0	10.0	-10.0
⊡	Predicted		0.20	0.0	10.0	0.0
△	Predicted		0.20	0.0	10.0	10.0
◇	327	33	0.20	0.0	10.0	0.0

ARC-12-327

E 205

$S_{REF} = 384.00$ ft.^{2}

$\overline{C}_{REF} = 142.68$ in.

E 205

ALPHA (DEGREES)

C_L

C_M

58
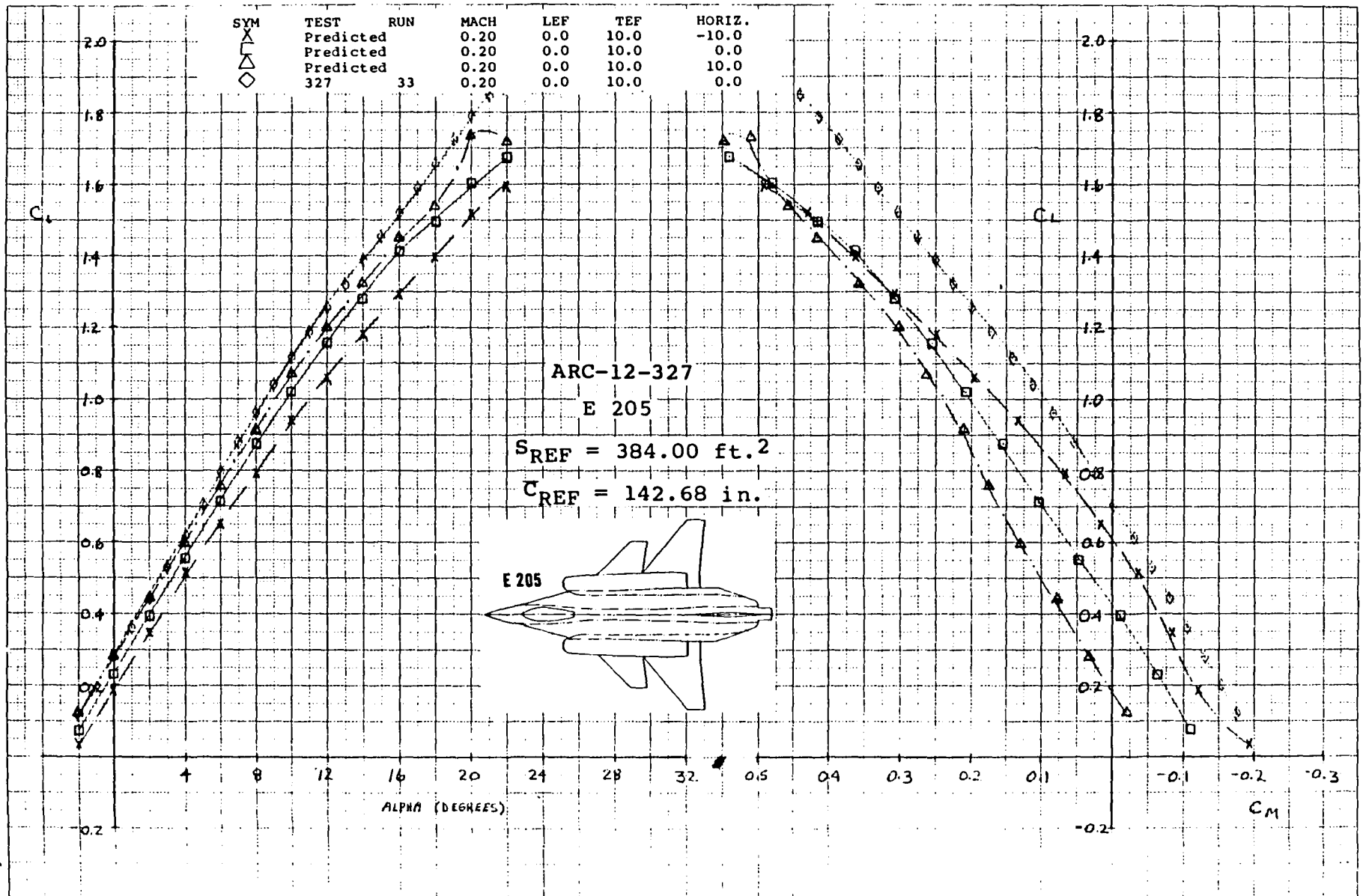
Figure 3-10a. Lift and Moment Comparison of Predicted and Test Longitudinal
Aerodynamic Characteristics of Baseline E205 Configuration with Wing
Trailing-Edge Flap Deflected +10°, Power-Off, Mach = .2
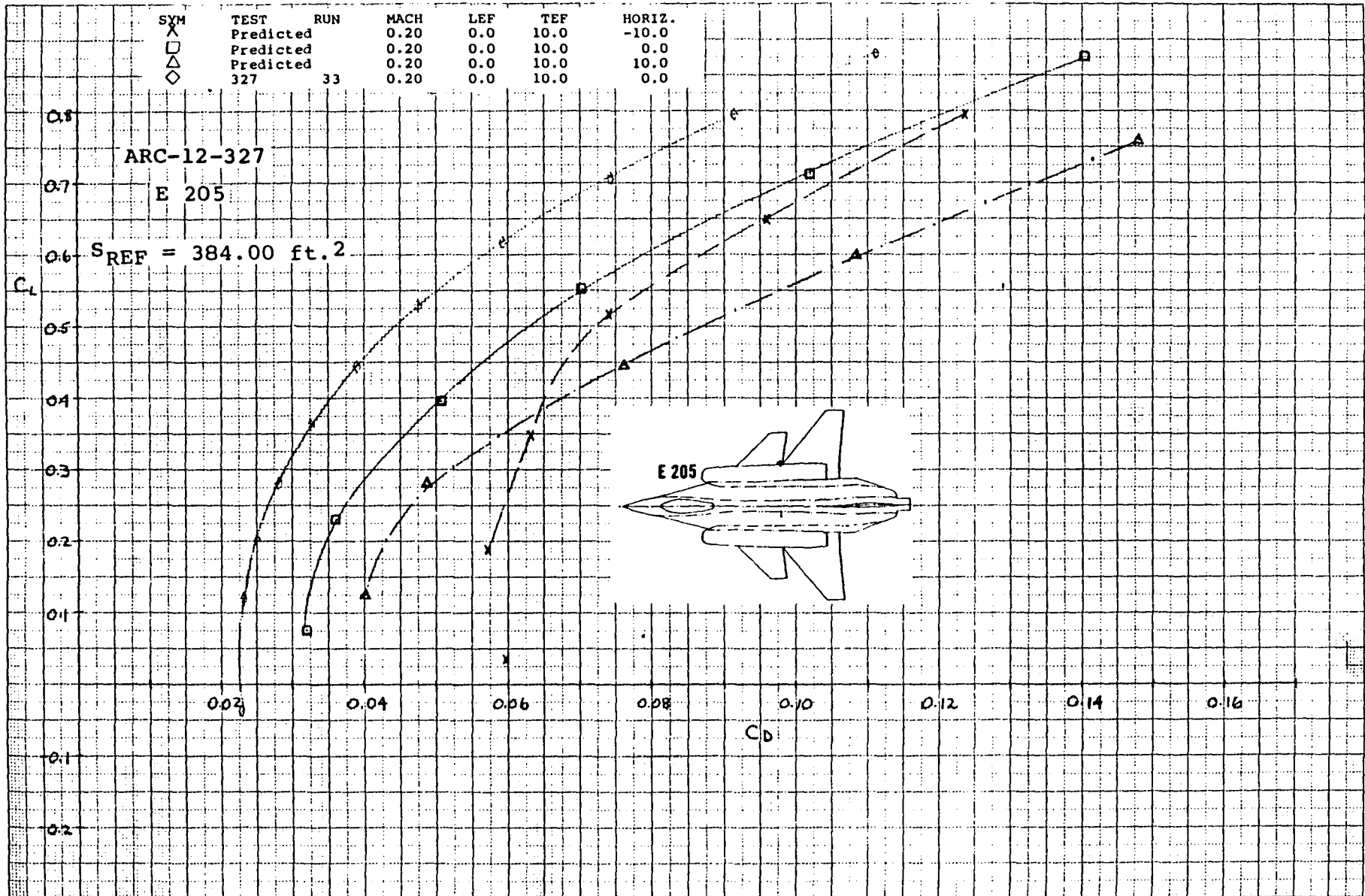
Figure 3-10b Drag Comparison of Predicted and Test Longitudinal Aerodynamic
Characteristics of Baseline E205 Configuration with Wing Trailing-Edge
Flap Deflected +10°, Power- Off, Mach = .2
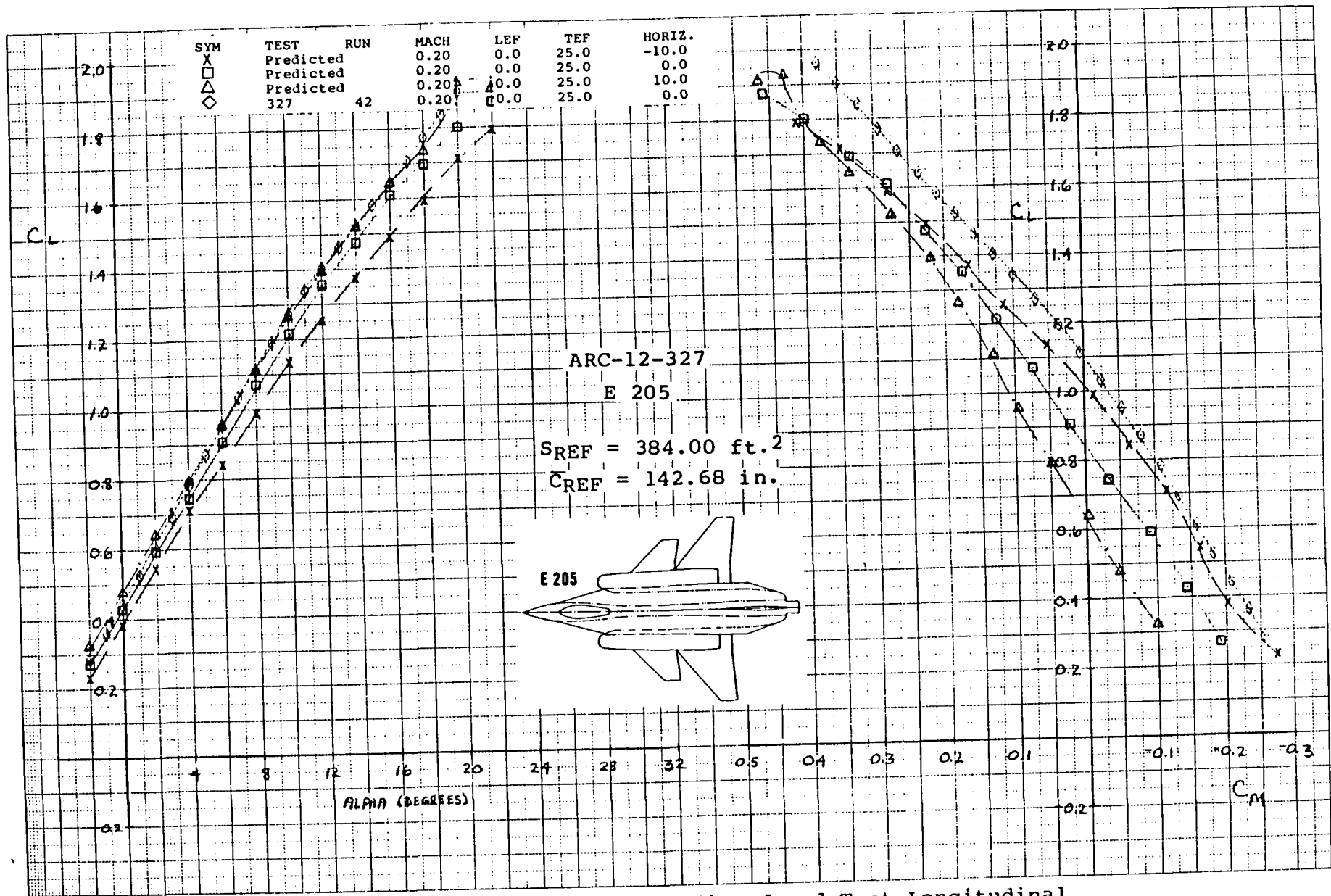
Figure 3-11a Lift and Moment Comparison of Predicted and Test Longitudinal Aerodynamic Characteristics of Baseline E205 Configuration with Wing Trailing-Edge Flap Deflected +25°, Power-Off, Mach = .2

SYM	TEST	RUN	MACH	LEF	TEF	HORIZ.
X	Predicted		0.20	0.0	25.0	-10.0
□	Predicted		0.20	0.0	25.0	0.0
△	Predicted		0.20	0.0	25.0	10.0
◇	327	42	0.20	0.0	25.0	0.0

ARC-12-327

E 205

$S_{REF} = 384.00$ ft.^{2}

E 205

C_L

C_D

0.8 0.7 0.6 0.5 0.4 0.3 0.2 0.1 -0.1 -0.2

0.02 0.04 0.06 0.08 0.10 0.12 0.14 0.16

Figure 3-11b Drag Comparison of Predicted and Test Longitudinal Aerodynamic
Characteristics of Baseline E205 Configuration with Wing Trailing-Edge
Flap Deflected +25°, Power-Off, Mach = .2
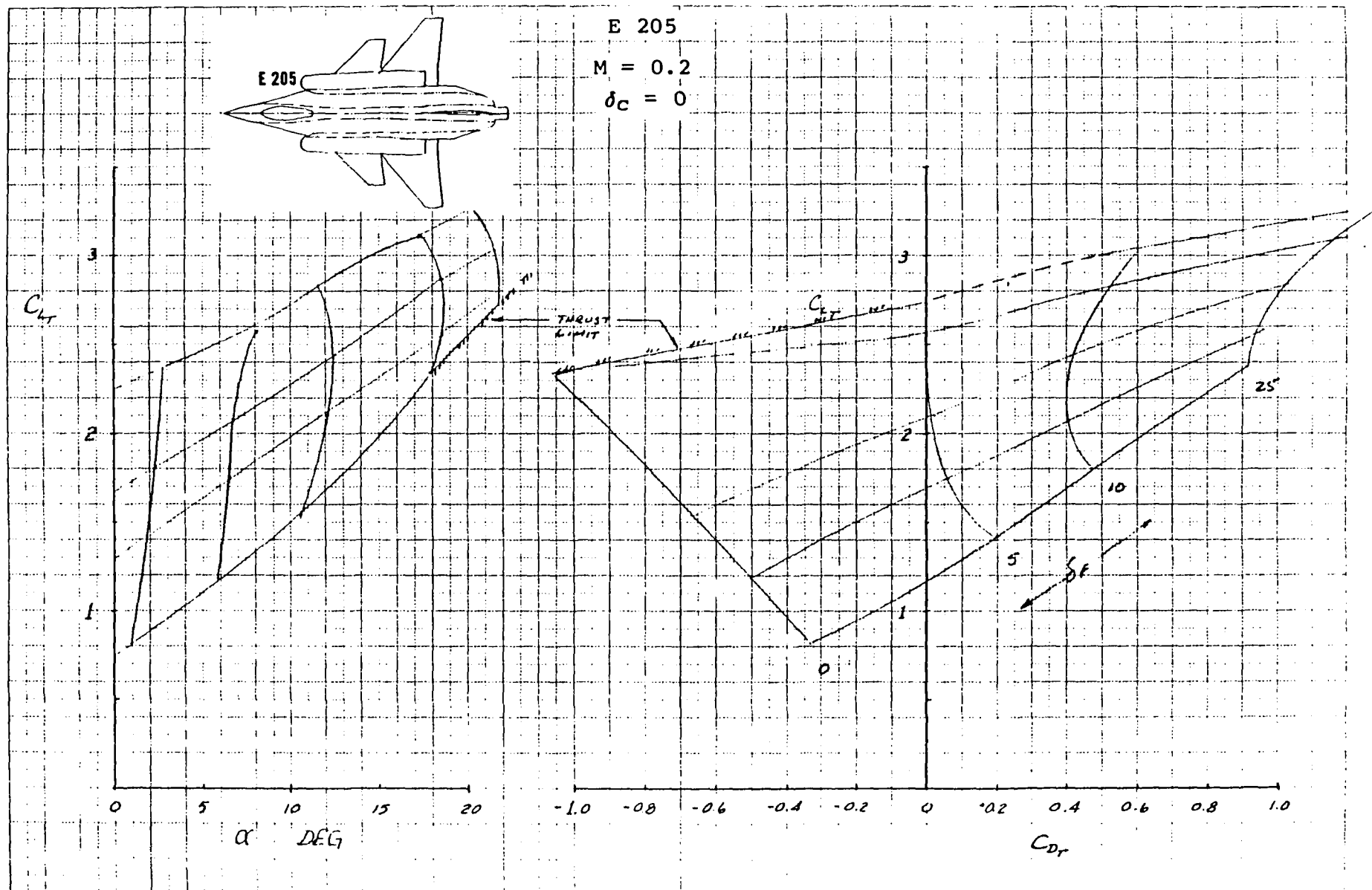
Figure 3-12 Full-Scale E205 Airplane Power-on, Trimmed Lift Curve- and Drag
Polar-Envelopes from Wind Tunnel Data for M = .2, $C_{T_{TOTAL}}$ = 1.81
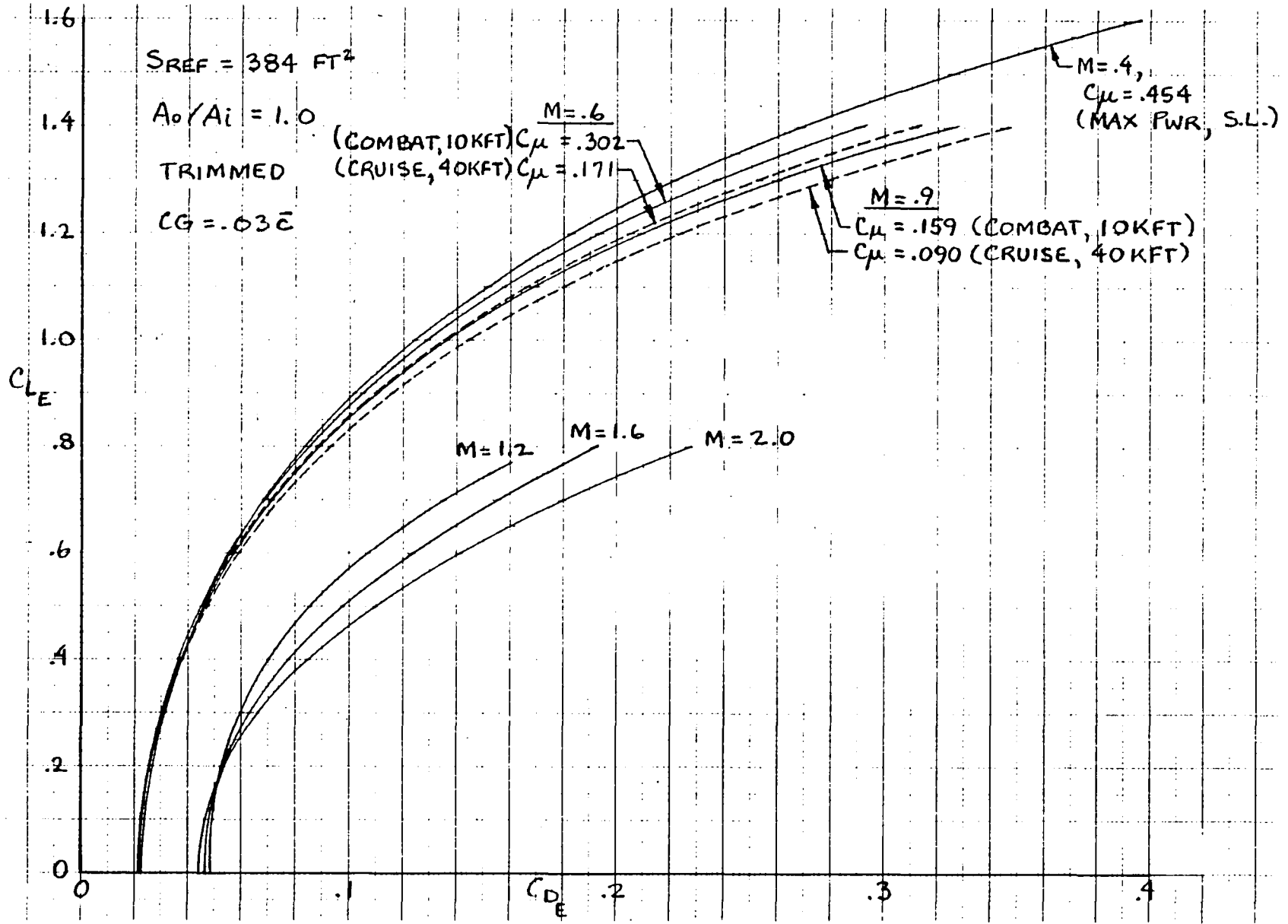
Figure 3-13. E205 Trimmed Cruise/Maneuver Drag Polars

1 — TEST DATA

$c^2_{L_E}$

$c_{D_C} + c_{D_S}$

c_{D_0}

c_{D_E}

2

δ_{TE} 0 5° 10°

e_E

C_{L_E}

3

δ_{TE} 10° 0 5° C_{L_T} $C_T = X$

TRIM

S_M

(+) C_{M_0} (−) C_{M_T}

4

$C_T = X$ MACH

C_{L_E} TRIM   .4   .8

$\delta_{TE_{TRIM}}$

5

M = XX
C_T = XX
$\delta_C = 0°$

e_E OPTIMUM ENVELOPE   TRIM

δ_{TE} δ_{TE} VARIES δ_{TE}

C_{L_E}

6

OPTIMUM e ENVELOPES

e_{TRIM} $C_T = X$

C_{L_E} .6   .8   1.0

MACH

$$e = \frac{1}{\pi AR} \frac{c^2_{L_E}}{c_{D_E} - c_{D_{0_E}}}$$

L_o ΔL_r ΔL_r

cg

S_m X_r X_r T

$L_T = L_o + \Delta L_r + \Delta L_R$

$M_T = M_o \, X \, \Delta L - X_R \, \Delta L_R$

WHERE L_o = POWER OFF AERODYNAMIC LIFT
ΔL_r = LIFT INCREMENT DUE TO SUPERCIRCULATION
L_R = REACTION LIFT DUE TO THRUST
X = SUPERCIRCULATION ARM
X_R = REACTION LIFT ARM
c_{D_C} = CAMBER DRAG
c_{D_S} = FLAP SCRUB DRAG

Figure 3-14   VEO-Wing Trim Method for Maneuver
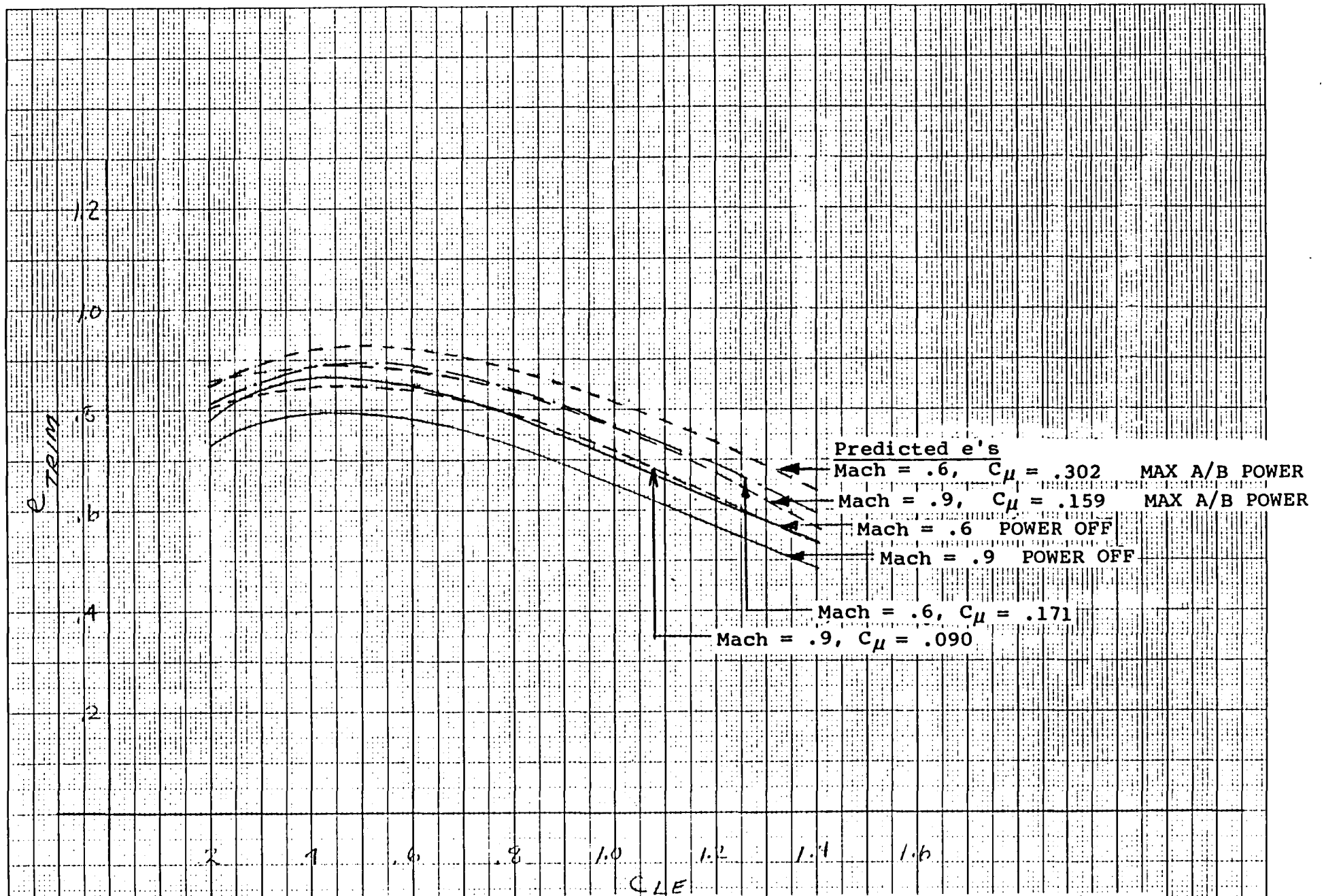
Figure 3-15 Power-on and Power-off Predicted Trimmed e's as a Function of Equivalent Lift Coefficient, C_{LE}, Mach Number, and C_μ (from Reference 1)

65

TOTAL COEFF = AERO-ONLY COEFFICIENTS ($\delta_F = 0°$)
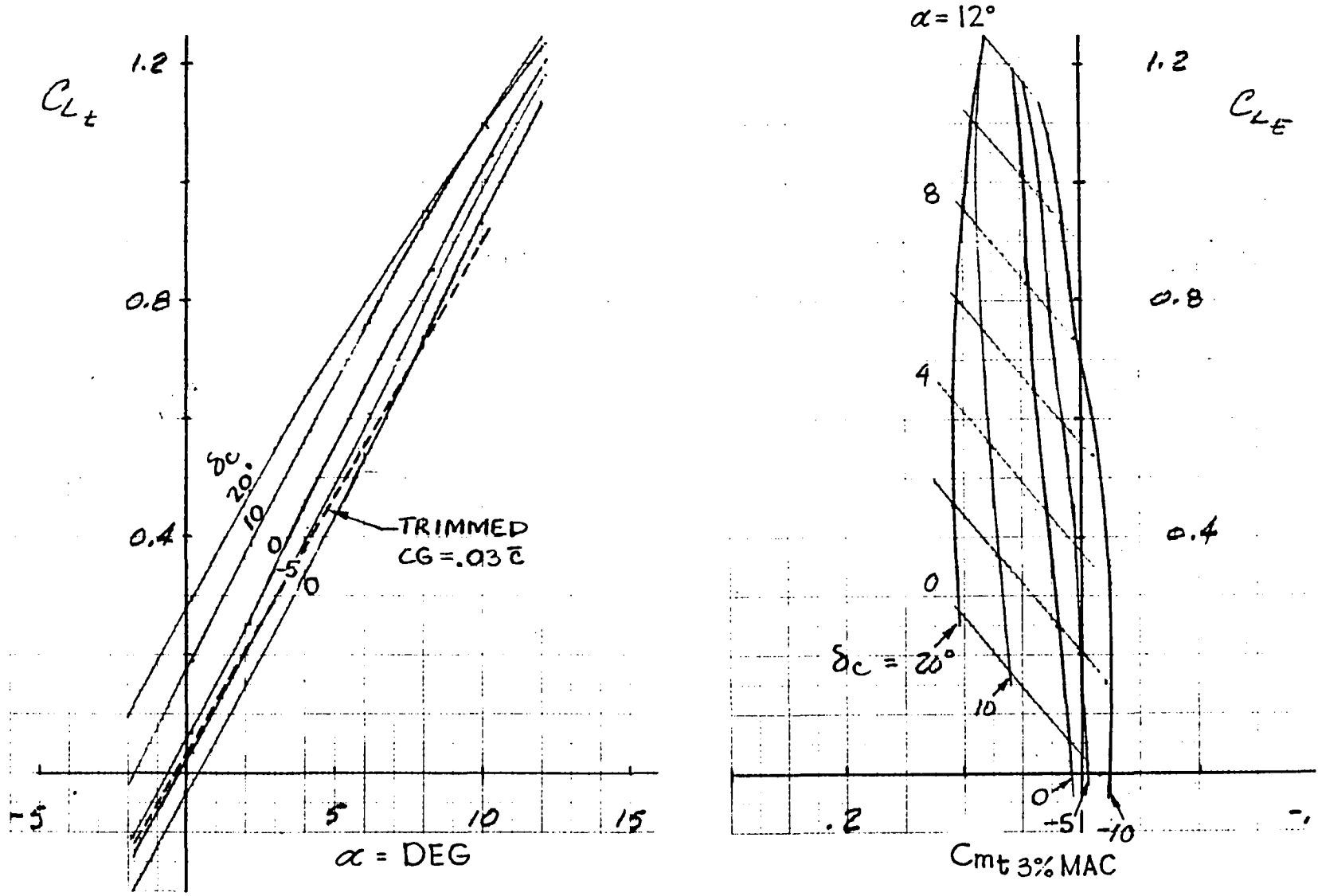
Figure 3-16a   E205 Lift and Pitching Moment Curves at M=1.2 with Canard Deflection
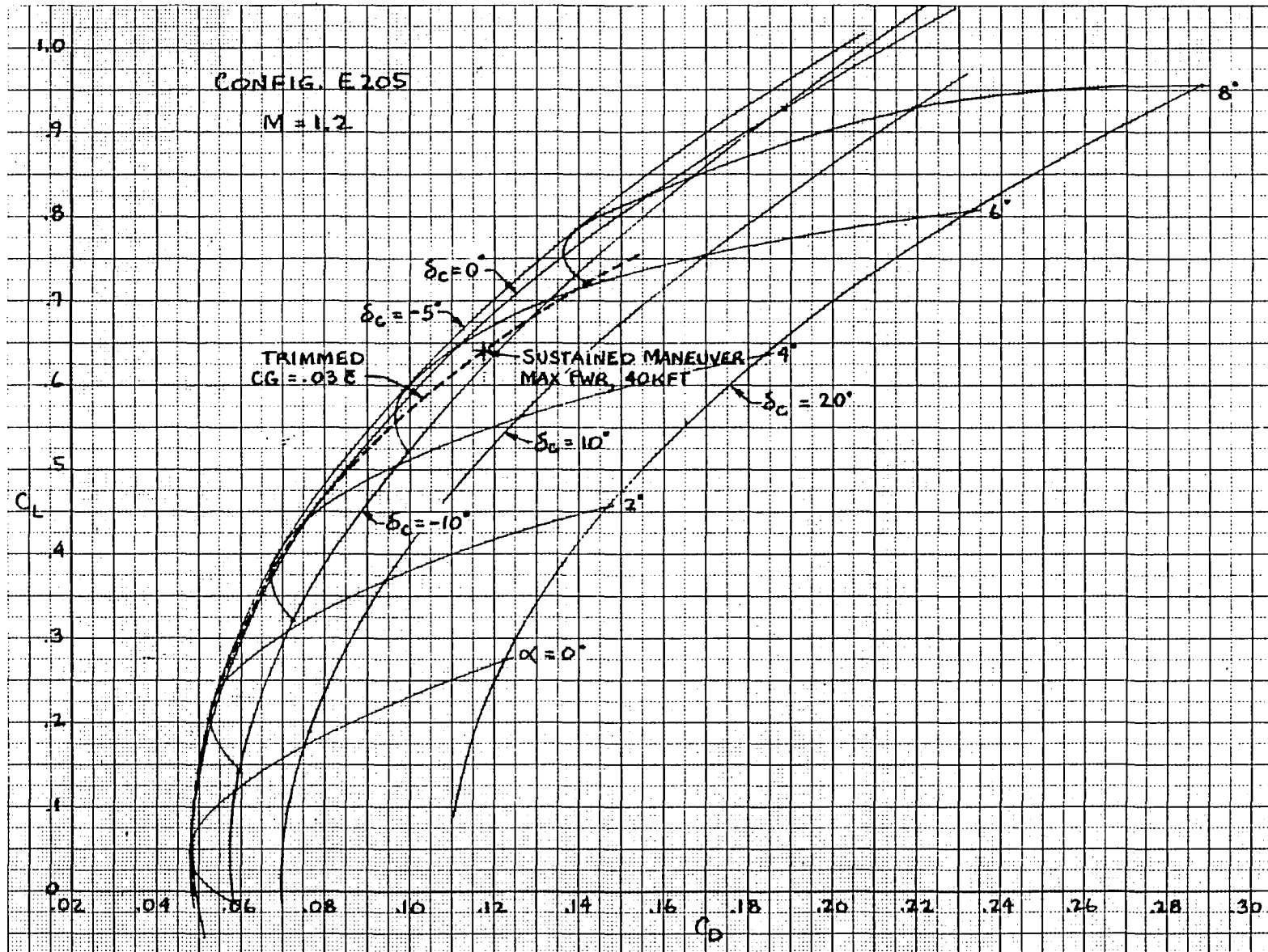
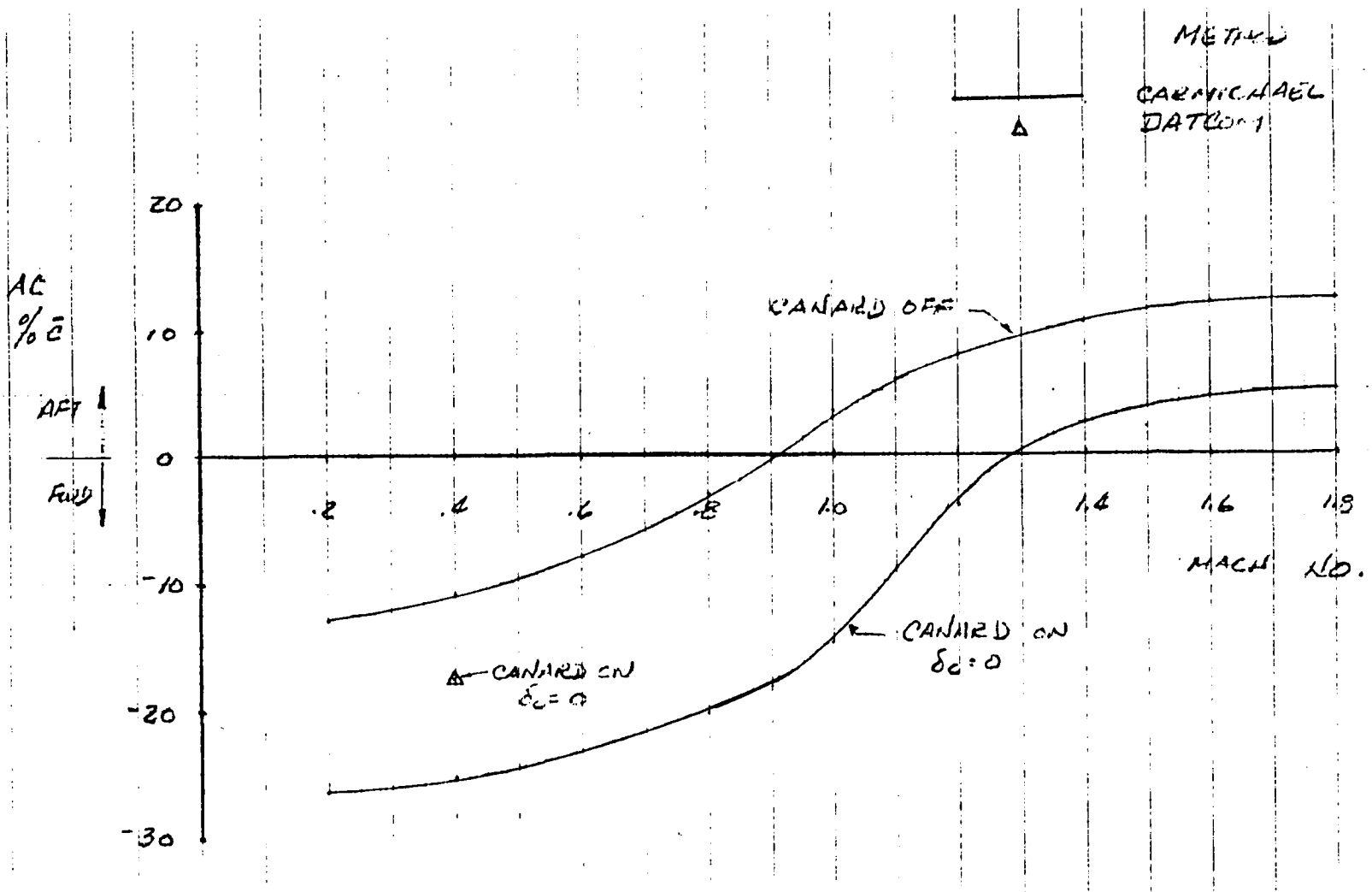Figure 3-16b   E205 Drag Polars at M=1.2 with Canard Deflection

TOTAL COEFF = AERO-ONLY COEFFICIENTS $(\delta_F = 0°)$
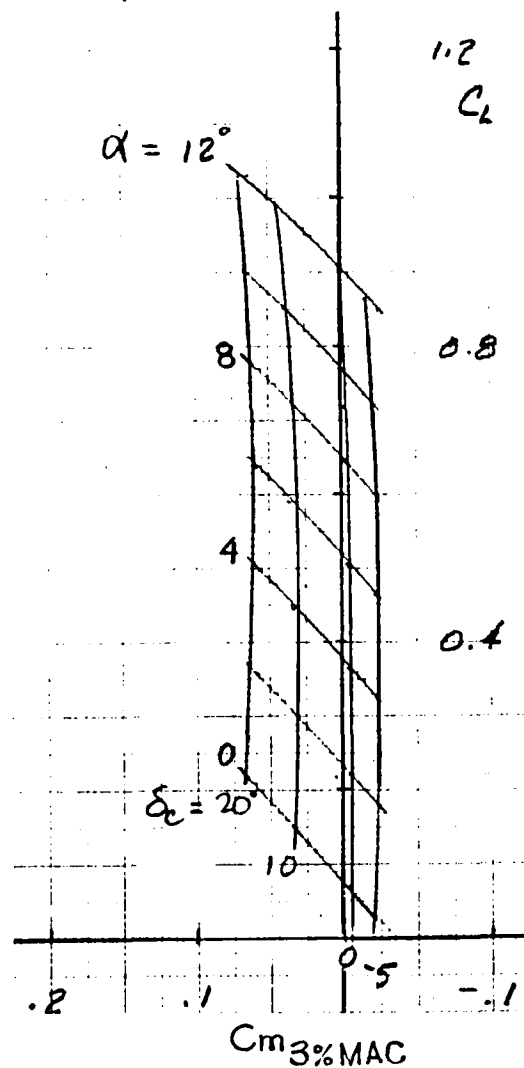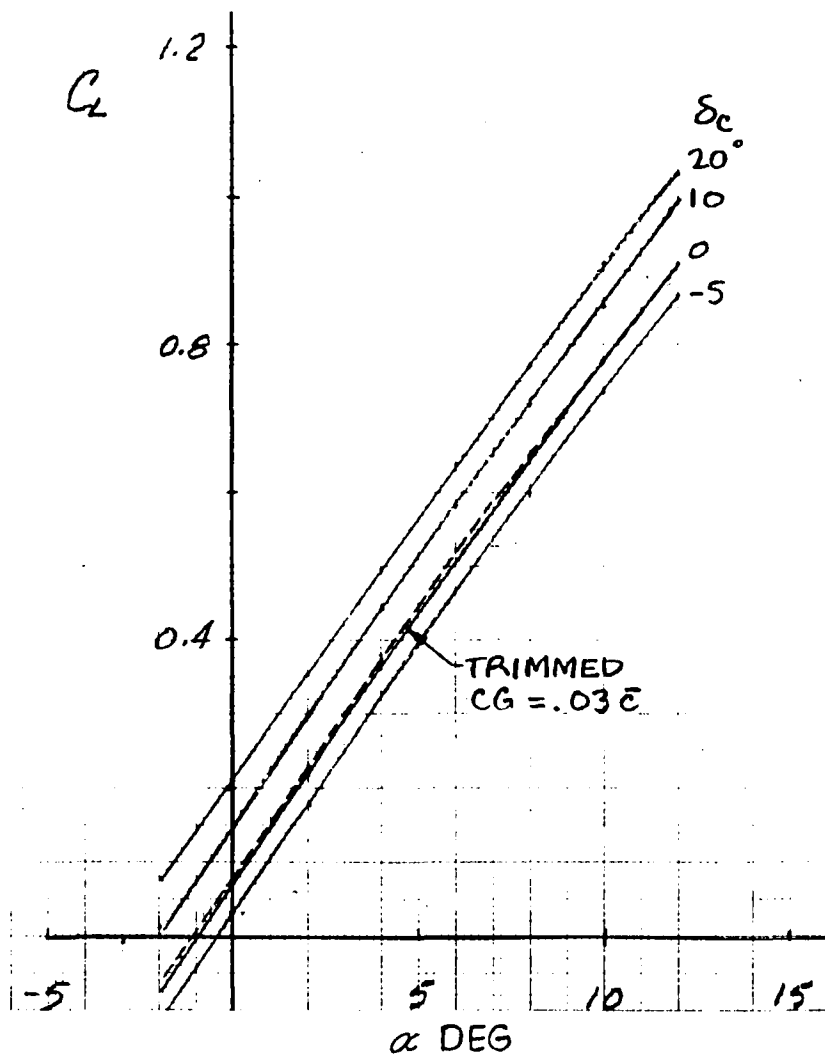
Figure 3-17a   E205 Lift and Pitching Moment Curves at M=1.6 with Canard Deflection
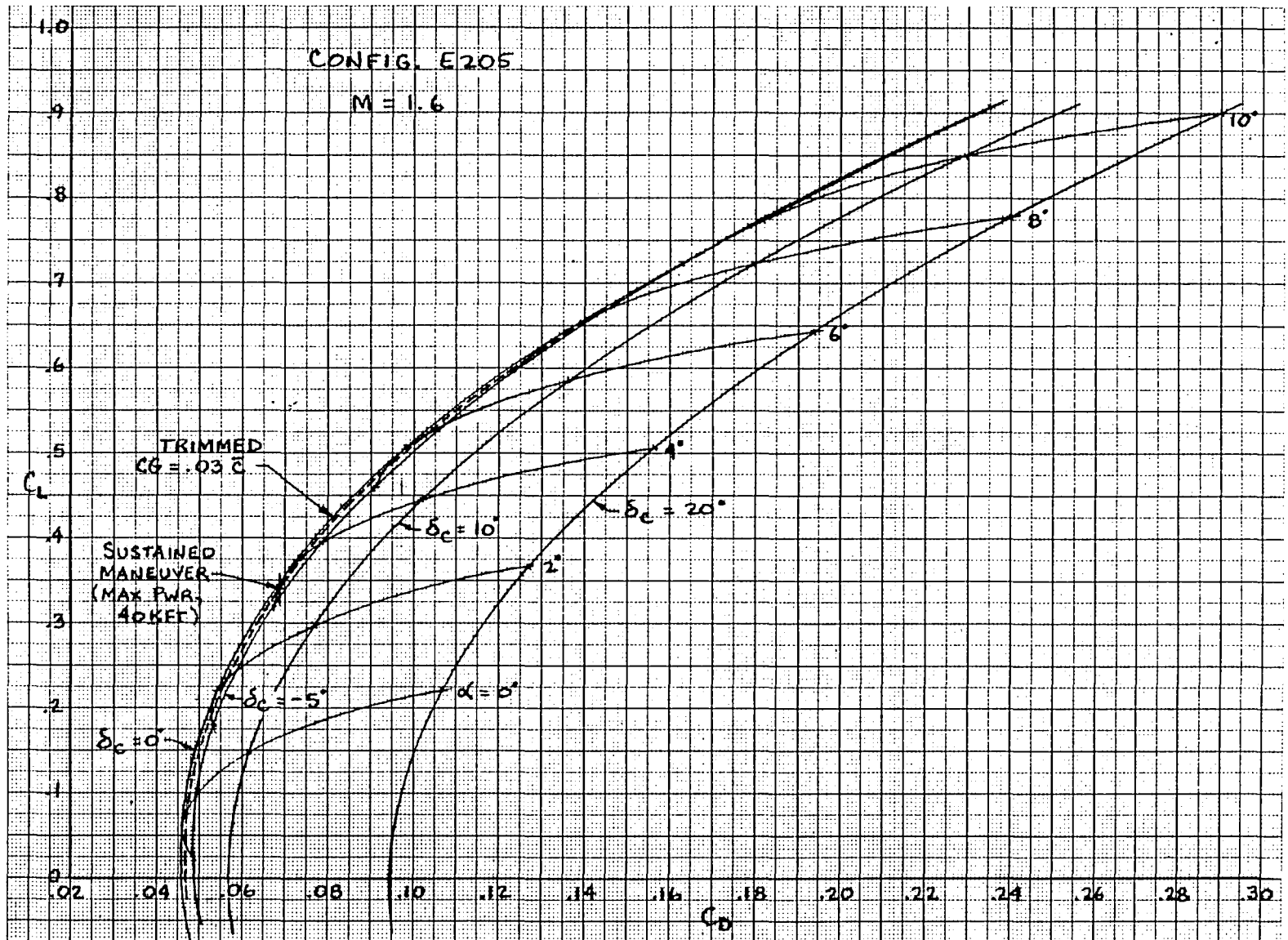
Figure 3-17b   E205 Drag Polars at M=1.6 with Canard Deflection

Figure 3-18   E205 Predicted Aerodynamic Center

70

THEORY: CARMICHAEL/WOODWARD ALL WING SIMULATION

NOTE: $+\Delta$ AC MEANS PREDICTED LOCATION AFT OF ACTUAL LOCATION

SYM	CONFIGURATION
ATW-4	$\Lambda = 15°$
	$\Lambda = 65°$
F-16A	
YF-16	
FB-111	$\Lambda = 26°$
1/10-SCALE VEO-WING RESEARCH MODEL	
GRUMMAN V/STOL AIAA 75-1013 CASE A, FLAG CASE D	
SUPER LEDE	
FX-132	$\Lambda = 20°$
B-1	$\Lambda = 67.5°$
	$\Lambda = 65°$
	$\Lambda = 25°$
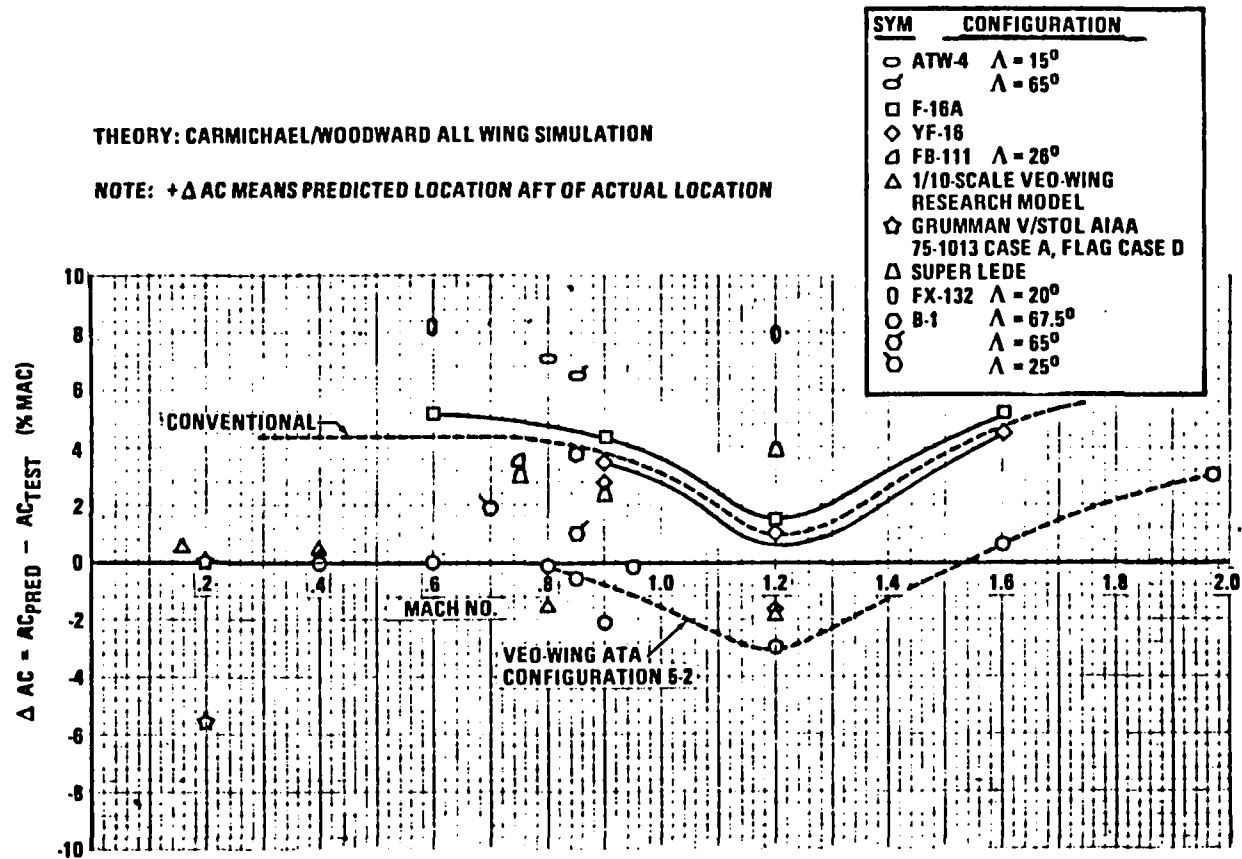
Figure 3-19 Aerodynamic Center Test/Theory Correlation

(a) EFFECTS OF CANARD

SYM	δ_C	δ_{LEF}	δ_{TEF}
⊙	0	0	0
△	10	0	0
⬯	OFF	0	0
⬭	-5	0	0

(b) EFFECTS OF FLAPS

SYM	δ_C	δ_{LEF}	δ_{TEF}
⊙	0	0	0
⬜	0	5	15
◇	0	0	15/5
△	0	20	15
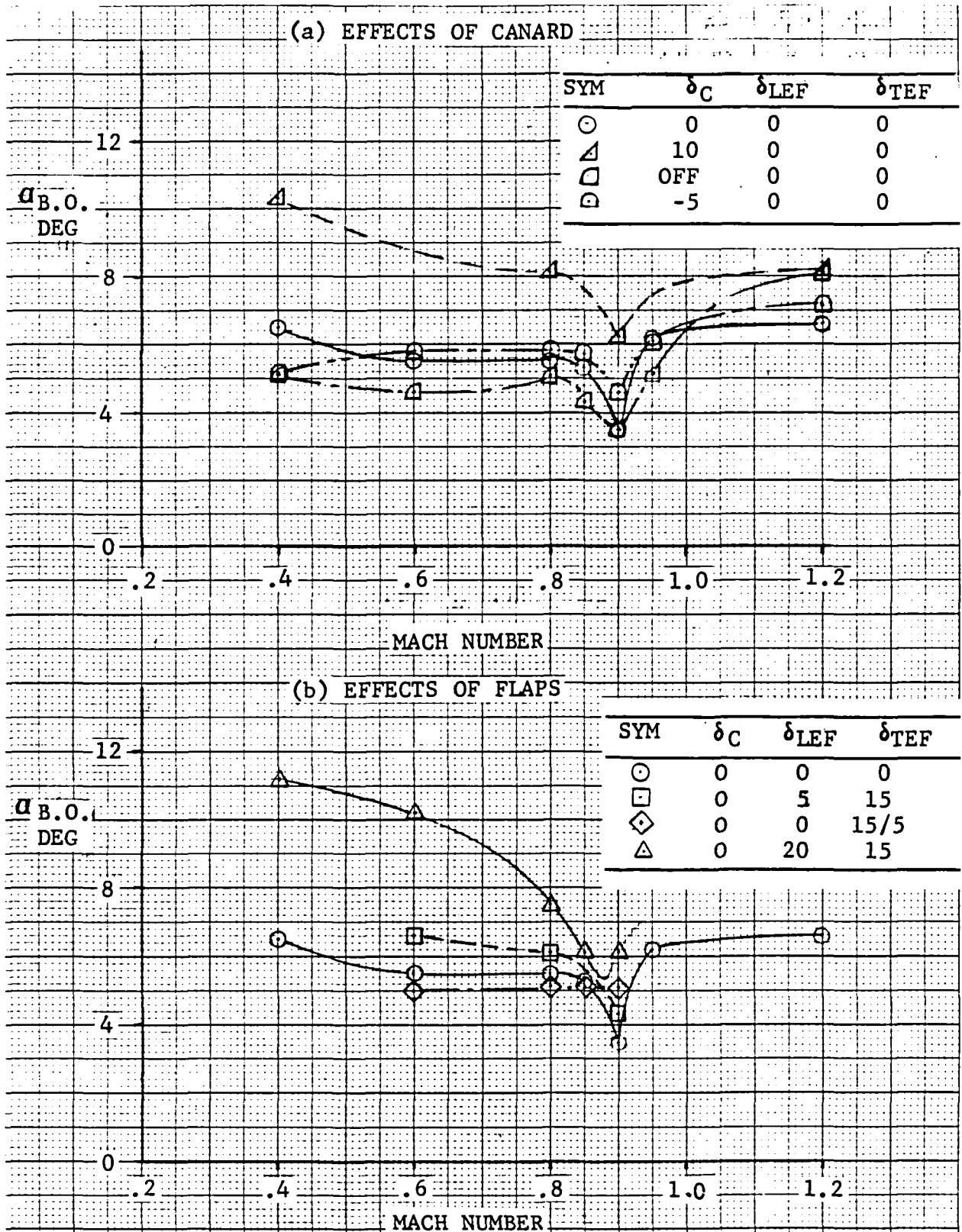
Figure 3-20   E205 Buffet-Onset Angle of Attack
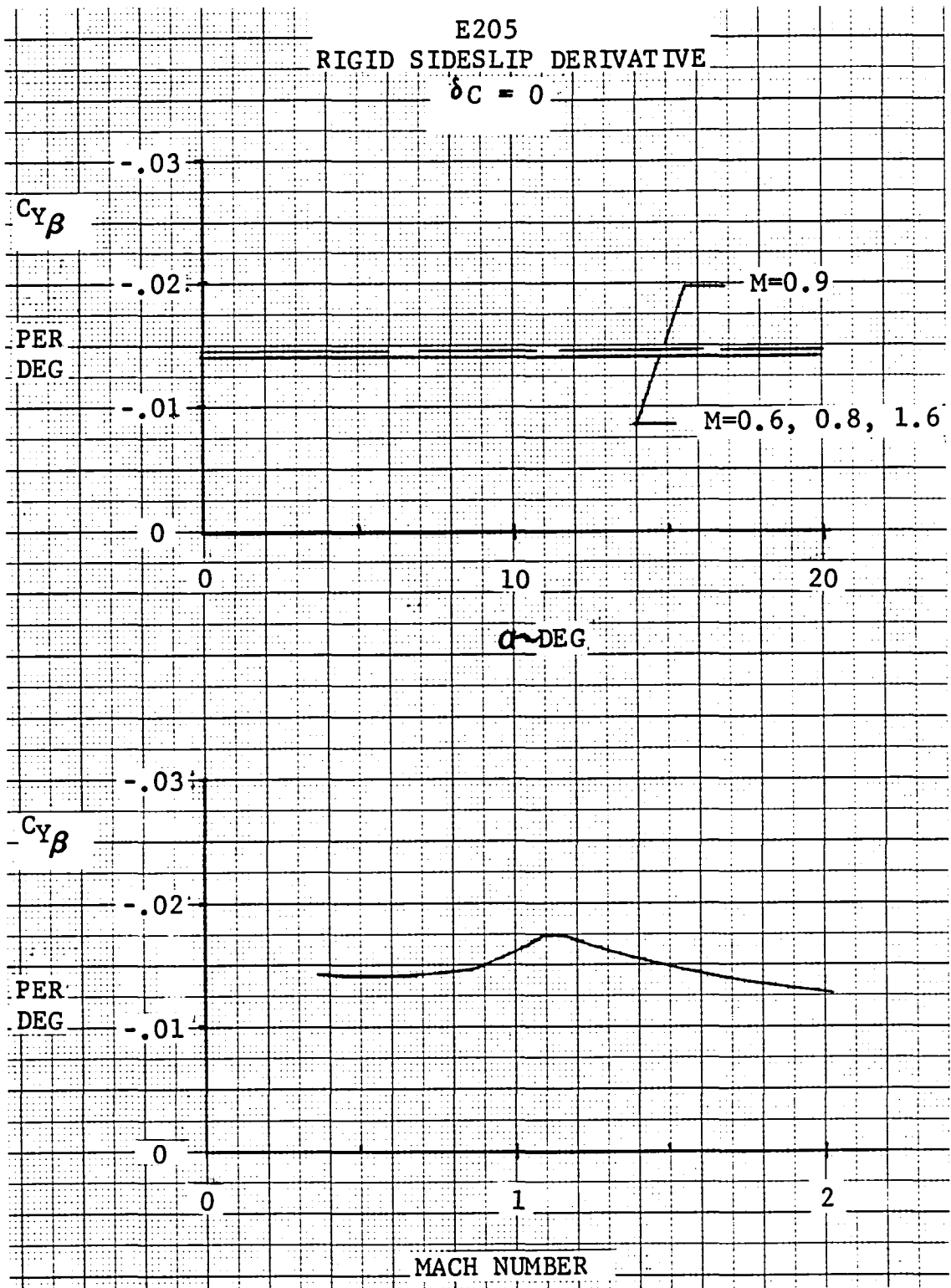
Figure 3-21a   E205 Lateral-Directional Characteristics
Cy_β vs. α and Mach No.

73

Figure 3-21b

C_{n_β} vs. α and Mach No.

74

Figure 3-21c

$C_{1\beta}$ vs. α and Mach No.

75
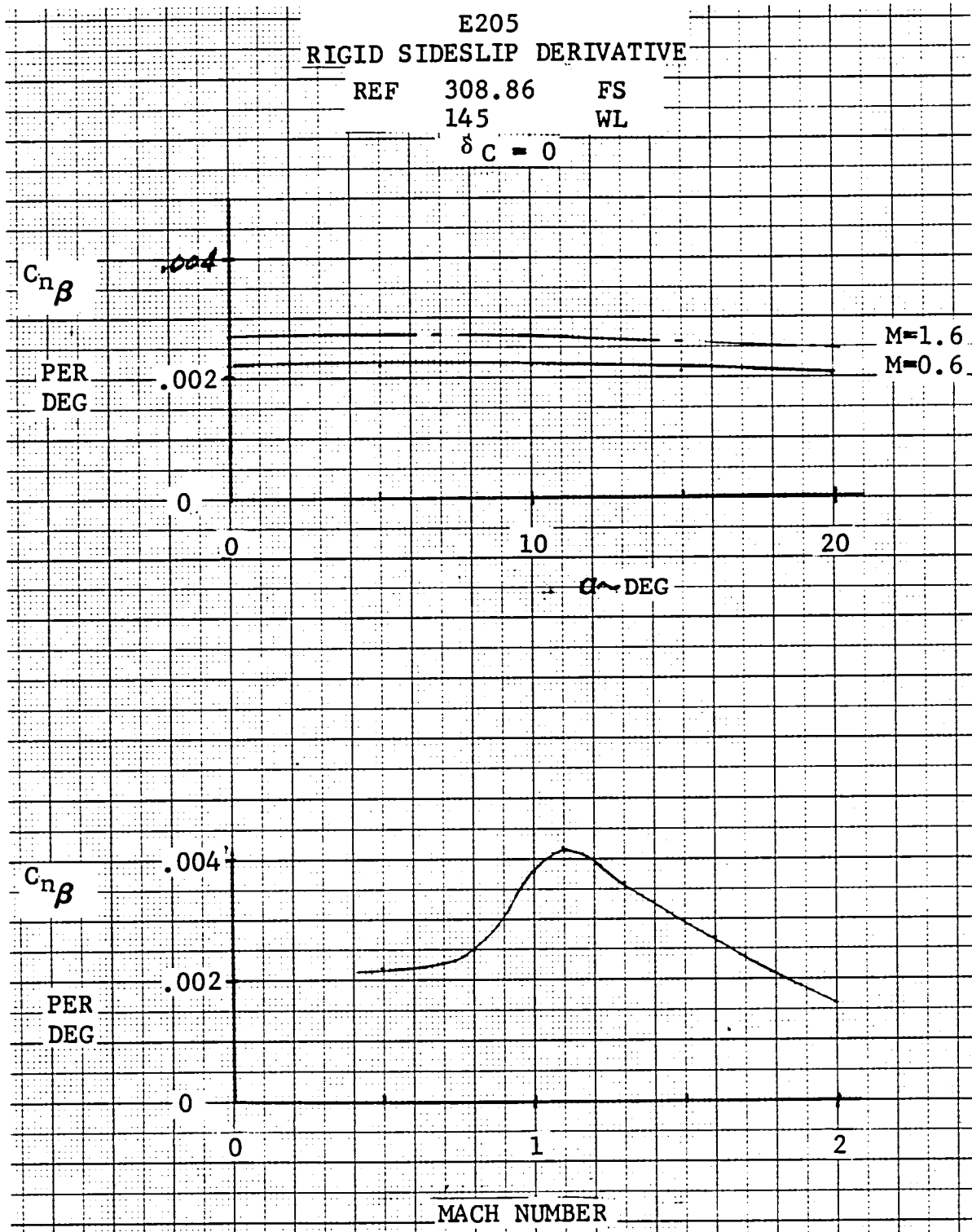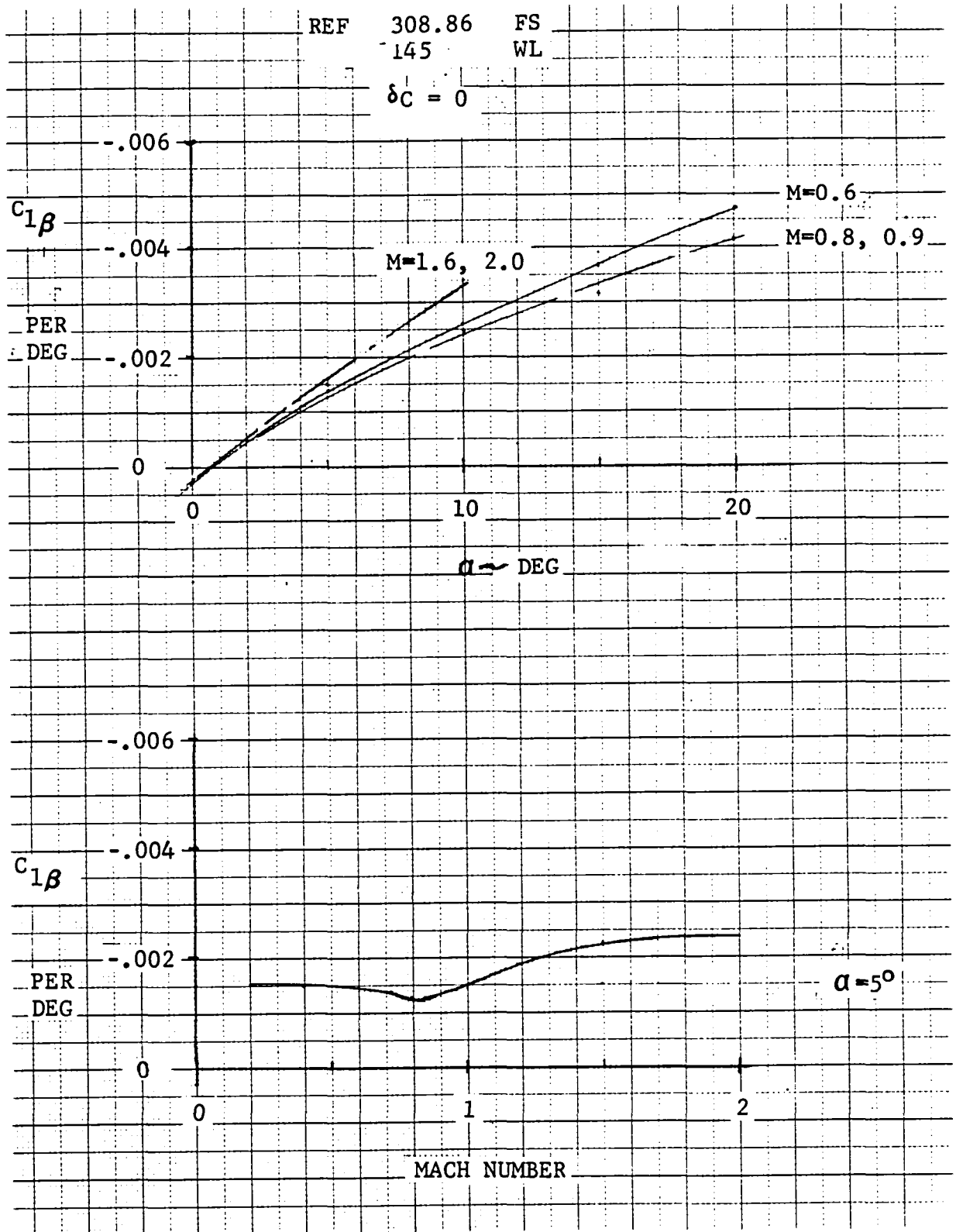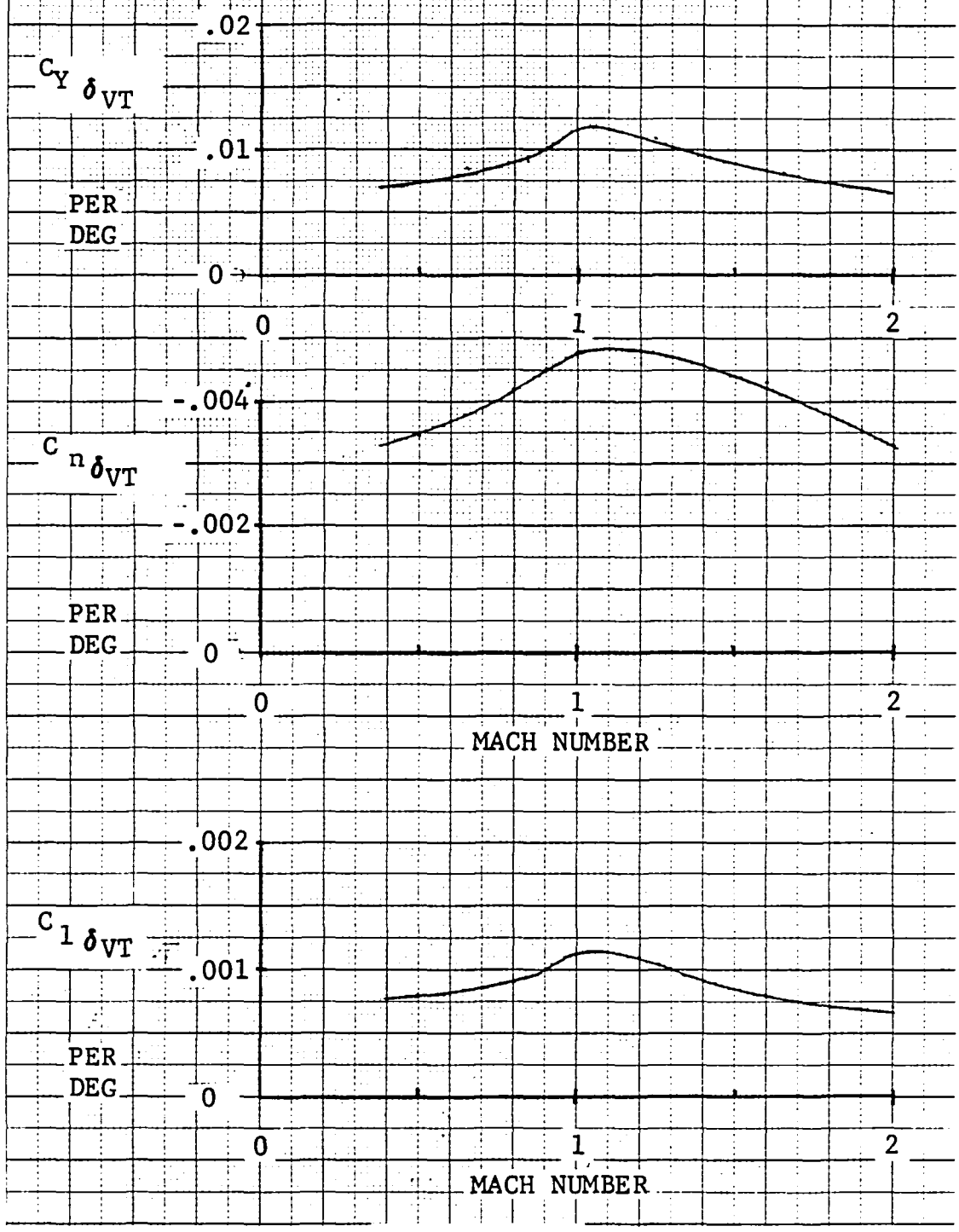
Figure 3-21d
Vertical Tail Effectiveness
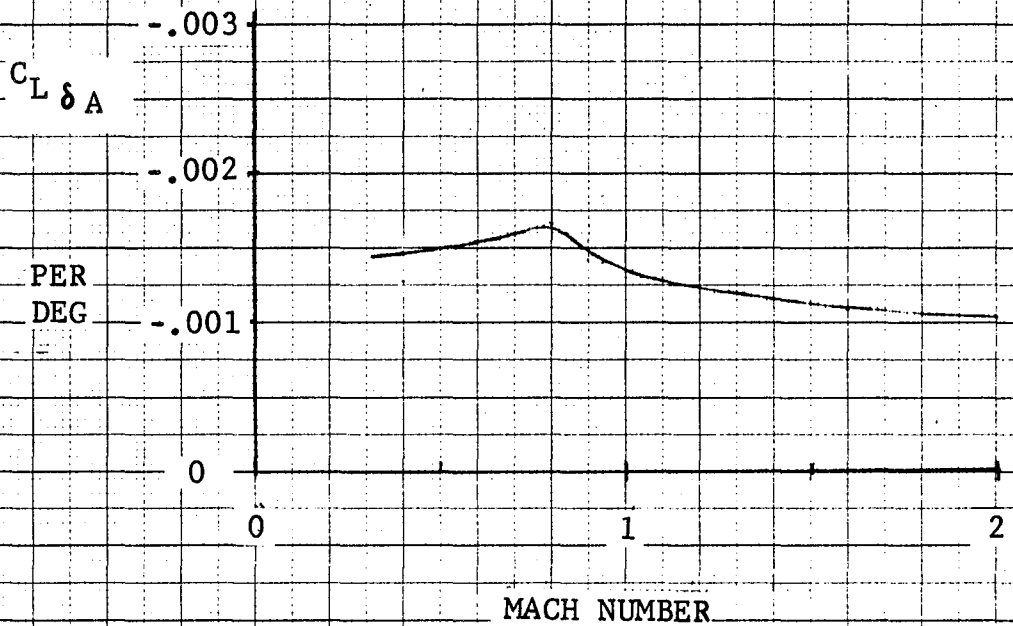
Figure 3-21e

Aileron Effectiveness

WING

THEO. AREA	3.3858 FT²	.3146 M²
SPAN	42.010 IN	1.067M
MAC	13.398 IN	.340M
L.E. SWEEP	40°	
TIP CHORD	3.706 IN	.094M
ROOT CHORD	19.505 IN	.495M
INCIDENCE	0°	
DIHEDRAL	0°	
ASPECT RATIO	3.62	
TAPER RATIO	.190	
AIRFOIL	NACA-64A204	

VERTICAL TAIL

THEO. AREA	.4188 FT²	.0389M²
SPAN	8.751 IN	.222M
MAC	7.256 IN	.184M
L.E. SWEEP	47°30'	
TIP CHORD	4.144 IN	.105M
ROOT CHORD	9.638 IN	.245M
ASPECT RATIO	1.27	
HINGE LINE @ F.S. 49.315		
H.L. SWEEP	0°	
TAPER RATIO	.43	
AIRFOIL @ Cʀ	5.3% BI-CONVEX	
Cᴛ	4.0% BI-CONVEX	

HORIZONTAL CANARD (MID-POSITION)

THEO. AREA (1 PANEL)	.3590 FT²	.0315M²
SPAN	7.2611 IN	.184M
MAC	7.1971 IN	.183M
L.E. SWEEP	45°	
T.E. SWEEP	8°26'	
TIP CHORD	5.631 IN	.092M
ROOT CHORD	9.815 IN	.249M
DIHEDRAL	0°	
HINGE LINE @ F.S. 24.414		
	B.L. 8.996	
	W.L. 15.587	
H.L. SWEEP	1°46'	
ASPECT RATIO (1 PANEL)	1.08	
AIRFOIL @ Cʀ	NACA-64A005	
Cᴛ	NACA-64A003	

Figure 3-22 Three View Drawing of E205 Wind Tunnel Model

3-VIEW .0939-SCALE V/STOL MODEL
CONFIGURATION E-205

78

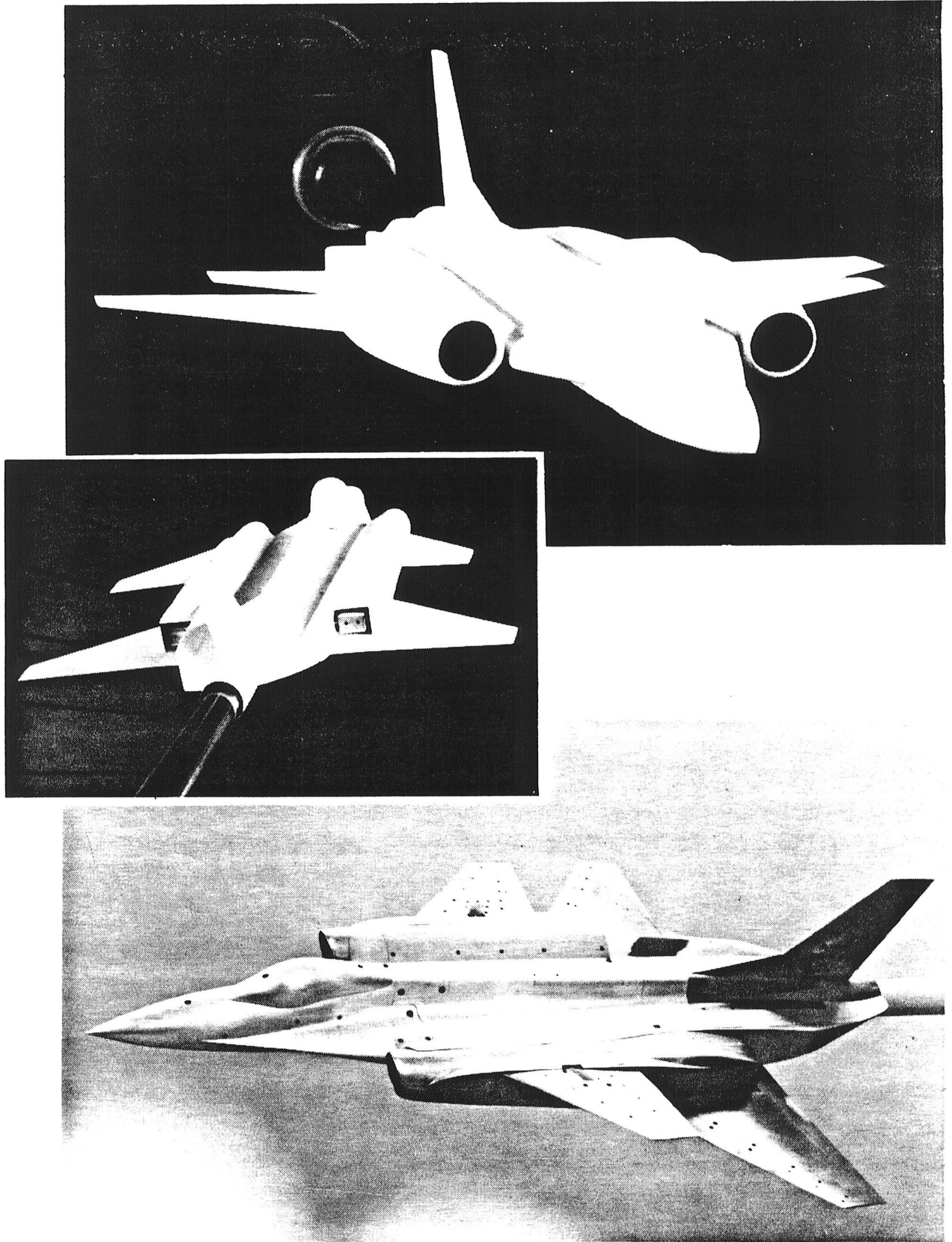Figure 3-23 VEO-Wing 0.0939-Scale V/STOL Fighter Model

79
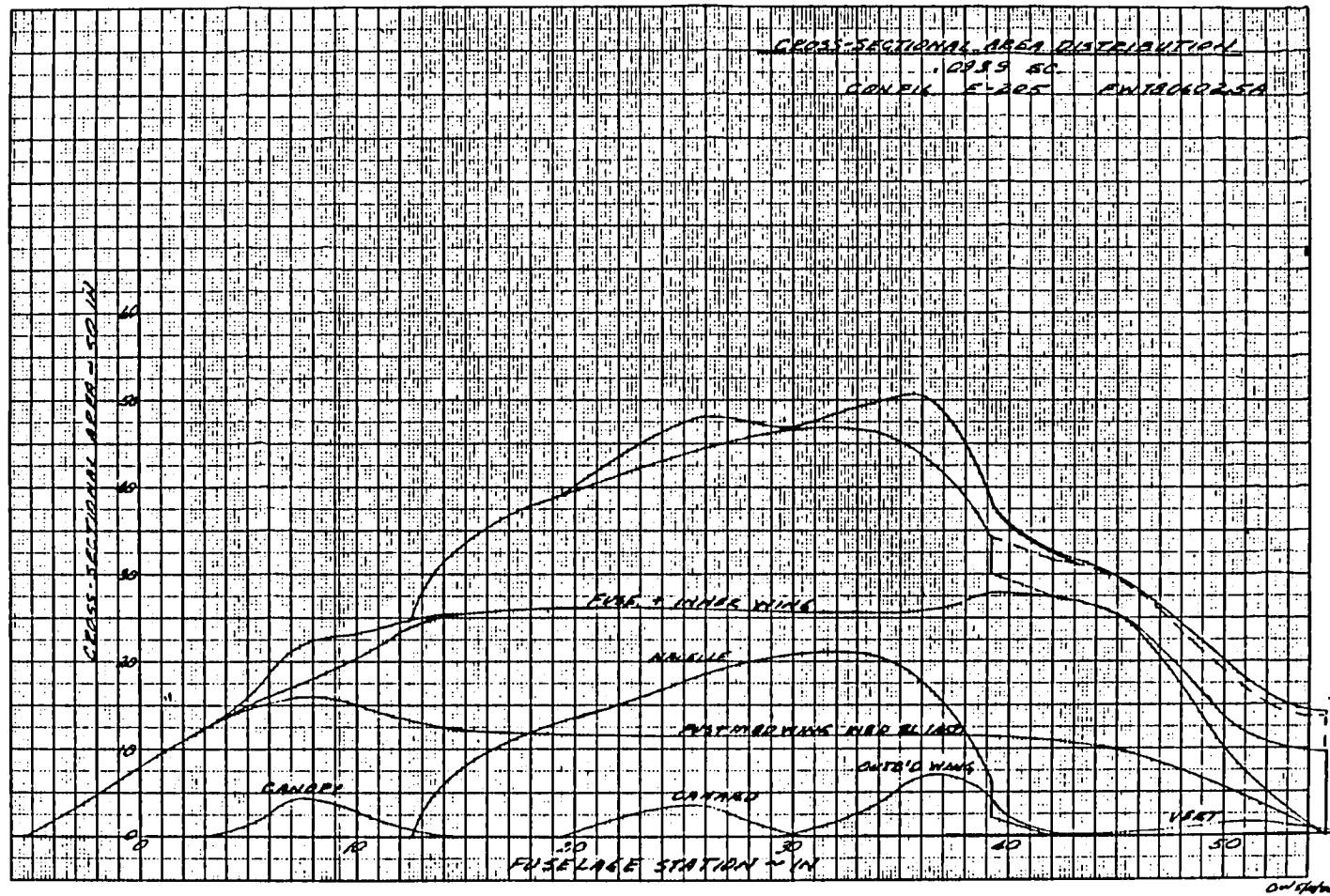
Figure 3-24   Cross-sectional Area Distribution of E205
              Wind Tunnel Model

WING

THEO. AREA	3.1541 FT²	.2930M²
SPAN	40.270 IN	1.023M
MAC	12.973 IN	.3295M
L.E. SWEEP	40°	
TIP CHORD	3.706	.094M
ROOT CHORD	18.851	.4788M
INCIDENCE	0°	
DIHEDRAL	0°	
ASPECT RATIO	3.57	
TAPER RATIO	.1966	
AIRFOIL	NACA-64A204	

VERTICAL TAIL

THEO. AREA	.4188 FT²	.0389M²
SPAN	8.751 IN	.222 M
MAC	7.256 IN	.184M
L.E. SWEEP	47°30'	
TIP CHORD	4.144 IN	.105M
ROOT CHORD	9.638 IN	.245M
ASPECT RATIO	1.27	
HINGE LINE @ F.S.	49.110	
HINGE LINE SWEEP	0°	
TAPER RATIO	.43	
AIRFOIL @ Cr	5.3% BI-CONVEX	
Ct	4.0% BI-CONVEX	

HORIZONTAL CANARD (MID-POSITION)

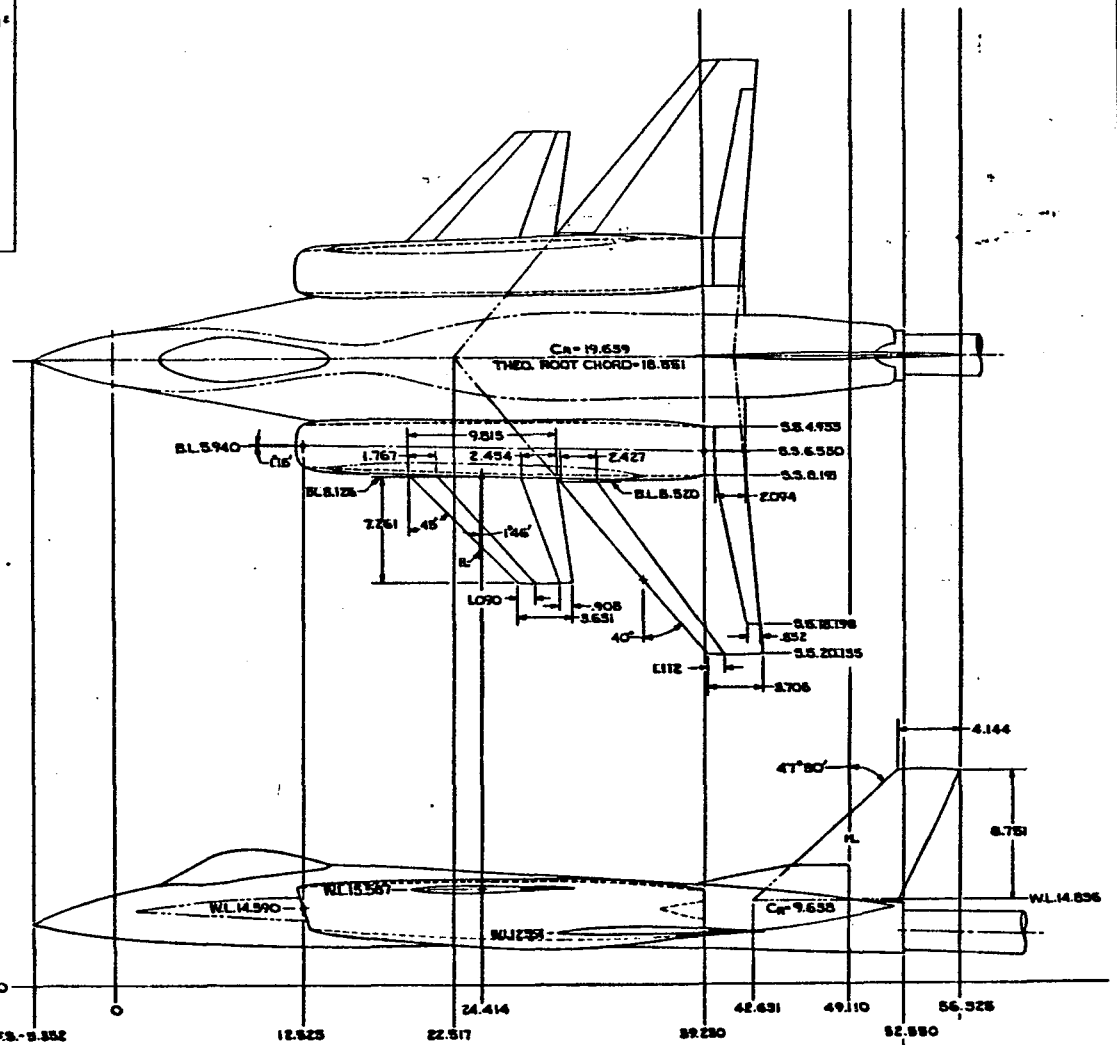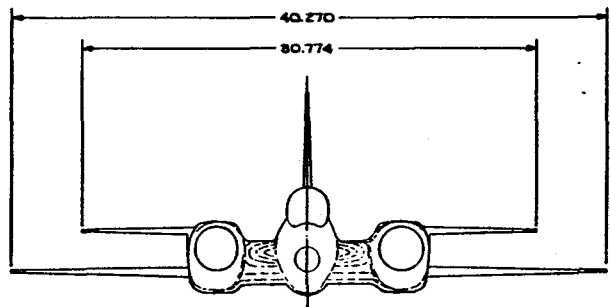|		
THEO. AREA (1 PANEL)	.3390 FT²	.0315M²
SPAN	7.261 IN	.184 M
MAC	7.197 IN	.183M
L.E. SWEEP	45°	
T.E. SWEEP	8°26'	
TIP CHORD	3.631 IN	.092M
ROOT CHORD	9.815 IN	.249M
DIHEDRAL	0°	
HINGE LINE @ F.S.	24.414	
B.L.	8.126	
W.L.	15.587	
HINGE LINE SWEEP	1°46'	
ASPECT RATIO (1 PANEL)		1.08
AIRFOIL @ Cr	NACA-64A005	
Ct	NACA-64A005	

Figure 3-25 Three View Drawing of R104 Wind Tunnel Model

3-VIEW .0939-SCALE V/STOL MODEL
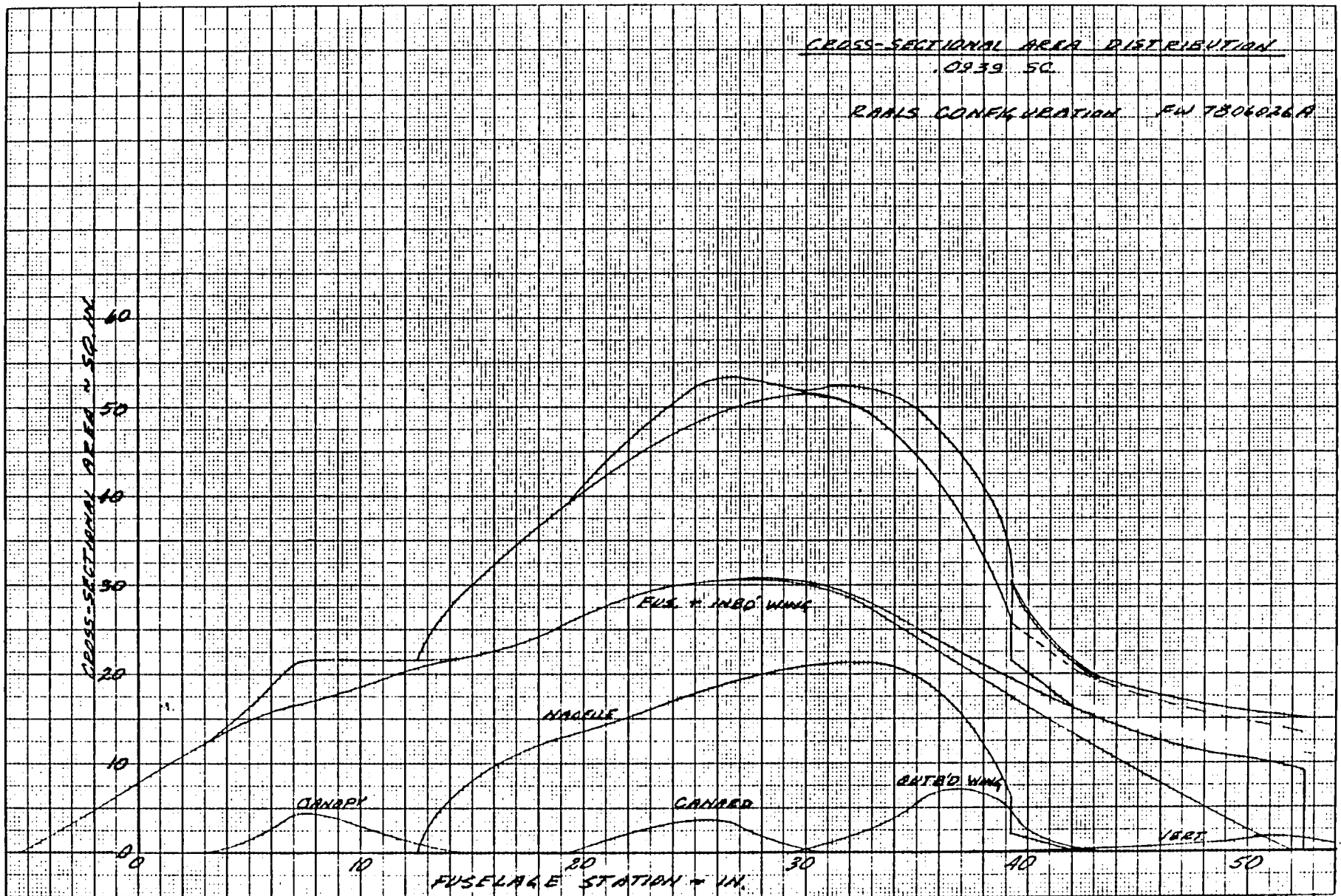RALS CONFIGURATION R-104 SIMULATION

81

Figure 3-26   Cross-sectional Area Distribution of R104
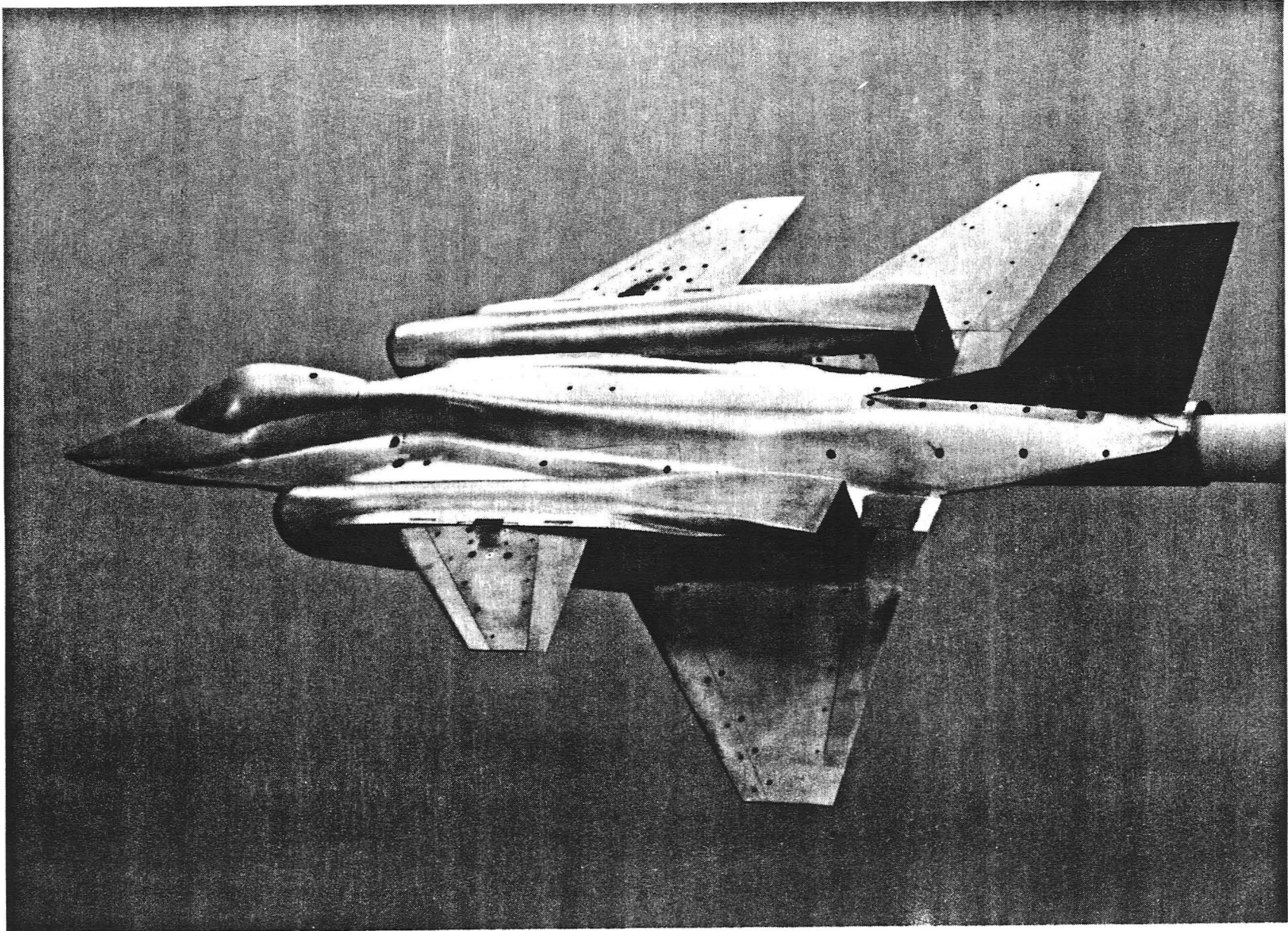Wind Tunnel Model
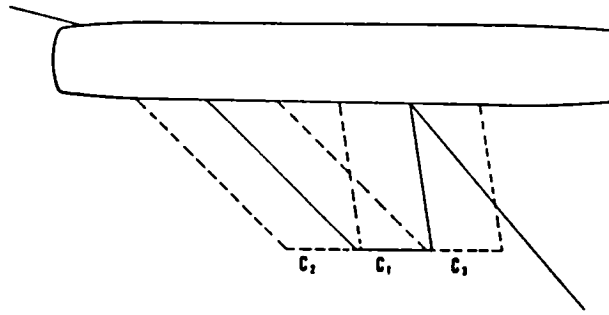
Figure 3-27 Photo of R104 Wind Tunnel Model

Figure 3-28a   Variations in CANARD Location for E205 and
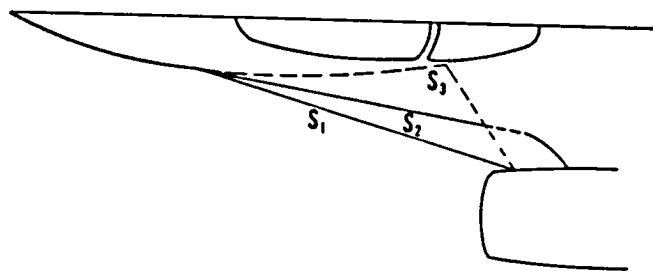R104 Wind Tunnel Models

Figure 3-28b   Variations in Strake Shape for E205
Wind Tunnel Model

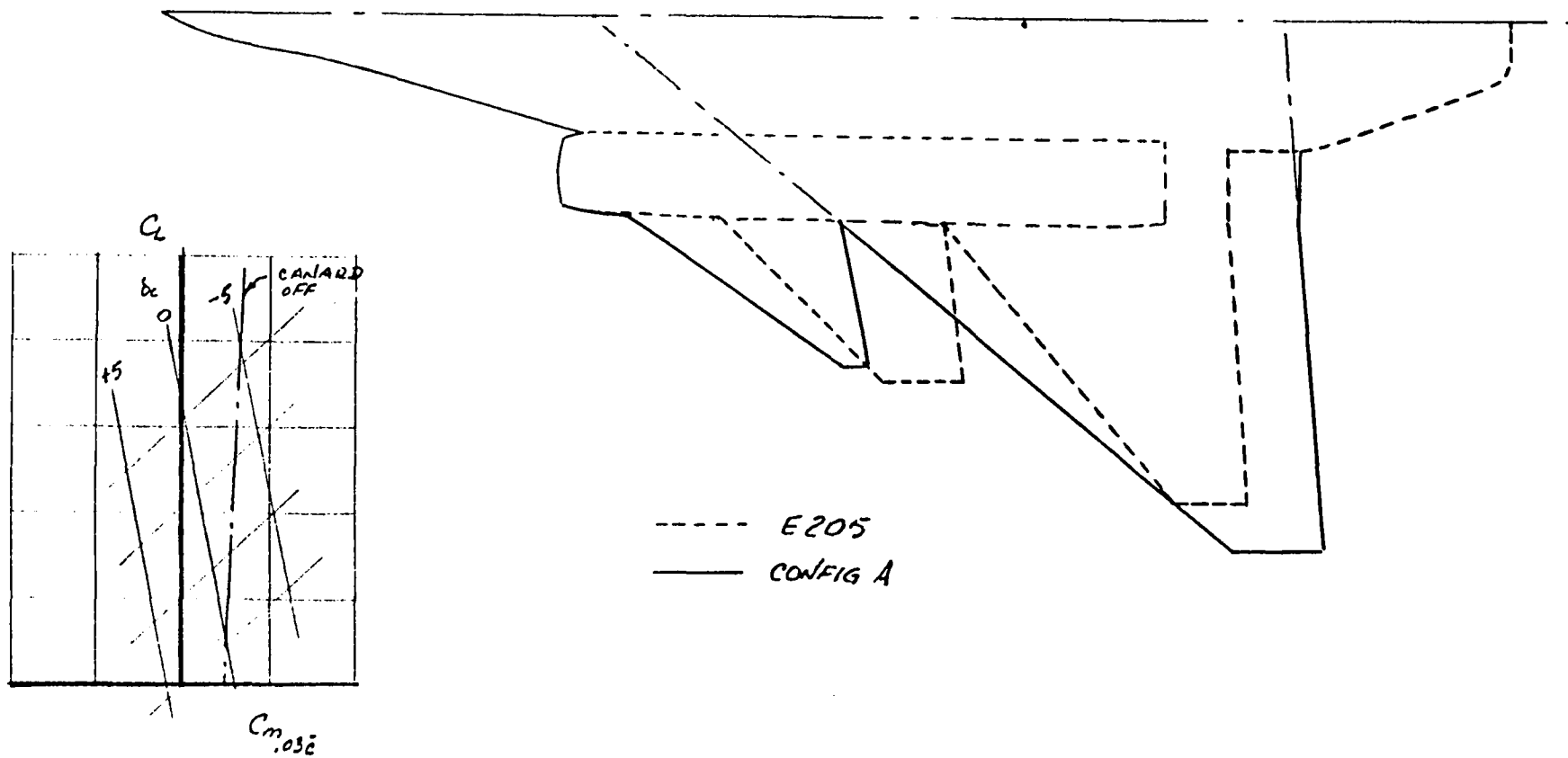|	WING	CANARD
λ	0.152	0.175
AR	2.7	2.46
S_{REF}	641.6	51.2
C_R	322.98	95.6
C_T	49.0	13.8

FIGURE 4-1   RECOMMENDED E205 CANARD AND WING PLANFORM CHANGE